University of Bath

PHD

Studies of cytochrome P450 in biomimetic films

Dash, Hayley

Award date:
2007

Awarding institution:
University of Bath

Link to publication

Alternative formats
If you require this document in an alternative format, please contact:
openaccess@bath.ac.uk

Copyright of this thesis rests with the author. Access is subject to the above licence, if given. If no licence is specified above, original content in this thesis is licensed under the terms of the Creative Commons Attribution-NonCommercial 4.0 International (CC BY-NC-ND 4.0) Licence (https://creativecommons.org/licenses/by-nc-nd/4.0/). Any third-party copyright material present remains the property of its respective owner(s) and is licensed under its existing terms.

Take down policy
If you consider content within Bath's Research Portal to be in breach of UK law, please contact: openaccess@bath.ac.uk with the details. Your claim will be investigated and, where appropriate, the item will be removed from public view as soon as possible.

Download date: 05. May. 2023

Studies of Cytochrome *P*450 in Biomimetic Films

Hayley Ann Dash

A thesis submitted for the degree of Doctor of Philosophy

University of Bath
Department of Chemistry

July 2007

COPYRIGHT

Attention is drawn to the fact that copyright of this thesis rests with its author.
This copy of the thesis has been supplied on condition that anyone who consults it is understood to recognize that its copyright rests with its author and that no quotation from the thesis and no information derived from it may be published without the prior written consent of the author.

This thesis may be made available for consultation within the University Library and may be photocopied of lent to other libraries for the purpose of consultation.

Hayley Dash

Abstract

Cytochrome *P*450 enzymes are a super family of haem-containing mono-oxygenases which are found in all kingdoms of life. They show extraordinary diversity in their reaction chemistry and are involved in the biotransformation of a plethora of both exogenous and endogenous compounds.
There has been a variety of approaches for the immobilisation of these biological redox systems and direct electrochemistry of these proteins can go towards providing biomimetic environments for fundamental studies together with a basis for designing devices without the need for electron transfer mediators.

The incorporation of these proteins into mesoporous films or onto various electrode surfaces has generated interest due to the possibility of direct electron exchange between the proteins redox active sites and the host electrode. Here, two different *P*450 protein systems were investigated. The water soluble *P*450cam or Cyp101, from the soil dwelling bacteria *Pseudomonas Putida* and Cyp6g1, a microsomal protein form the fruit fly *Drosophila Melanogaster.*

In this work, firstly the Cyp101 proteins were expressed and purified from a microbial culture starting material. The various steps in the purification process freed the protein from a confining matrix followed by the separation of the protein and non-protein parts of the mixture. In the latter system the enzyme is already embedded into a microsomal unit, thus more likely to mimic a biologically active environment.

The utilisation of methoxy-resorufin ether (MRES) is described as an electrochemical probe for investigating the activity of the microsomal protein. This substrate also exhibits fluorescent properties which provided a dual detection system for the enzymes activity.
The work then went on to investigate the absorption and reactivity of Cyp101 in porous nanoparticulateTiO_2 film electrodes and on an edge plane graphite electrode.

Declaration of work carried out in conjunction with others:

All experimental work in this thesis was carried out by the author.

Acknowledgements:

Funding: EPSRC and National Physical Laboratory, UK.

Dr. A.T.A. Jenkins, Dr. F. Marken. E.V.Milsom, Dr. S. Boundy, J.A.Olds, Professor D.R. Brown, Dr. P.J.Clegg. Dr. S. Flower, Capt. P.P. van Bergen.

Table of Contents

Table of Figures

1 Introduction

1.1. The origins of Electrochemical Investigations of Biological molecules.

1.2. Metalloproteins in biological systems.

1.3. Cytochromes and Haem proteins.

1.4. Cytochrome *P*450

1.5 Discovery of Cytochrome *P*450 (CYP) proteins

1.6 Cytochrome *P*450 Nomenclature

1.7. A review of Cytochrome *P*450 protein electrode investigations.

1.8. Direct electron transfer of Cytochrome *P*450 proteins in electrochemical sensors.

1.9. Cytochrome *P*450 proteins on bare electrode surfaces.

1.10. Phospholipid modified electrodes.

1.11. Electrodes modified with multilayer films.

1.12. Review summary.

1.13. Aims of the project

1.14. Chapter Summary

1.15. References

1.1 The origins of Electrochemical Investigations of Biological molecules

The Italian anatomist and physician Luigi Galvani was one of the first to investigate experimentally the phenomenon of what can be called bio electrochemistry. In a series of experiments started around 1780, Galvani, working at the University of Bologna, found that the electric current delivered by a Leyden jar or a rotating static electricity generator would cause the contraction of the muscles in the leg of a frog and many other animals, either by applying the charge to the muscle or to the nerve. In the strange case of Galvani's frog, this twitching happened even when its legs were not in a direct circuit with the machine. Galvani had placed the lower section of a dissected frog on a table near a plate-type electrical machine.

Then things occurred simultaneously causing Galvani to stop and wonder. An assistant was drawing a spark from the brass conductor of the electrical machine when a knife held in his hand touched the sciatic nerve passing through the lower part of the spine into the frog's legs. There was an immediate twitch of the muscles and a kick of the legs as if a severe cramp had set in. Galvani wrote, "While one of those who were assisting me touched lightly, and by chance, the point of his scalpel to the internal nerves of the frog, suddenly all the muscles of its limbs were seen to be so contracted that they seemed to have fallen into tonic convulsions" [1].

Galvani knew that metals transmitted this mysterious substance called electricity, and came to the obvious conclusion that some kind of electricity which he called "animal electricity" was generated in the tissue of the frog and flowing through the metal skewer and fence, activated the frog's muscles. He distinguished this kind of electricity from "artificial electricity" generated by friction (static electricity) and from "natural electricity" such as lightning. He thought of "animal electricity" as a fluid secreted by the brain, and proposed that flow of this fluid through the nerves activated the muscles. Galvani's remarkable experiments helped to establish the basis for biological study in many areas. The paradigm shift was complete: nerves were not water pipes or channels, as Descartes and his contemporaries thought, but electrical conductors. Information within the nervous system was carried by electricity generated directly by the organic tissue. As the result of the experimental demonstrations carried out by Luigi Galvani and his followers, the electrical nature of the nerve-muscle function was unveiled. However, a direct proof could only be made when scientists could be able to measure

or to detect the natural electrical currents generated in the nervous and muscular cells. Galvani did not have the technology to measure these currents, because they were too small.

Leland C. Clark had studied the electrochemistry of oxygen gas reduction at platinum metal electrodes, pioneering the use of the latter as an oxygen and therefore chemi-sensor. In fact, platinum electrodes used to detect oxygen electrochemically are often referred to generically as "Clark electrodes". More than almost any single invention, the Clark Oxygen Electrode has revolutionised the field of medicine for the past fifty years. This electrode remains the standard for measuring dissolved oxygen in biomedical, environmental, and industrial applications. The electrode can measure blood oxygen levels rapidly enabling many thousands of life saving procedures such as open heart surgery and associated emergency care. Oxygen monitoring is now a requirement for hospital accreditation [2]. It is also used to measure oxygen levels in rivers and oceans which may protect wildlife populations and monitor environmental pollution.

The electrochemical reduction of oxygen was discovered by Heinrich Danneel and Walter Nernst in 1897 [3]. Polarography using dropping mercury was discovered accidentally by Jaroslav Heyrovsky in Prague in 1922 [4]. This method produced the first measured oxygen concentration values in plasma and blood in the 1940s. Brink, Davies, and Bronk implanted platinum electrodes into tissue to study oxygen supply, or availability, from about 1940, but these bare electrodes became poisoned or contaminated when immersed in blood [5].

Leland Clark sealed a platinum cathode in glass and covered it first with cellophane; he then tested other membranes of polyethylene. In 1954 Clark conceived and constructed the first membrane covered oxygen electrode having both the anode and cathode behind a nonconductive polyethylene membrane. The limited permeability of polyethylene to oxygen reduced depletion of oxygen from the sample, making possible quantitative measurements of oxygen concentration in blood and many other solutions as well as gases. This invention led to the introduction of the modern blood gas analysis apparatus. These analysers are now found in most hospital emergency wards and in all biomedical laboratories. There is currently a great deal scientific interest in this kind of

technology and the investigation of biological molecules using electrochemical techniques has seen a significant increase in recent years.

1.2 Metalloproteins in biological systems.

In biochemistry, a metalloprotein is a generic term for a protein that contains a metal ion in its structure. The metal may be an isolated ion or may be coordinated with a nonprotein organic compound, such as the porphyrin found in haem proteins. In some cases, the metal is co-coordinated with a side chain of the protein and an inorganic nonmetallic ion. This kind of protein-metal-nonmetal structure is seen in iron-sulfur clusters.

A living system controls its activity through enzymes. An enzyme is a protein molecule that is a biological catalyst with three characteristics. Firstly, the basic function of an enzyme is to increase the rate of a reaction. Secondly, most enzymes act specifically with one substrate to produce products. The third and most remarkable characteristic is that enzymes are regulated from a state of low activity to high activity and vice versa. The activity of an enzyme depends, at the minimum, on a specific protein chain. In many cases, the enzyme consists of the protein and a combination of one or more parts or cofactors. A cofactor is a non-protein substance which may be derived from an inorganic metal.

The inorganic metal ions may be bonded through coordinate covalent bonds. The major reason for the nutritional requirement for minerals is to supply such metal ions as Zn^{+2}, Mg^{+2}, Mn^{+2}, Fe^{+2}, Cu^{+2}, K^{+1}, and Na^{+} for use in enzymes as cofactors .

Proteins associated with metals serve many important biological functions. The amino acid residues provide the functional groups in a protein which are the potential ligands for a metallic ion. Metals impart various effects on protein structure and bring about overall structural stability. These effects are seen in quaternary, secondary and tertiary structures of the protein [6].

1.3 Cytochromes and Haem proteins

Cytochromes are generally membrane-bound proteins that contain haem groups and carry out electron transport or catalyse reductive/oxidative or redox reactions. They are found in the mitochondrial inner membrane and endoplasmic reticulum of eukaryotes, in the chloroplasts of plants, in photosynthetic microorganisms, and in bacteria.

The heam group is a highly conjugated ring system so its electrons are very mobile. The ring surrounds a metal ion, which readily interconvert between the oxidation states. For many cytochromes the metal ion present is that of iron which interconvert between Fe^{2+} (reduced) and Fe^{3+} (oxidized) states during electron-transfer processes. Cytochromes are thus capable of performing oxidation and reduction. Because the cytochromes, as well as other complexes, are held within membranes in an organized way, the redox reactions are carried out in a highly organised sequence for maximum efficiency.

In the process of oxidative phosphorylation, which is the principal energy-generating process undertaken by organisms which need oxygen to survive, other membrane-bound and soluble complexes and cofactors are involved in the chain of redox reactions, with the additional net effect that protons (H^+) are transported across the mitochondrial inner membrane. The resulting transmembrane proton gradient is used to generate adenosine triphosphate (ATP), which is the universal chemical energy currency of life. ATP is consumed to drive cellular processes that require energy, such as rotation of flagella, transport of molecules across the membrane, and synthesis of macromolecules. ATP is an unstable molecule and tends to be hydrolysed in water. If ATP and ADP are in chemical equilibrium, almost all the ATP will be converted to ADP. Any system that is far from equilibrium contains potential energy, and is capable of doing work. Biological cells maintain the ratio of ATP to ADP at a point ten orders of magnitude from equilibrium, with ATP concentrations a thousand fold higher than the concentration of ADP. This displacement from equilibrium means that the hydrolysis of ATP in the cell releases a great amount of energy [7].

Several kinds of cytochrome exist and can be distinguished by way of spectroscopy, structure of the heam group, inhibitor sensitivity, and reduction potential:

Heam proteins have an extraordinary number of different functions in life processes including oxygen and electron transport, charge separation in photosynthesis and catalysis in the synthesis and breakdown of chemicals in the cell. All of these functions are based on an iron atom coordinated by a porphyrin and one or two axial ligands from the protein [7].

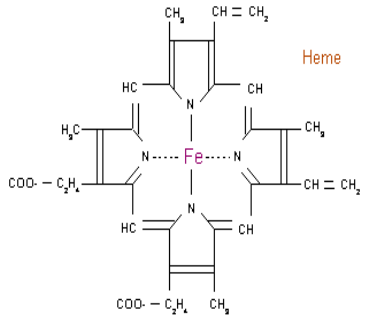

Haemoglobin

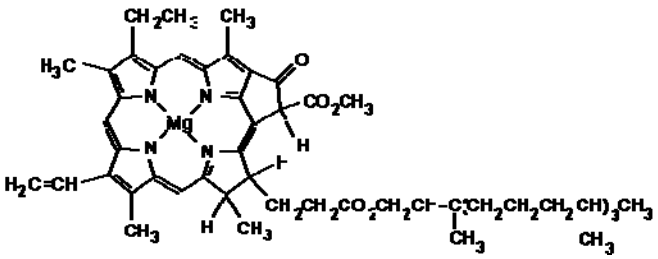

Chlorophyll

Figure 1 Two examples of metal centred proteins (adapted from Alberts 2001)

Prosthetic groups differ from cofactors in being tightly, often covalently, bound to a particular enzyme molecule, two example of which are shown in figure 1. Heam, which is found in cytochromes and haemoglobin, and carries oxygen and/or electrons. Another example of a metal centred protein can be found in Chlorophyll which is the molecule that absorbs sunlight and uses its energy to synthesise carbohydrates from CO_2 and water.

Haemoglobin

Haemoglobin (Hb) is the iron-containing oxygen-transport metalloprotein in the red cells of the blood in mammals and other animals. Haemoglobin in vertebrates transports

oxygen from the lungs to the rest of the body, such as to the muscles, where it releases the oxygen load. Haemoglobin also has a variety of other gas transport and effect modulation functions, which vary from species to species, and which in invertebrates may be quite diverse [8].

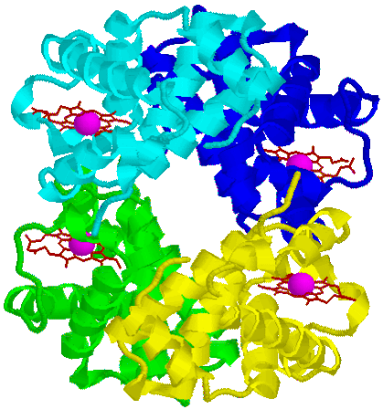

Figure 2 Diagrammatic representation of a haemoglobin molecule (Da Silva 2001)

The four globin components consisting, of two alpha chains and two beta chains, are shown in figure 2 as blue, turquoise, green, and yellow, and the four haem groups are shown in red with the iron atoms in purple.
Another example is a small heam protein found loosely associated with the inner membrane of the mitochondrion. Cytochrome C is a soluble protein, unlike other cytochromes, and is an essential component of the electron transfer chain. It is capable of undergoing oxidation and reduction, but does not bind oxygen. It transfers electrons between Complexes III and IV of the electron transport chain [9].

Cytochrome *c*

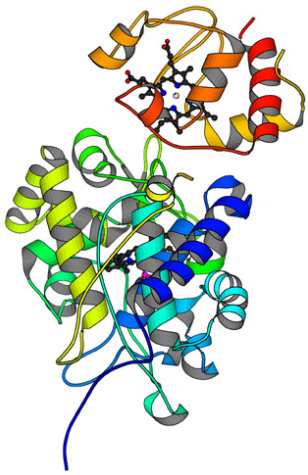

Figure 3 Diagrammatic representation of Cytochrome C. (Da Silva 2001)

Shown in blue and yellow which is complexed with Cytochrome C peroxidase in orange and red.

The differences in the structure of the cytochromes means that the redox potential of the ferrous to ferric redox couple can be tuned to the requirements of the particular cytochrome function. Different cytochromes have quite different redox potentials. It is also important to compare Cytochrome C, shown in figure 3, with the oxygen transporting haem proteins myoglobin and haemoglobin. The function of myoglobin requires that the ferrous iron atom is bound to oxygen but is not oxidised to the ferric form. Once again the function of the iron atom is modulated by the environment provided by the porphyrin ring of the haem and the surrounding protein [10].

1.4 Cytochrome *P*450

Cytochrome *P*450 oxidase, commonly abbreviated as CYP, is a generic term for a large number of related, but distinct, oxidative enzymes important in animal physiology. The cytochrome *P*450 mixed function mono-oxygenase system is probably the most important element of Phase I metabolism of therapeutic drugs in humans and most animals. Cytochrome *P*450 sequence homologs have been determined in all lineages of life, including mammals, birds, fish, insects, worms, sea squirts, sea urchins, plants, fungi, slime molds and bacteria .

Small molecule drugs are xenobiotics, foreign molecules, which the human body attempts to deal with through a number of responses. Some drugs are excreted from the human body intact. Most drugs, however, need to be modified structurally to facilitate excretion. These modification processes are called drug metabolism. Drug metabolism is a detoxification function the human body possesses to defend itself from environment hostility. When a person is sick, however, the body needs some kind of medication to fight the disease. Ideally, a drug should reach the site of action intact, cure the disease and leave the body after it completes its mission. However, drug developers often face the dilemma that a potential drug is either metabolised/excreted from the body too fast and the drug cannot reach its therapeutic effect. Or too slow and the drug stays in the body for a long time, causing unwanted side effects.

The study of drug metabolism, therefore, serves primarily two purposes: to elucidate the function and fate of the drug, and to manipulate the metabolic process of a potential drug.

The liver is the primary site for metabolism. The liver contains the necessary enzymes for metabolism of drugs and other xenobiotics. These enzymes induce two metabolism pathways: Phase I (functionalisation reactions) and Phase II (biosynthetic reactions) metabolism. Some typical examples of Phase I metabolism include oxidation and hydrolysis. The enzymes involved in Phase I reactions are primarily located in the endoplasmic reticulum of the liver cell (microsomal enzymes). Phase II metabolism involves the introduction of a hydrophilic endogenous species, such as glucuronic acid or sulfate, to the drug molecule. Enzymes involved in phase II reactions are mainly located in the cytosol, except glucuronidation enzyme, which is also a microsomal enzyme.

Drugs are usually lipophilic substances (Oil-like) so they can pass plasma membranes and reach the site of action. Drug metabolism is basically a process that introduces hydrophilic functionailities onto the drug molecule to facilitate excretion. When the drug molecule is oxidised, hydrolysed, or covalently attached to a hydrophilic species, the whole molecule becomes more hydrophilic, and is excreted more easily. Drugs often undergo both Phase I and II reactions before excretion. The Phase I reaction introduces a functional group such as a hydroxyl group onto the molecule, or exposes a pre-existing functional group, and Phase II reaction connects this functional group to the endogenous species such as a glucuronic acid. The modified drug molecule may then be hydrophilic enough to be excreted.

Although the liver is the primary site for metabolism, virtually all tissue cells have some metabolic capabilities. Other organs having significant metabolic activities include the gastrointestinal tract, kidneys, and lungs. When a drug is administered orally, it undergoes metabolism in the gastro-intestinal (GI) track and the liver before reaching systemic circulation. This process is called first-pass metabolism. First-pass metabolism limits the oral bioavailability of drugs, sometimes significantly.

Drugs are ultimately excreted from the body through various routes. The kidney is the major organ for drug excretion. It excretes hydrophilic drugs and drug metabolites through glomerular filtration. Macromolecules such as proteins are retained. Lipophilic drug molecules are not directly excreted from the kidney. Only after they are metabolised into more hydrophilic molecules, can they be excreted through the kidneys into the urine. Drugs and their metabolites are also excreted into bile. This is usually mediated by protein transporters. Drugs and their metabolites in bile are eventually released into the intestinal tract. The drugs may be reabsorbed into the body from the intestine. Drug metabolites such as glucuronide conjugates, may be converted back to the parent drug in the intestine through glucuronidase enzyme, and then reabsorbed into systemic circulation. This drug recycling process is called enterohepatic recycling. This process, if extensive, may prolong the half-life of the drug. The bile drugs and drug metabolites, if not reabsorbed by intestine, are excreted from the body through faeces. Also, a variety of orally administrated drugs are excreted through faeces because they are not absorbed through the intestine. Oral bioavailability constitutes a major challenge for drug developers. Other routes of excretion, such as sweat, tears, and saliva, are quantitatively less important. Excretion

through breast milk is not important to the mother, but may be of key importance to the baby, because the drug may be toxic to the baby. Pulmonary excretion is important for anaesthetic gases and vapour drugs.

As is pointed out, small molecule drugs are usually lipophilic substances that can penetrate cell membranes to reach the site of action, and drug metabolism is a process of introducing hydrophilic functional groups onto the drug molecule. The most common phase I reactions are oxidative processes that involve cytochrome P450 enzymes.

These enzymes catalyze the following reactions: aromatic hydroxylation; aliphatic hydroxylation; N-, O-, and S-dealkylation; N-hydroxylation; N-oxidation; sulfoxidation; deamination; and dehalogenation.

These enzymes are also involved in a number of reductive reactions, generally under oxygen-deficient conditions. Hydrolysis is also observed for a wide variety of drugs. The enzymes involved in hydrolysis are esterases, amidases, and proteases. These reactions generate hydroxyl or amine groups, which are suitable for phase II conjugation.

Phase II conjugation introduces hydrophilic functionalities such as glucuronic acid, sulfate, glycine, or acetyl group onto the drug or drug metabolite molecules. These reactions are catalyzed by a group of enzymes called transferases. Most trasferases are located in cytosol, except the one facilitates glucuronidation, which is a microsomal enzyme. This enzyme, called uridine diphosphate glucuronosyltransferase (UGTs), catalyzes the most important phase II reaction: glucuronidation. Glucuronic acid contains a number of hydroxyl groups and one carboxylic acid functionality. This molecule is extremely hydrophilic, and improves the hydrophilicity of a drug molecule when they are covalently bound.

The following is a partial list of common metabolism motifs:

Aliphatic/Aromatic carbons: hydroxylation.
Methoxyl/methylamine group: demethylation.
Amine: N-oxidation, or deamination.
Sulfur: S-oxidation.
Phenol/alcohol: glucuronidation/sulphation.
Esters/amides: hydrolysis.

In reality, drug metabolism is an extremely complicated process. Often, a drug is metabolised into many products, some major, others minor. A complete picture of the metabolism of a drug is, in many cases, not possible, and not usually necessary.

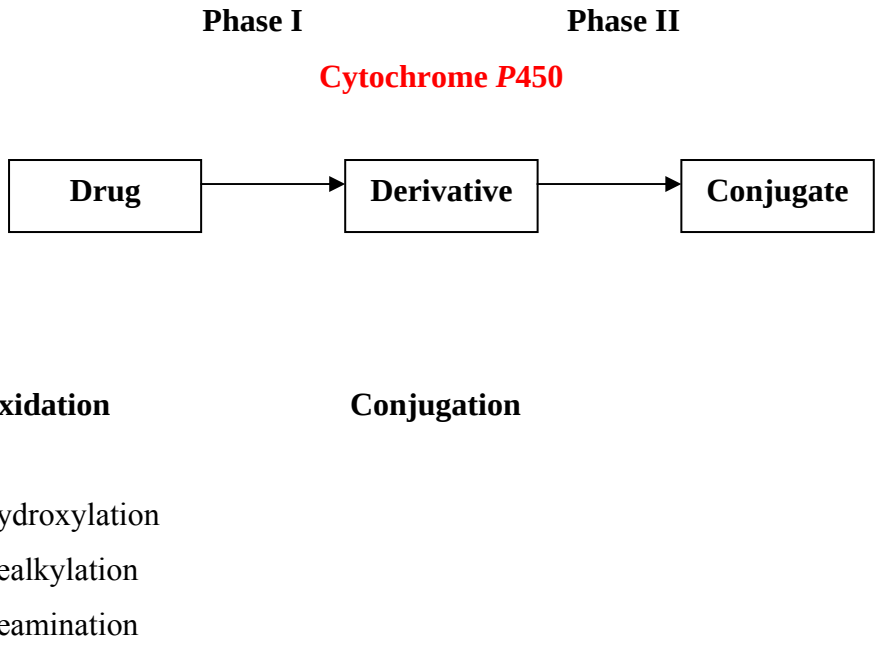

Figure 4. Schematic interpretation of the two phases of drug metabolism. This shows the association and involvement of Cytochrome P450 proteins during phase I biotransformation.

*P*450s are membrane-associated proteins, either in the inner membrane of mitochondria or in the endoplasmic reticulum of cells where they metabolise thousands of endogenous and exogenous compound. The involvement of *P*450 is shown in Figure 4. In the liver, these substrates include drugs and toxic compounds as well as metabolic products such as the breakdown product of haemoglobin, bilirubin. *P*450s are present in many other tissues of the body including the mucosa of the gastrointestinal tract, and play important roles in hormone synthesis including estrogen and testosterone synthesis and metabolism, cholesterol synthesis, and vitamin D metabolism. In most animals, including humans, hepatic *P*450s are the most widely studied of these enzymes.

1.5 Discovery of Cytochrome *P*450 (CYP) proteins

A major class of oxidative transformations was initially characterized in 1955 by O.Hayaishi in Japan and H.S.Mason in the United States. This class of Oxygenases had requirements for both an oxidant and a reductant and hence was given the trivial name "mixed-function oxidases" [11]. The general reaction is shown in figure 5.

$$RH + O_2 + 2H^+ + 2e^- \longrightarrow ROH + H_2O$$

Figure 5. General reaction mechanism of the mixed function oxidase system.

The most common reaction catalysed by P450 enzymes is a monooxygenase reaction, i.e. insertion of one atom of oxygen into substrate while the other oxygen atom is reduced to water 11.

An understanding of the biochemical nature of these reactions grew out of early studies on liver pigments by Garfinkel and Klingenberg who observed in liver microsomes an unusual carbon monoxide binding pigment with an absorbance maximum at 450 nm [12]. (In cell biology, a microsome is a small vesicle that is derived from fragmented endoplasmic reticulum produced when cells are homogenized).

This pigment was ultimately characterized as a cytochrome by Omura and Sato. Through the use of detergent solubilisation of microsomes and interaction with isocyanide ligands, they showed that the resultant *P*450, or pigment which absorbs strongly at 450nm, was indeed a cytochrome with a typical Soret absorption band, shown in Figure 6. The technique showed a very strong absorption in the blue region of the optical absorption spectrum of the heam found in this protein [13].

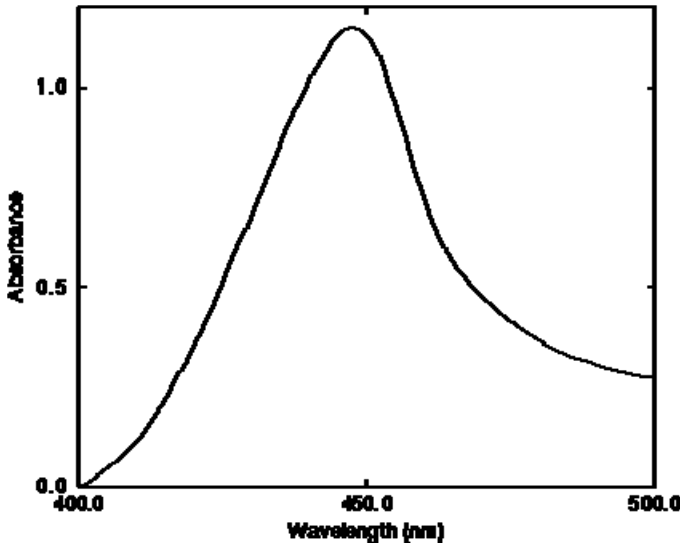

Figure 6 Ultra Violet absorption spectra of a *P*450 carbon monoxide complex.

This shows the characteristic Soret peak at around 450nm. (Spectra adapted from Omura and Sato) [13]

The reason why absorption occurs at this wavelength is related to one of the six ligands associated with the iron atom contained in the haem. The heam ring itself provides four ligands (nitrogens), but in *P*450 the fifth is an unusual, negatively charged sulphur atom. This is generally known as a thiolate anion and proteins containing this unusual moiety are referred to as haem-thiolate proteins.

Cytochrome *P*450

Figure 7 The Haem-thiolate protein Cytochrome *P*450.
P450s are large, multidomain proteins typically with a single active haem site shown in Figure 7 near the centre in dark red. Different domains, often separate subunits, are used to bind the redox partners, store reducing equivalents and act as controls of the enzymatic activation (Da Silva 2001)

As a result of this, CYP chemistry is fascinating and challenging. It is important to note that the bond between the two atoms in an oxygen molecule is very strong. This implies that a substantial amount of energy is required to break the bond. This energy is supplied by the addition of electrons to the iron atom of haem. These electrons in turn come from the last protein in an electron transfer chain. There are two such chains in cellular structure involved in CYP catalysis. The first is found in the endoplasmic reticulum. This protein, nicotinamide adenine dinucleotide phosphate (NADPH) cytochrome *P*450 reductase, passes electrons to flavin adenine dinucleotide (FAD) to flavin mononucleotide (FMN) and then to the heam. The second chain is found within mitochondria where electrons are passed down to the haem. NADPH then passes electrons to ferredoxin reductase, then to ferredoxin, which itself has an iron-sulphur cluster, and from there to CYP. An interpretation of this reaction is shown in Figure 8.

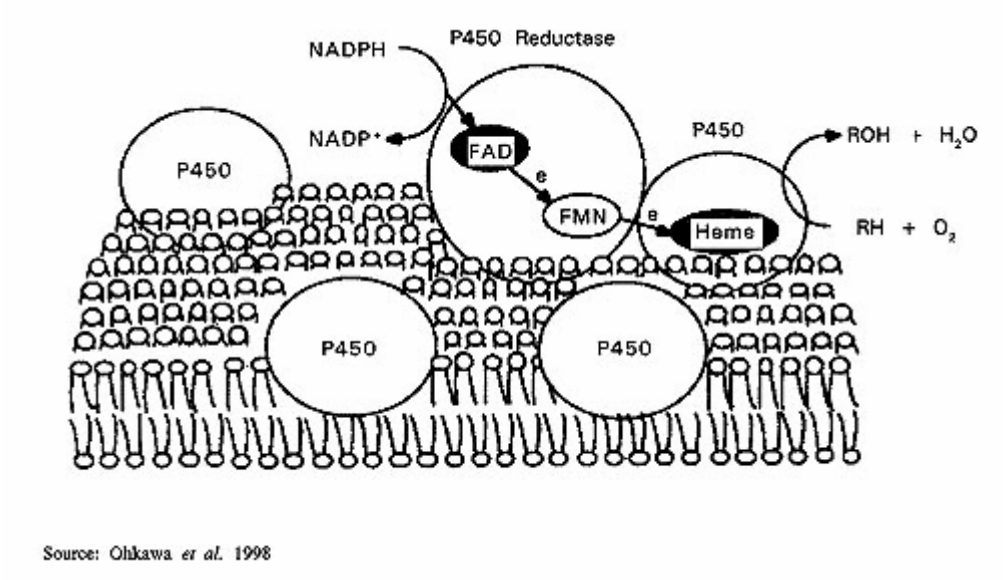

Figure 8 Schematic interpretation of the chain of electron transfer in Cytochrome *P*450 monooxigenases in plant microsomes.

1.6 Cytochrome *P*450 Nomenclature

*P*450 research is a field that has benefited by having a systematic standardised nomenclature. The need for such a system only appeared gradually, since early work in the 1960s debated if there was more than one *P*450. The purification of multiple forms from rat and rabbit gave rise to a nomenclature started by the labs that were writing the papers on these forms. The tendency was to make the forms a, b, c or 1, 2, 3 with some prefix to identify the source or inducer, like RLM for rat liver microsomes or PB1 for Phenobarbital form 1. This quickly became unworkable as every lab had their own naming convention. The 1980s saw cloning of many *P*450s so the problem got worse. The visionary who saw where this was leading and proposed a solution was Dan Nebert. Dan, along with Frank Gonzalez put together the first *P*450 nomenclature. An official nomenclature proposal was published that same year with a large number of influential *P*450 researchers as co-authors [14].

Nomenclature, e.g. for CYP2D6

CYP = cytochrome *P*450
2 = genetic family
D = genetic sub-family
6 = specific gene
Note that this nomenclature is genetically based. It has no functional implication.

*P*450 nomenclature is based on the homology of the gene, firstly to members of the same family where the homology at the amino acid level is greater than 40%, (this is shown as the first number). The members of a subfamily have greater than 55% homology at the amino acid level (as shown by the letter). Members of each family are then classed by a second number usually dependant on when they are discovered [15].
These proteins can also be grouped by two different schemes. One scheme was based on a taxonomic split: class I (prokaryotic/mitochondrial) and class II (eukaryotic microsomes). The other scheme was based on the number of components in the system: class B (3-components) and class E (2-components). These classes merge to a certain degree. Most prokaryotes and mitochondria (and fungal CYP55) have 3-component systems (class I/class B) - a FAD-containing flavoprotein (NAD(P)H-dependent reductase), an iron-sulphur protein and *P*450. Most eukaryotic microsomes have 2-component systems (class II/class E) - NADPH: *P450* reductase (FAD and FMN-containing flavoprotein) and P450 however there are exceptions to this scheme.

Over 200,000 chemical compounds are metabolised by the CYP superfamily of enzymes. Many different reactions are catalysed including oxidations, reductions and dehalogenations. Although the initial characterisation was by UV spectra, methods such as immunoblotting with specific antibodies and amino acid gene sequencing are now used. Full sequencing has been successfully carried out on animal, fungi, plant and bacterial CYP enzymes [16].

Members of the human CYP superfamily play a role in the metabolism of many drugs and several of them, CYP2D6, CYP2C9 and CYP2C19, have been shown to be polymorphic as a result of single nucleotide polymorphisms (SNPs), gene deletions, and gene duplications [16]. These polymorphisms can impact on the pharmacokinetics

(PK), metabolism, safety and efficacy of drugs and because of the availability of automation, genotyped human tissue, recombinant CYP preparations (rCYPs) and reagents, most pharmaceutical companies have increasingly screened out compounds that are metabolised solely by polymorphic CYPs. In the absence of suitable animal models, it has been widely accepted that such *in vitro* data are useful because one can obtain information prior to dosing in man and select the most appropriate clinical studies with prospectively genotyped and phenotyped subjects. Overall, current trends in the industry have been fuelled by increasing managed healthcare, the desire to minimise the need for therapeutic drug monitoring and CYP genotyping in medical practice and a very competitive market place. In the past, such paradigms have not been as influential and there are numerous examples of marketed drugs that are metabolised by polymorphic CYPs.

For example, many individuals lack functional 2D6. These subjects will be predisposed to drug toxicity caused by antidepressants or neuroleptics, but will find codeine and tramadol to be ineffective due to lack of activation. Other drugs that have caused problems in those lacking 2D6 include dexfenfluramine, propafenone, mexiletine, and perhexiline. Perhexiline was in fact withdrawn from the market due to the neuropathy it caused in those 2D6 inactive patients unfortunate enough to be treated with it [17]. Even beta-blocker removal may be impaired in 2D6-deficient people. Occasionally one derives benefit from an unusual CYP phenotype. For example, cure rates for peptic ulcer treated with omeprazole are substantially greater in individuals with defective CYP2C19, owing to the high plasma levels achieved [18].

Designing and ultimately marketing a drug is very costly. The interaction between CYP and newly designed drugs is therefore rather important to pharmaceutical companies, so much so that predominant degradation of a drug by one of the polymorphic CYPs is often enough to stop further research on that drug in its tracks. This is a very important point. Variable expression of CYP has substantial clinical consequences, not only in different people and different race groups, but also in individuals as they progress from infancy to old age [19]. CYP1A2 is not expressed in neonates, making them particularly susceptible to toxicity from drugs such as caffeine. These issues drive the need for research into the understanding of how these proteins function [20].

1.7 A review of Cytochrome *P*450 protein electrode investigations.

In the thirty five years since the identification of Cytochrome *P*450 as the terminal component of oxygenation reactions, the field has grown from an area of narrow interest for drug metabolism scientists to a major field of interest to molecular biologists, pharmacologists, biochemists and physicians. From the isolation of membrane bound *P*450 by Lu and Coon [21] in 1969 to the first crystallization of a mammalian *P*450 in 1999 by Eric Johnson and co-workers [22], the area of *P*450 research has established the crucial role of P450s in controlling the biotransformation of drugs and other xenobiotics. CYP has probably been one of the most extensively researched families of redox active proteins studied over the past fifty years. The enzymes multi domain structure makes it an ideal model system for studying the mechanism of electron transfer and for understanding the architecture and activity of membrane bound CYP proteins.

Horecker first identified mammalian NADPH cytochrome *P*450 reductase in 1950. Studies in the 1960's linked mammalian *P*450 to the newly discovered microsomal electron transport chains, cytochromes *P*450 and b_5 and their involvement in drug and steroid hydroxylations [23, 24].

The work on the bacterial protein, *P*450cam, so named due to its natural substrate being camphor, carried out in 1996 by Kazlauskaite and co workers, reported the observation of unprompted electrochemistry of recombinant *P*450cam on an edge-plane graphite (EPG) electrode [25]. All previous redox studies on this *P*450 system had been carried out using spectroscopic studies [16]. *P*450cam mechanisms are considered in more detail later.

The pioneering work carried out by Eddowes and Hill highlighted that the problem of slow electron transfer between an electrode and a protein could be overcome using an electron shuttle or mediator [26]. The work carried out by Fleming and co workers determined the redox properties of Cytochrome *P*450$_{BM3}$, found in the soil dwelling bacterium Bacillus Megaterium, when incorporated into a lipid bilayer. Direct electrochemistry determined an outline of some of the redox properties of this membrane bound protein [27].

Studies carried out in 1973 by Sharrock and colleagues reported that ferric *P*450cam underwent a low to high spin transformation in its electronic state upon substrate binding. Subsequent work found this to be a characteristic feature of many other *P*450s. It was suggested that this model offered a possible insight as to why ferrous *P*450 cannot be generated in the absence of its substrate, thus potentially toxic reduction of O_2 to superoxide or peroxide is avoided [28]. However, studies carried out by Kondo and co workers questioned the mechanisms in this model [29].

In general, direct electrochemistry of CYP enzymes on unmodified electrodes has proved extremely problematic due to the deeply buried haem moiety and instability of the biological matrix upon interaction with the electrode surface. A fundamental aspect of *P*450 reactions is the substrate induced modulation of the haem spin state upon binding. This can have a significant effect on both the redox potential of the protein whereby the change from predominantly low spin to high spin brings about a lowering of the haem protein redox potential so it becomes less negative. This is discussed later in more detail.

The first electrochemical study of human *P*450 2E1 was reported in January 2004 by Fantuzzi and colleagues [30.] The work highlighted the important aspects of immobilisation of proteins in the production of biosensors, as sensitivity may strongly depend on both concentration and orientation of the protein at the surface. In order to address these requirements thiol terminated chains covalently bound to a metal surface and functionalised at the other end with a group able to specifically interact with the protein surface was found to generate an oriented and tightly packed monolayer. The liver CYP used in this work was N-terminally modified and expressed in E coli. The results highlighted the extent of the monolayer coverage and the electron transfer rate and showed that an electrochemical response on a gold surface was only obtainable after modification of the surface [30].

Several ways have been used to investigate electron transfer between redox proteins and electrodes, particularly using chemically modified electrodes in combination with electrochemical techniques like cyclic voltammetry (CV) and square wave voltammetry (SWV). This is particularly important in the case of haem proteins like CYP in which the electrochemically active centre is buried in the protein structure and is surrounded by an amino acid chain in order to gain a hydrophobic environment for catalysis.

1.8 Direct electron transfer of Cytochrome *P*450 proteins in electrochemical sensors.

On unmodified electrodes, enzymes tend to denature. *P*450 proteins are naturally involved in electron transport pathways of protein redox partners, which require specific docking sites. Therefore, it would be natural to assume electrical contact to CYP enzymes should be possible with suitable surface modifications of electrodes. However, this has been shown to be very problematic.

The electrochemistry of CYP has been investigated using a variety of metal electrodes such as Au, Pt and Tin oxide, represented in Figure 9, as well as non metal electrodes such as glassy carbon (GC), pyrolytic graphite (PG), edge-plane graphite (EPG), and carbon electrodes. Although direct electron transfer has been observed on bare electrodes, modifying the electrode with an appropriate medium like a polymer or another linker molecule in order to attain native structure and appropriate orientation thus increasing electron transfer between the enzyme and the electrode has been very popular in recent years. The bioelectrocatalysis by proteins and enzymes such as cytochrome *c*, CYP, glutathione peroxidase and haem flavo enzymes at modified electrodes has been recently reviewed [31].

In the first biosensor based on the direct electron transfer between the electrode and CYP, solubilised protein from rabbit liver showed a reduction step at a mercury electrode of −580 mV versus SCE [32].

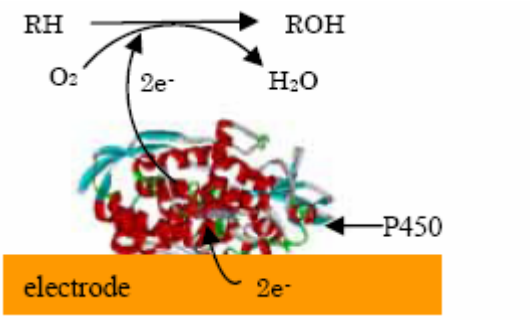

Figure 9. A schematic representation of a Cytochrome *P*450 sensor.
The enzyme could be adsorbed or immobilised in a variety of ways on many different electrode surfaces (Garrett & Grisham 1998)

1.9 Cytochrome *P*450 proteins on bare electrode surfaces.

Hill and co workers had used bare EPG electrodes to characterize the electrochemistry of recombinant CYP101 [31]. In this work, cyclic voltammetric measurements were carried out in the presence and in the absence of the substrate camphor. Strictly anaerobic conditions were used to prevent formation of the binding of oxygen to Fe^{2+} and the possibility of second electron transfer. The results indicated reversible oxidation and reduction. The interaction of the CYP101 with the bare EPG has been proposed by the authors to be possible via the positively charged amino acid residues on the surface of CYP101.

The formal potential ($E°'$) was −526 mV versus SCE with the camphor free CYP101 and an $E°'$ of −390 mV versus SCE for the camphor bound form. These values are in agreement with the redox potential of CYP101 in solution for the substrate free form with an $E°'$ of −547 versus SCE and substrate bound form, with an $E°'$ of −394 versus SCE [32]. The binding of camphor to the active site of the enzyme shifts the spin state of the haem prosthetic group from low to high. The authors also claim that a catalytic response upon camphor addition was observed, although details are not given.

In order to investigate the role played by amino acids on the immobilisation of CYP101 on the electrode surface, Lo and colleagues carried out site directed mutagenesis to modify the surface of the enzyme [33]. In this study the cysteine residues were replaced by chemically inert alanines. Electrochemistry of wild type (WT) CYP101 and the mutants could be observed with bare EPG electrodes with formal potentials ranging from −428 to −449 mV versus SCE at a range of scan rates. However, a quasi

reversible or irreversible electrochemistry was obtained with bare gold electrodes. The electrochemistry of cysteine free CYP101 was in both cases indistinguishable with that of the WT and the single cysteine mutant enzyme, which indicated that electron transfer was not affected by these residues. Furthermore, electrochemistry of CYP2E1 could be seen with bare GC electrodes with a midpoint potential of −334 mV versus SCE, indicating that CYP2E1 was adsorbed on the electrode surface [30].

1.10 Phospholipid modified electrodes.

The majority of CYP enzymes are located in a hydrophobic environment in the endoplasmic reticulum of cells, although cytosolic enzymes also exist, such as CYP101 [10]. In order to mimic the physiological environment of CYP enzymes, a number of groups have used phospholipids, such as didodecyldimethylammonium bromide (DDAB)dimeristoyl Lphosphatidylcholine (DMPC),dilauroylphosphatidylethanolamine (DLPE) and distearoylphosphatidylethanolamine (DSPE), for the construction of biosensors. Phospholipid layers form vesicular dispersions that bear structural relationship with the phospholipid components of biologically important membranes. Using this method, a membranous environment is created that facilitates electron transfer between the enzymes redox centre and the electrode.In a similar study Zhang and co workers in addition to DDAB, used DMPC to incorporate CYP101 and then modify PG disc electrodes [34]. CV responses with DMPC showed reversible electrochemistry. Work carried out to investigate the protein in the presence of carbon monoxide (CO) indicated that electron transfer involved the haem $Fe^{3+/2+}$ couple of the enzyme.

1.11 Electrodes modified with multilayer films.

In order to improve the direct electron transfer between Au electrodes and haem proteins like CYP, Rusling and co workers investigated the direct electrochemistry of CYP101 using a layer-by-layer approach to the construction of films of CYP101 protein with polyions [35] .In these studies Au and pyrolytic graphite (PG) electrodes were modified by sequential adsorption of polystyrenesulfonat (PSS) and CYP101 thus creating CYP101 multilayer films.

The motivation behind the development of a biosensor with human CYP3A4 as a novel drug screening tool was created due to CYP enzymes playing an important role in the metabolism of endogenous compounds as well as in pharmacokinetics and toxicokinetics. The sensor was constructed by assembling enzyme films on gold electrodes by alternate adsorption of a layer of CYP3A4 on top of a layer of PDDA. The biosensor was used in the detection of verapamil, midazolam, quinidine and progesterone. Electrochemical investigation of the enzyme bound film revealed well defined anodic and cathodic redox peaks, which indicated reversible oxidation and reduction of the haem group in these experiments.

Catalytic responses have also been obtained with fluoxetine using CYP2D6 on a polyaniline-doped GC electrode. The enzyme exhibited reversible electrochemsitry with an $E^{\circ\prime}$ of −120 mV versus SCE, which upon increasing concentrations of fluoxetine a cathodic shift was observed [36].

1.12 Review summary

Regarding protein electrochemistry, the number of papers on CYP ranks very highly after cytochrome *c* and glucose oxidase. The binding sites for electron transferring proteins at the molecule surface, which are essential for the fast electron transfer and subsequent oxygen activation, characterise the CYP family. Therefore, the engineering of the electrode surface for appropriately orienting the active site towards the electrode is crucial for the observation of the proteins activity. However, due to the well known low conformational stability of these proteins, pronounced structural changes are plausible in the process of embedding in the matrix at the electrode surface. These deviations from the behaviour in solution are reflected by the anodic shift of the structure free protein and may be reflected by the smaller anodic peak in cyclic voltammetry measurements.

Glucose oxidase is an intrinsic redox enzyme with the prosthetic group buried deep within the protein fabric. For the fast heterogenous electron transfer within this protein, the coupling of the redox relay to the protein has been established [37]. This concept has been transferred to CYP electrochemistry by Archakov's group by attempts at binding riboflavin to the protein surface [38]. The concept of a ‘redox wire’ transferring the

electrons via immobilized mediators from the electrode to the prosthetic group has not yet been realised for the electrochemical substrate hydroxylation by CYP.
Interpretations of the reaction mechanism are complicated by the fact that substrate conversion requires oxygen. Most probably, both reduction of the prosthetic group and of oxygen proceed in parallel at the electrode. To unravel the complexity, the influence of CYP inhibitors is a useful diagnostic criterion. In most cases biosensors based on CYP can catalyze a variety of substrates, as has been described above. In recent years a great deal of interest and effort has been invested in the use of protein engineering. This implies the introduction of specific attachment regions and electron transfer regions to overcome the kinetic limitations. Furthermore, engineering of the protein surface could provide means of immobilising the protein directly on the electrode, thus shortening the distance between the redox centre and the electrode and achieving faster electron transfer. Recent work indicates the potential of engineering sites for surface binding and redox active dyes [39, 40].

Nature offers almost unique biocatalysis of the Cytochrome *P*450 family exhibiting almost absolute specificity for recognising a given substrate in mixtures of very similar compounds like steroid hormones, and conversion of highly different compounds following the same reaction type, e.g., demethylation of various drugs. Using genetic engineering, both recognition types may be optimised for the analytical system under investigation. In this respect, arrays carrying different CYP isoforms will eventually be developed for characterising the metabolism of drug converting organs, like the liver, of different species. Full interaction of specific substrate conversion and a deeper understanding of electrochemical investigations can be expected in the next generation of research in this fascinating area.

1.13 Aims of the project

The direct electrochemistry of cytochrome *P*450 has been reported in published articles over many years but has never been conclusively demonstrated. The main objective of this project was to attempt to investigate further the proposed mechanisms seen in surface bound *P*450 proteins and to attempt to identify further experiments that are required before the statement “direct electrochemistry of cytochrome *P*450 has been

achieved" can be reported with some validity. The biggest question here is "is the *P*450 functioning as an active enzyme on or at the electrode?"

To date, in the published work, the possibility that the observed electrochemical response is due to such things as displaced haem, denatured protein or that measured catalysis is due to hydrogen peroxide formed following the electrochemical reduction of dioxygen (the so-called peroxide shunt mechanism) has not been addressed fully. This mechanism bypasses the need for the external co factor NADPH, bypasses the requirement for the electron transfer reductase proteins and the requirement for oxygen [41, 42.] In this mechanism hydrogen peroxide oxidises Fe3+ directly to the high valent oxyferryl form. Therefore, in an electrochemical experiment it maybe possible that hydrogen peroxide formed at the electrode surface via dioxygen reduction would react chemically to drive some turnovers. The drawback of the peroxide shunt mechanism is that the presence of peroxide eventually "poisons" the enzyme so that the usefulness is limited. However, very recent work has investigated the possible effects of protein denaturation and the likelihood of observation of displaced iron electrochemistry only being observed in *P*450 experiments [43.]

When substrates bind to *P*450s a large positive shift in what is referred to in the electrochemical literature as the formal potential and in the biological literature as the midpoint potential, is reported to occur. These potentials are the redox potentials in the prevailing medium. Measurements of the redox potentials of *P*450s that are reported in the literature are generally made under anaearobic conditions because the experimental methods used to determine the redox potential typically requires the exclusion of dioxygen. The exclusion of dioxygen from the redox potential measurement produces a measurement in an experimental medium that is unrelated to the prevailing medium during real life enzyme catalysis which would take place an aerobic medium [44].

Electrochemical enzyme studies are typically performed to determine fundamental parameters, such as the redox potential of the enzyme, or to study the electron transfer

between the enzyme and various electrodes, either directly or through the use of mediators [45]. In addition to fundamental studies, electrochemical studies of *P*450s are of great interest due to the possibility of developing applications such as biosensors for analyte detection.

The electrochemical behaviour of enzymes is more complicated than that of smaller molecules which have traditionally been the subject of studies by electrochemists. The most important complication is the possibility of conformational changes occurring within the enzyme during the measurement process.
The important question to ask here is how do we know that an electrochemical response is due to the functioning enzyme and not some altered conformation of the enzyme in which its activity is reduced or eliminated altogether?
As discussed earlier, many different methods of immobilising these enzymes onto an electrode surface or adsorbed into a film or matrix have been reported but we have no way of knowing, based on published electrochemical experiments, what conformational form *P*450 takes on when in contact with these materials.

Spectroscopic characterisation of the enzyme in a film on, say a glass slide, does not tell us what happens to the enzyme when it comes into contact with the electrode surface. Such experiments do however provide valuable information about the stability of the enzyme within various films and coatings but do not reveal the structure/activity relationship of the enzyme.

It is common in reported work on *P*450 enzymes to use non natural substrates. Thus it is also important to remember that ultimately non-natural substrates may be of more interest, particularly when considering the use of *P*450s for biosensors and biocatalysts, however it would be useful to demonstrate the enzyme functionality with the natural substrate as many non-specific catalytic reactions can also be performed by hemin and haem containing proteins such as myoglobin.

It is vital to remember that in using enzymes immobilised on an electrode we are presumably endeavouring to electrochemically drive a specific catalytic reaction. Thus we are not endeavouring to demonstrate catalysis per se but very specific catalysis of the type that only enzymes generally perform.

1.14 Chapter Summary

In this chapter the origins of electrochemical investigations of biological molecules and numerous model metalloprotein systems were considered. The early experimental investigations and the various electrochemical methods employed to probe the enzymes' activity were reviewed, also the aims of the project were introduced. Next, experimental electrochemical methods and their theory will be considered along with the complex *P*450 protein mechanisms.

1.15 References

1. Kandel E.R., Schwartz, J.H., Jessell, T.M. **2000**. *Principles of Neural Science, 4th ed* pp 6. McGraw-Hill, New York, USA.

2. Garrett, R.H. & Grisham, C.M. *Biochemistry.* **1998** Thompsom Learning, UK

3. W. Nernst. Ueber die Berechnung chemischer Gleichgewichte aus thermischen Messungen. Nachr. Kgl. Ges. Wiss. Gött., **1906**,1, pp. 1 - 40

4. Heyrovský J*, Critical Reviews in Analytical Chemistry* **2001**, 31(4) pp. 2 – 10.

5. Athel Cornish-Bowden, *Fundamentals of Enzyme Kinetics*. **2004** 4th Ed.Portland Press, USA.

6. Gregory P and Dagmar R. **2003.** *Protein Structure and Function*. Blackwell Publishing, UK.

7. Frausto Da Silva and Williams. **2001.** *The Biological Chemistry of the Elements*: The *Inorganic Chemistry of Life.* Oxford University Press, UK.

8. Alberts B. **2001** *Molecular Biology of the Cell*. Garland Science, UK

9. Rang H.P, Dale M, Ritter J. **2003.** *Pharmacology.* Churchill Livingstone, UK.

10. Lewis, D.F.V. **2001**. *Cytochromes P450. Structure and Function.* Taylor and Francis, London, UK.

11.Hayaishi O and Nozaki M, **1969** *Science.* 164 (2) pp 389-96

12. Hayaishi O, **1964** *Proc.Plen.Session*, 6th Int.Cong.Biochem. New York, p.31.

13. Garfinkel D, **1958** *Arch.Biochem.Biophys*. 77: pp493-509

14. Ingelman-Sundberg M, Oscarson M, Daly A, Garte S and Nebert D, **2001.** *Cancer Epidemiology Biomarkers & Prevention.* 10, pp1307-1308

15. Feyereisen, R. **1999**. *Insect P450 enzymes*. 44: pp507 – 533.

16. Ortiz de Montellano **1995**. *Cytochrome P450. Structure, Mechanism and Biochemistry.* Kulwer Academic, USA

17. Friedrich J, Ebner R, Kunz-Schughart L. **1989** *Scandinavian journal of gastroenterology*. 24 (9) pp. 1107-1112

18. Ingelman-Sundberg **1999**. *Trends in Pharm Sci* 12 (2) pp342 -350.

19. Cupp MJ and Tracy TS. **1998** *Amer Fam Phys* 57 (1) pp107-116

20. Chang G W and Kam T. **1999.** *Trends in Pharm Sci* 60 (9) pp380-384

21. Bailey C and Markwell J, **2006.** *Biochemistry and Molecular Biology Education.* 34, (2), pp. 66-74,

22. Williams, P.A., Cosme, J., Sridhar, V. and Johnson, E.F. J. **2000** *Inorg.Biochem*. 31. pp183-190

23. Horecker BL. **1950**, *J Biol Chem***,** 183. pp593-605

24. Vermilion JL, Coon MJ. **1978** *J Biol Chem* 253(24) pp 8812-9.

25. Kazlauskaite, J., Westlake, A.C.G., Wong, L.L. and Hill, H.A.O. *Chem. Comm.* **1996**, 18, pp 2189-2190.

26. Eddowes, M.J. and Hill, H.A.O. **1977** *J.Chem. Soc Chem. Commun.*, 771 pp10 - 15

27. Fleming B.D **2003** *Eur. J. Biochem.* 270, pp 4082-4088

28. Sharrock, M., Muenck, P.G., Debrunner, V., Marshall, J.D., Lipscombe, J.D. & Gunsalus, I.C. **1973**, *Biochemistry,* 12, 258 pp 254 - 259

29. Kondo, F., Zinsou, A., Bernhardt, P.V., De Voss, J. & Slessor, **2003** K.E. *Chem Chom*, pp 418-419.

30. Fantuzzi, A., Fairhead, M and Gilard, G. *JACS*, **2004**, 5040-5041.

31. Bistolasa N, Wollenbergera U, Jungb C and Schellera F. **2005** *Biosensors and Bioelectronics* . 20 (12) pp 2408-2423

32. Bistolasa N and Jungb C **2006** *Biosensors and Bioelectronics* .18 (1) pp 1998 - 1003

33. Lo Conte L, Chothia C and Janin J, **1999** *Journal of Molecular Biology* . 285 (5) pp 2177-2198.

34. Zhang, Z., Nassar, A.F., Zhonqging, L., Schenkman, J.B, & Rusling, J.F. *Faraday Transactions*, **1997**, 93 pp1769-1774

35. Lvov,Y.M., Lu,Z., Schenkman,J.B., Zu,X. and Rusling,J.F. **1998** *J. Am. Chem. Soc.*, 120, pp 4073–4080

36. Huang Y, Okochi H, May, Legname B, Prusiner S, Benet L, Guglielmo J, and Lin E, **2004,** *Clinical Pharmacology*, 435 (12) pp 278 - 282

37. Degani Y and Heller A **1987** *J. Phys. Chem: 91*(6) pp1285-1289.

38. Shumyantseva V, Bulko T, Bachmann T, Bilitewski B, Schmid R and Archakov A, **2000** *Arch Biochem Biophys* **,** 377 pp 43-48

39. Wong S and Arnold **2004,** *Biotechnology and Bioengineering*. 85 (3) pp 351-358.

40. Johnson D, Conley C and Martin L **2003.** *Journal of Molecular Endocrinology* 36**,** pp349-359

41. Denisov I, Makris T, Sligar S, and Schlichting I, **2005** *Chem. Rev*. 105 pp2253.

42 Ortiz de Montellano, **1995** *Cytochrome P450 Structure, Mechanism, and Biochemistry,* Plenum Press, New York, USA

43. Milsom E, Dash H, Jenkins A, Opallo M, Thetford A, Bligh N, Nogalab W and Marken F.**2007** *Journal of Electroanalytical Chemistry*. (Accepted April 2007)

44. Garrett, R.H. & Grisham, C.M. *Biochemistry.* **1998** Thompsom Learning, UK

45. Armstrong F and Wilson G, **2000** *Electrochim. Acta*, 45 pp 2623.

2 Theory of Electrochemical Techniques and Cytochrome *P*450 mechanisms.

2.1. Interfacial electrochemistry.

2.1.1. Mass transport Mechanisms.

2.1.2. Diffusion Currents

2.2 The Nernst Equation

2.3 The three electrode cell.

2.3.1. Reference Electrodes.

2.4 The Electrical Double Layer.

2.5 Cyclic Voltammetry (CV).

2.6. Differential Pulse Voltammetry (DPV).

2.7 Current decay due to capacitive charging.

2.8. Chronoamperometry (CA) and the Cottrell Equation.

2.9 Surface adsorbed species.

2.10 Interactions between protein and surface.

2.10.1 Van der Waals forces.

2.11 Physisorption and Chemisorption.

2.12 The Langmuir Isotherm.

2.13. Protein electrochemistry and Cytochrome *P*450 enzyme mechanisms.

2.13.1. Haem spin state of Cytochrome *P*450 proteins.

2.13.2. The Cytochrome *P*450 catalytic cycle.

2.14. Cytochrome *P*450 Protein Model Systems.

2.14.1. Class I Bacterial *P*450 proteins from Pseudomonas Putida.
(*P*450cam, Cyp101).

2.14.2. Class II Microsomal *P*450 proteins from Drosophila melanogaster (Cyp6g1).

2.14.3. *P*450 substrates and their associated activities.

2.14.4. Nicotinamide Adenine Dinucleotide (NADPH) as an indicator for *P*450cam activity.

2.14.5. Resorufin Methyl Ether (MRES) as an indicator for the detection of microsomal *P*450 activity.

2.14.6. Inhibition of Cytochrome *P*450 enzyme activity.

2.14.7. Chapter Summary.

2.14.8. References.

2.1 Interfacial electrochemistry

In interfacial electrochemistry it is important to appreciate the difference between the bulk and the surface. Reactants are often at very different concentrations in these two regions. It is frequently this concentration difference that drives the transfer of molecules from the bulk to the surface.

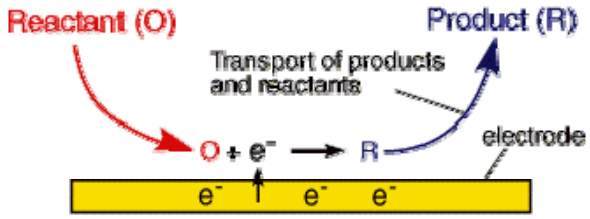

Figure 10.Schematic interpretation of the transfer of products at an electrode surface.

Reactant (O) has to be transported to the surface from the bulk, in order that it might react for a current to flow, shown in Figure 10. The product (R) then needs to be transported back into the bulk. (Adapted from *Electrode Dynamics*, A Fisher 1996)

2.1.1 Mass transport Mechanisms

There are essentially three mechanisms for transporting molecules through space.

1. Diffusion is the movement of molecules along a concentration gradient, from an area of high concentration to an area of low concentration.

2. Migration is the transport of a charged species under the influence of an electric field.

3. Convection is the transport of species by hydrodynamic transport (e.g. natural thermal motion and stirring).

Generally, in most electrochemical experiments, a background electrolyte of a salt that does not participate directly in the reaction is present. This is typically one or two orders of magnitude higher in concentration than the reactive species and is used to remove the effects of migration in experiments. Therefore, normally only the effects of diffusion and convection need to be considered. If a system is changed quickly (i.e. a potential step is applied to an electrode), then diffusion becomes the principal mechanism of mass transport, provided the solution is not externally stirred or agitated.

2.1.2 Diffusion Currents

One of the most simple and useful ways of understanding the time dependent effects of current flow through an electrode is the concept of the diffusion layer introduced by Walter Nernst in 1904 [1]. When an electrode is polarised, the surface concentration of the species that is either being oxidised or reduced falls to zero. Additional material will then diffuse to the electrode surface towards this region of lower concentration.

2.2 The Nernst Equation

The Nernst equation relates the concentrations of ions taking part in an electrochemical reaction at equilibrium with the potential that the electrode takes up relative to the standard electrode potential of the system.

$$E = E^{o} - \frac{RT}{nF} \ln \frac{^{a}Ox}{^{a}\mathrm{Re}\,d} \qquad \textbf{Equation 1}$$

The Nernst Equation. In electrochemistry, the Nernst equation gives the electrode potential (E), relative to the standard electrode potential, (E0), of the electrode couple.

Where:

- R is the universal gas constant, equal to 8.314510 J K^{-1} mol^{-1}

- T is the temperature in kelvin (kelvin = 273.15 + °C.)
- a the chemical activities on the reduced and oxidized side, respectively
- F is the Faraday constant (the charge per a mole of electrons), equal to $9.6485309*10^4$ C mol^{-1}
- n is the number of electrons transferred in the half-reaction.
- $[^aRed]$ is the concentration of oxidizing agent (the reduced species).
- $[^aOx]$ is the concentration of reducing agent (the oxidized species).
- $E^{0'}$ is the formal electrode potential

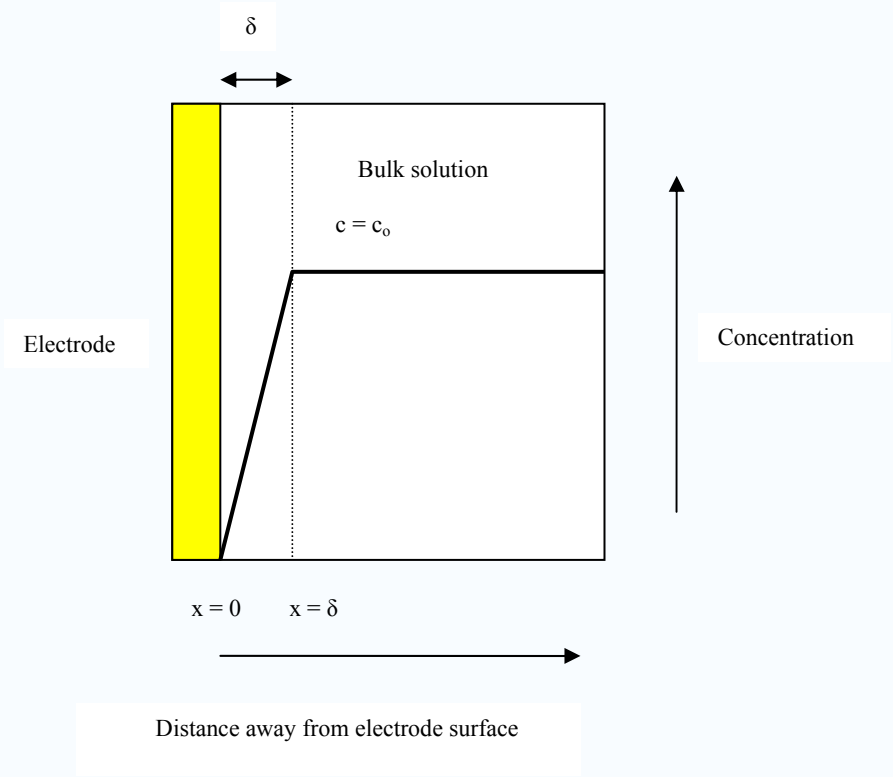

Figure 11. A simple schematic model of the Nernst diffusion layer showing the linear variation in concentration.

The electrode is represented by the yellow bar on the left in Figure 11. The x-axis represents distance away from the electrode. The point of origin (x = 0) represents the surface of the electrode and the y-axis represents concentration. The maximum concentration is represented by c_o which is the concentration of the analyte in the bulk solution.

There are two regions of concentration to consider. Because the solution is well mixed, in the bulk region the concentration is constant with respect to distance. This is represented by the horizontal line known as the convective region. There is then a region where the concentration drops, falling to zero at the electrode surface. This region, known as the Nernst diffusion layer, has thickness δ. The exact thickness of the Nernst diffusion layer depends upon the nature of the solution into which it extends. An important assumption of this model is that when material reaches the surface of the electrode it is instantaneously oxidised or reduced thereby maintaining a zero concentration at the electrode surface. In practice, this can be achieved by selecting a suitable polarising voltage.

In summary, the Nernst diffusion layer theory tells us that there is a stationary thin layer of solution in contact with the electrode surface which has a thickness equal to δ. Within this layer, diffusion alone controls the transfer of analyte to the electrode. This occurs down a concentration gradient. Outside this layer, diffusion is negligible and the concentration of analyte is maintained at a value of c_o by convective transfer. Because of the heterogeneous nature of the electrochemical process, the reaction depends upon both the rate of electron transfer at the interface and on the mass transport of analyte to the electrode from the bulk solution. An electrochemical experiment therefore should be designed so that the mode of transport of the electroactive species to the electrode surface is well defined. The most important mass transport processes in electrochemical measurements are diffusion and convection.

In diffusion, the driving force is a concentration or activity gradient. The movement is from a region of high concentration to one of low concentration.
Before the initiation of the electrolysis, the concentration of the reactant is uniform throughout the solution. (It can be assumed that at the start of the experiment, the solution has been well mixed and is completely homogeneous). When current flows, the concentration of the reactant at the electrode surface becomes less than in the bulk solution due to the electrochemical conversion of reactant into product. In a quiet solution diffusion is the only mode of transport so the flux of reactant to the electrode surface at a given time and distance from the electrode surface is proportional to the

steepness of the concentration gradient. The flux of reactant is therefore given by Fick's first law of diffusion:

$$J = -D\frac{\partial \phi}{\partial x}$$ **Equation 2**

Ficks first law. Fick's first law is used in steady state diffusion when the concentration within the diffusion volume does not change with respect to time

Where

J is the diffusion flux in dimensions of [(amount of substance) length^{-2} time^{-1}], [mol m^{-2} s^{-1}]

D is the diffusion coefficient or diffusivity in dimensions of [length^2 time^{-1}], [m^2 s^{-1}].

ϕ is the concentration in dimensions of [(amount of substance) length^{-3}], [mol m^{-3}]

x is the position [length], [m]

D is proportional to the velocity of the diffusing particles, which depends on the temperature, viscosity of the fluid and the size of the particles according to the Stokes-Einstein relation. For the biological molecules the diffusion coefficients normally range from 10^{-11} to 10^{-10} [m^2 s^{-1}].

$$\frac{\partial \phi}{\partial t} = D\frac{\partial^2 \phi}{\partial x^2}$$ **Equation 3**

Fick's second law. Fick's second law is used in non-steady or continually changing state diffusion, i.e., when the concentration within the diffusion volume changes with respect to time.

Where

ϕ is the concentration in dimensions of [(amount of substance) length^{-3}], [mol m^{-3}]

t is time [s]

D is the diffusion coefficient in dimensions of [length^2 time^{-1}], [m^2 s^{-1}]

x is the position [length], [m]

2.3 The three electrode cell

In dynamic electrochemistry, the three electrode cell is one of the most common configurations used to study electrochemical reactions. The cell consists of a counter electrode (CE) which is used to polarise the electrode of interest: the working electrode. In order that the potential (voltage) on the working electrode is precisely known, a third electrode, the reference electrode (RE), is held close to the surface of the working electrode (WE) and the potential difference measured. This is because the RE has no current passing through it, but maintains an invariant constant potential regardless of what is happening around it.

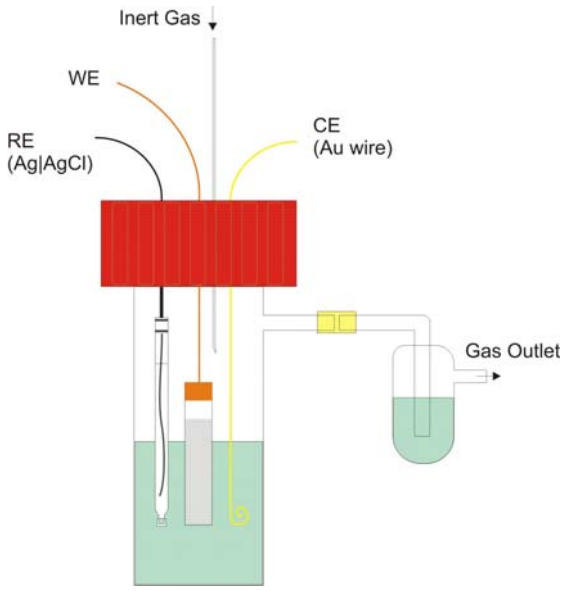

Figure 12. Interpretation of the three electrode cell. RE = reference electrode, WE = working electrode, CE = counter electrode.

A potentiostat, shown in Figure 12, is used to supply a constant potential or current to the WE, regardless of the chemical changes taking place on the WE at that time. It is

like a feedback circuit, constantly ensuring the potential or current is maintained to that which the operator has set.

2.3.1 Reference Electrodes

All electrode potentials are measured vs. the standard hydrogen electrode (SHE). This electrode couple is arbitrarily defined as 0.00 Volts [2]. However, in reality using this electrode is not at all practical. It requires a steady flow of hydrogen bubbling onto a high surface area of platinum. It is much easier is to use an electrode couple that has a clearly defined potential relative to the SHE.

A commonly employed system is the Silver/Silver Chloride (Ag / AgCl) electrode. The potential of this system is determined by the concentration of Cl^- ions in the solution measured according to the Nernst equation. By measuring relative to this electrode one can determine the potential, relative to the SHE. In electrochemical experiments, voltages must always be given relative to a known reference electrode.

2.4 The Electrical Double Layer

The earliest model of the electrical double layer is usually attributed to Helmholtz in 1879 [2]. Helmholtz treated the double layer mathematically as a simple capacitor, based on a physical model in which a single layer of ions adsorbed at a surface.

Later Gouy and Chapman (1910-1913) made significant improvements by introducing a diffuse model of the electrical double layer, in which the potential at a surface decreases exponentially due to adsorbed counter-ions from the solution [3].

The current classical electrical double layer is the Gouy-Chapman-Stern model, which combines the Helmholtz single adsorbed layer with the Gouy-Chapman diffuse layer. The nature of the electrode interface is fundamentally important in electrochemistry, since this is where electron transfer takes place and is therefore the region where molecules have to move in order to be oxidised or reduced. The nature of the electrode interface has been intensely debated; however the Helmholtz model is currently the most popular [2].

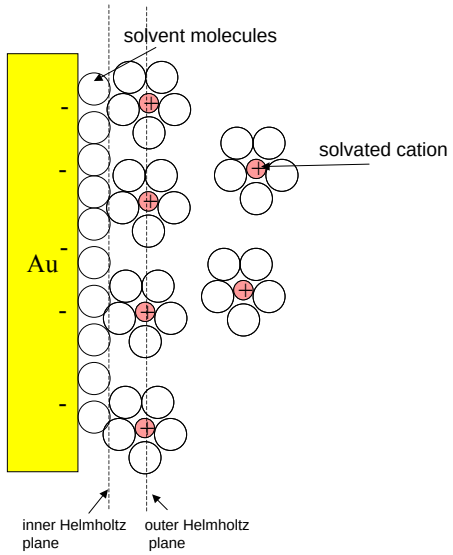

Figure 13. Schematic interpretation of the 'diffuse double layer model' at the electrode interface (adapted from Bard & Faulkner, *Electrochemical methods* 2nd Ed.)

The concept of the double layer, shown in Figure 13, is such that when an electrode is polarised by the application of potential, ions of opposing charge will assemble at the electrode surface. This is also true of surfaces that are not formally polarised since most metal interfaces have an excess of electrons at the surface, producing a slightly negative net charge.

The important points to note from this model are that it is the double layer region where the potential difference between the electrode surface and the bulk electrode change the most. However, since there are two layers of charge, electrons in the metal and cations at the outer Helmholtz plane which are separated by a dielectric, the interface can be modelled as a capacitor.

Capacitors are simply two charged interfaces separated by an insulator.

The charge, q, which can be stored on a capacitor, depends on the *capacity* C, of the capacitor and the potential difference between the charged interfaces, E. The relationship is simply:

$$q = CE$$ **Equation 4**

Where

q is charge

C is capacitance

E is potential difference

The capacitance depends on the overlap area A, between the charged interfaces, the distance d, and the dielectric permittivity or dielectric constant of the dielectric material, ε_τ

$$C = \frac{\varepsilon_0 \varepsilon_\tau A}{d}$$ **Equation 5**

Where

ε_o is the permittivity of free space which is a constant: $8.854 \text{ x } 10^{-12} \text{ C}^2 \text{ N}^{-1} \text{ m}^{-2}$.

As charge can be stored on a capacitor, a current must flow when a potential difference is applied.

Since by definition:

$$i = \frac{dq}{dt}$$ **Equation 6**

Where:

i is current

q is charge

t is time

So the current that flows when a capacitor is charged is:

$$i = C\frac{dE}{dt} \qquad \textbf{Equation 7}$$

Where

$\frac{dE}{dt}$ is the sweep rate in say a cyclic voltammetry experiment.

It is now possible to model the electrode interface as a capacitor and demonstrate that a polarised electrode in an experiment provides the capacitive charging component of the total measured current together with the Faradaic current which results from oxidation or reduction of an electroactive species:

$$i_{total} = i_{Faradaic} + i_{capacitative} \qquad \textbf{Equation 8}$$

So the capacitive charging current is frequently termed the *double layer* charging current.

2.5 Cyclic Voltammetry (CV)

A simple potential waveform that is often used in electrochemistry is the linear waveform, that is, the potential is continuously changed as a linear function of time, shown in Figure 14. The rate of change of potential with time is referred to as the scan rate (v).

The simplest technique that uses this waveform is linear sweep voltammetry. The potential range is scanned in one direction, starting at the initial potential and finishing at the final potential. A more commonly used variation of the technique is cyclic voltammetry, in which the direction of the potential is reversed at the end of the first scan. Thus, the waveform is usually of the form of an isosceles triangle. This has the

advantage that the product of the electron transfer reaction that occurred in the forward scan can be probed again in the reverse scan. In addition, it is a powerful tool for the determination of formal redox potentials: detection of chemical reactions that precede or follow the electrochemical reaction and evaluation of electron transfer kinetics.

An example waveform that can be used in cyclic voltammetry is shown below: In this example it is assumed that only the reduced form of the species is initially present. Thus, a positive potential scan is chosen for the first half cycle during which an anodic current is observed. The product generated during the forward scan is available at the surface of the electrode for the reverse scan resulting in a cathodic current.

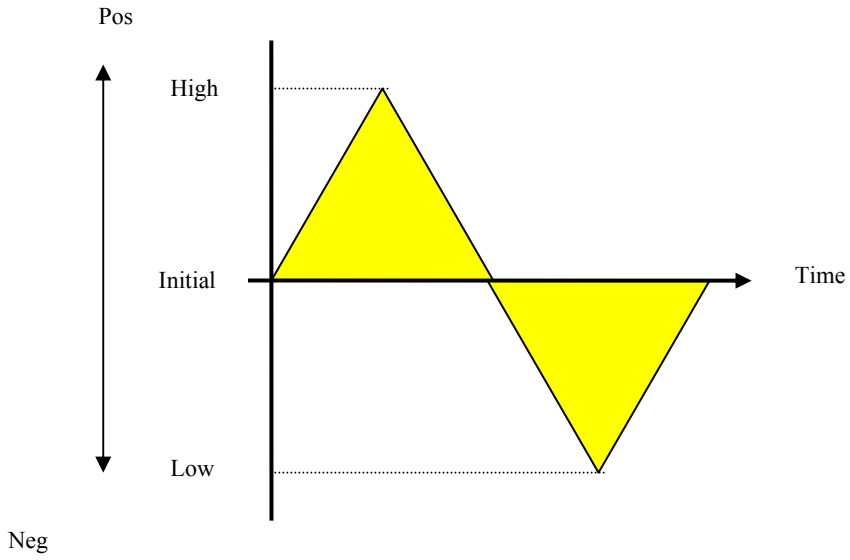

Figure 14. A simple schematic model of the complex waveform composed of two equilateral triangles.

As the voltage is scanned in the positive direction, so the reduced compound is oxidised at the electrode surface. At a particular set value, the scan direction is reversed and the material that was oxidised in the outward excursion is then reduced. Once the voltage is returned to the initial value, the experiment can be terminated. In this example

however, a further voltage excursion takes place to more negative or more reducing values. This may be useful in probing for other species present in the sample or for investigating any electroactive products formed as a result of the first voltage excursion.

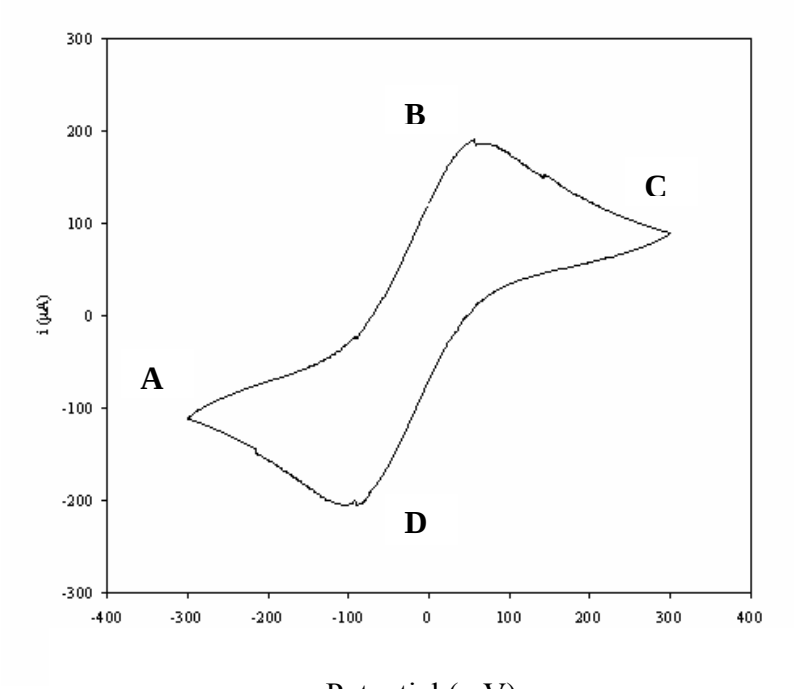

Figure 15. A simple schematic model of the basic shape of the current response for a cyclic voltammetry experiment (Adapted from *Electrode Dynamics*, A Fisher 1996)

At the start of the experiment, shown in Figure 15, the bulk solution contains only the reduced form of the redox couple so that at potentials lower than the redox potential there is no net conversion of R into O, the oxidised form (point A). As the redox potential is approached, there is a net anodic current which increases exponentially with potential. As R is converted into O, concentration gradients are set up for both R and O, and diffusion occurs down these concentration gradients. At the anodic peak (point B), the redox potential is sufficiently positive that any R that reaches the electrode

surface is instantaneously oxidised to O. Therefore, the current now depends upon the rate of mass transfer to the electrode surface.

Upon reversal of the scan (point C), the current continues to decay until the potential nears the redox potential. At this point, a net reduction of O to R occurs which causes a cathodic current, which eventually produces a peak shaped response (point D). If a redox system remains in equilibrium throughout the potential scan, the electrochemical reaction is said to be reversible. In other words, equilibrium requires that the surface concentrations of O and R be maintained at the values defined by the Nernst Equation.

The response observed during a voltammetry experiment depends strongly on the rate that material approaches the electrode surface.

The concentration of electroactive species present in a solution also plays a major role in determining the response observed in a voltammetric experiment

2.6 Differential Pulse Voltammetry (DPV)

The basis of all pulse techniques is the difference in the rate of the decay of the charging and the Faradaic currents following a potential step pulse. The charging current decays exponentially, whereas the Faradaic current (for a diffusion-controlled current) decays as a function of $1/(\text{time})^{½}$ [34], that is, the rate of decay of the charging current is considerably faster than the decay of the Faradaic current. Therefore, after this time, the measured current consists solely of the Faradaic current. So measuring the current at the end of a potential pulse allows discrimination between the Faradaic and charging currents.

The parameters to be considered for pulse techniques are:

Pulse amplitude. The height of the potential pulse.

Pulse width. The duration of the potential pulse.

Sample period. The time at the end of the pulse during which the current is measured.

The potential waveform for differential pulse voltammetry is shown in Figure 16. The potential waveform consists of small pulses (of constant amplitude) superimposed upon a staircase waveform. The current is sampled twice in each Pulse Period (once before the pulse, and at the end of the pulse), and the difference between these two current values is recorded and displayed.

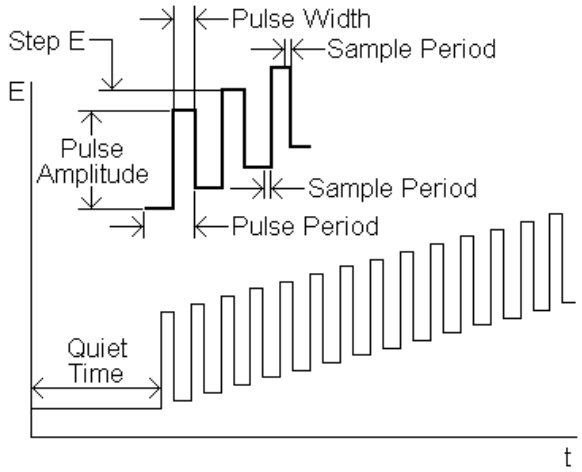

Figure 16. Schematic interpretation of a potential waveform for differential pulse voltammetry. (Adapted from Bard & Faulkner, *Electrochemical methods* 2nd Ed.)

2.7 Current decay due to capacitive charging.

The charging current is also part of the total measured current which decays with time. If the solution/electrode interface is modelled as a solution resistance (R_s) in series with a double layer capacitor (C_{dl}), then the potential difference across the double layer can be resolved as having two components as shown below.

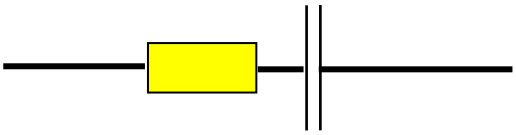

Rs **Cdl**

Figure 17.A basic schematic model of a resistor and double layer capacitor in parallel.

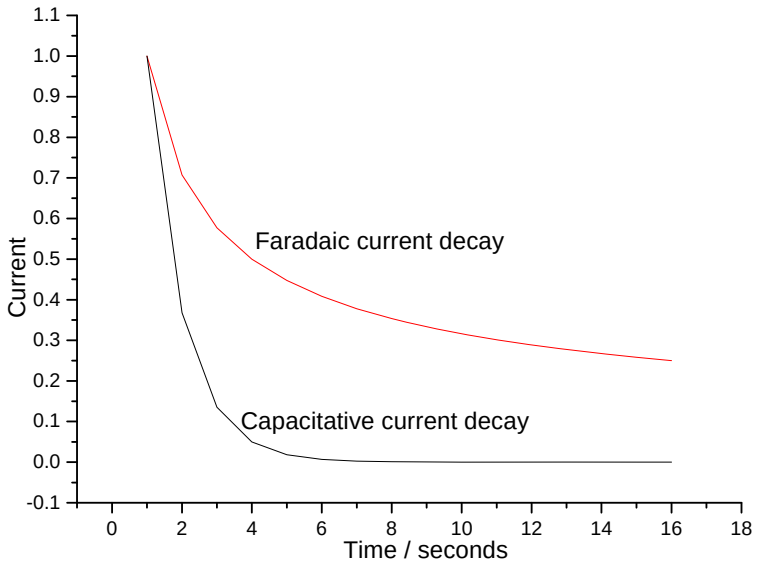

Figure 18. **Voltammogram illustrating Faradaic and capacitative current decay over time.**

The charging current is largely dependent on the concentration of the electroactive species one is trying to measure. The Faradaic current is directly proportional to the concentration of that electroactive species shown in Figure 18.

This leads to potential difficulties if the electrode surface is rough or if the electroactive species is low.

In the case of a rough electrode, the real surface area will be very high, but the diffusion layer (which relates to the rate at which species diffuse to the surface) will be much lower, since the diffusion is some distance from the electrode surface. Hence the capacitance will be very high, as will be the capacitive charging current.
In the case of low concentration of electroactive species, the Faradaic current will be very low. In both cases, the capacitive current may 'swamp' the signal of interest, or distort the measured values, leading to inaccuracies in measurements or no measurement at all.
In a typical cyclic voltammetry experiment, it can be imagined that the linear voltage one applies with respect to time, is actually a staircase shape (this is in fact true for most modern digital potentiostats). The result is that electrode charging can be problematic.
This can be overcome by applying a potential step, waiting a few seconds and then measuring the current. By waiting a few seconds (generally milliseconds in practise), the capacitive charging current will have decayed, but the Faradaic current will still be significant. In addition, the differential current, that is the difference in current before the pulse and at some time after the pulse, can also be measured.

2.8 Chronoamperometry (CA) and the Cottrell Equation

Chronoamperometry is used to study diffusion-controlled electrochemical reactions and complex electrochemical mechanisms. It is performed by applying an initial potential at which no faradaic reaction is occurring, then stepping the potential to a value at which the electrochemical reaction of interest takes place. The solution is generally unstirred and the current is measured throughout the experiment.
Immediately following the step, a large current is detected which falls steadily with time, shown in Figure 19. This arises since the magnitude of the current is controlled by the rate of diffusion of electroactive species to the electrode. The concentration gradients shortly after the step are extremely large since there has been little time for any depletion of the electroactive material to occur. Consequently, the currents flowing

are initially large. Gradually, as depletion occurs, the diffusion layer thickness increases and the current decreases. The Cottrell Equation describes the current response as a function of time.

CA uses the potential wave form, the potential step, which is one of the simplest potential wave forms. As shown below, the potential is changed instantaneously from the Initial Potential to the First Step Potential, and it is held at this value for the First Step Time. This is a single potential step experiment. In a double potential step experiment, the potential is changed to the Second Step Potential after the First Step Time, and it is then held at this value for the Second Step Time. In CA, the current is monitored as a function of time. It is important to note that the basic potential step experiment on the epsilon is CA; that is, during the experiment, the current is recorded as a function of time. However, after the experiment, the data can also be displayed as charge as a function of time (the charge is calculated by integrating the current).

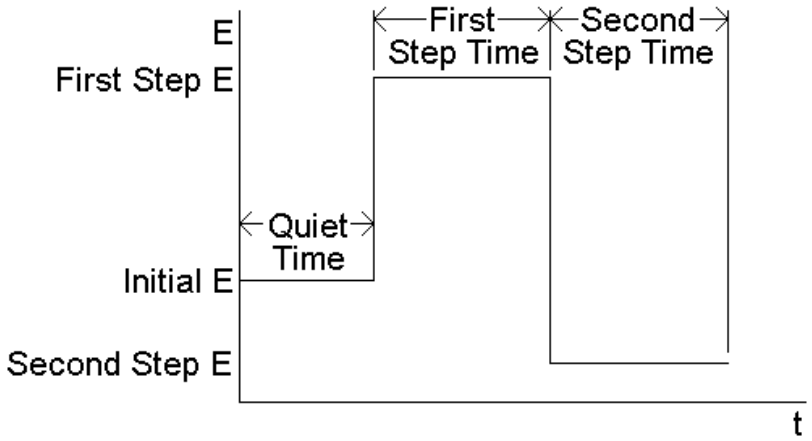

Figure 19. Potential wave form for chronoamperometry. (Adapted from Bard & Faulkner, *Electrochemical methods* 2nd Ed.)

The analysis of chronoamperometry (**CA**) data is based on the Cottrell equation, which defines the current-time dependence for linear diffusion control:

$$i = nFACD^{1/2} p^{-1/2} t^{-1/2} \qquad \textbf{2.8.1}$$

The Cottrell Equation

Where

n = number of electrons transferred/molecule

F = Faraday's constant (96,500 C mol^{-1})

A = electrode area (cm^2)

C = concentration (mol cm^{-3})

D = diffusion coefficient (cm^2 s^{-1})

P = Pi (3.14)

t = time

This indicates that, under these conditions, there is a linear relationship between the current and the inverse square root of time. A plot of i vs. $t^{-1/2}$ is often referred to as the Cottrell plot. Although the current decay may appear to be exponential (in the case of adsorbed redox species), it actually decays as the reciprocal of the square root of time. This dependence on the square root of time reflects the fact that physical diffusion is responsible for transport of the analyte to the electrode surface.

2.9 Surface adsorbed species

The voltammetric behaviour of a molecule adsorbed uniformly on the electrode surface must also be considered here. If the species is capable of undergoing a reversible one electron transfer, the resulting voltammogram will display a two-peak relationship as shown in Figure 20. On the forward scan, a peak is seen which corresponds to the reduction of adsorbed species A to from B, which remains adsorbed on the surface. On the return scan, a current is observed which indicates the reverse, where B is

reconverted to adsorbed A. When compared to a solution phase one-electron transfer voltammogram, several differences become apparent.

Firstly, both forward and reverse peaks are symmetrical and the observed current returns to zero. Also, an absence of current at potentials greater than the reduction potential of A is observed, due to the limited amount of A adsorbed onto the surface. Once this limited amount of A has been converted to B no further electron transfer can take place. When compared to the solution phase reaction: reactant is continually transported to the electrode by diffusion from the bulk, the observed symmetry of the peaks occurs since the electrode reaction is controlled by a one electron transfer mechanism and not by a coupled mechanism of diffusion and electron transfer. This also explains why the maxima of the forward and reverse peaks coincide. The areas of each peak will be identical and can provide a direct measure of the amount of charge required to drive the reaction, which in turn will indicate the amount of species adsorbed onto the surface. However, these reactions and resulting voltammograms may occur in ideal behaviour but deviation will occur if, for example, the surface adsorbed species is not charge stable or if it becomes desorbed from the surface during the experiment. If a reduction in the height of the reverse peak is observed, it is likely that the species is desorbing slowly. More importantly here, deviations from the model voltammetric behaviour can then be used to probe the stability and nature of the surface/species bond and provide some insight into the electrochemical behaviour of the molecule under investigation.

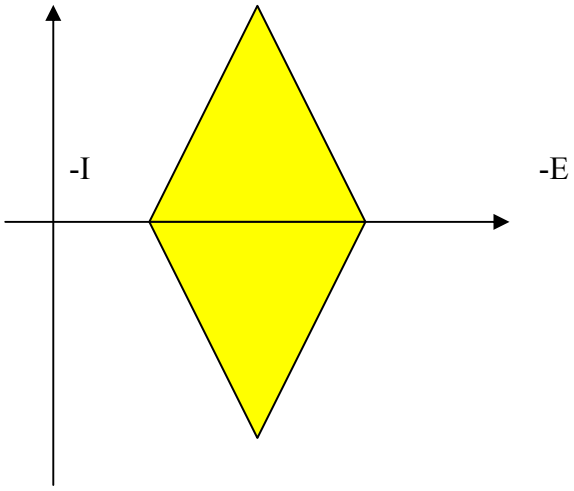

Figure 20. A simple schematic model of a Cyclic voltammogram from a surface adsorbed species (Adapted from *Electrode Dynamics*, A Fisher 1996)

2.10 Interactions between protein and surface.

The apparent activity of an enzyme can be reduced after immobilisation and this in turn may be due to several factors. Firstly, the chosen immobilisation chemistry may not be optimal and may lead to modification of the active site. Even when the immobilisation does not interfere with the active site, the nature of the support may produce diffusional barriers. Also, the very act of immobilisation may lead to unfavourable conformational changes in the protein or reduce the conformational mobility of the enzyme. Although the immobilisation matrix is often seen as solely a support for the enzyme, it may nevertheless introduce partitioning effects. A positively charged matrix for example will exclude protons so an enzyme in this matrix will exhibit a lower optimal pH than usual.

2.10.1 Van der waals forces

These bonds exist between non-polar molecules or atoms. They are the weakest of all the intermolecular forces.On average the negative charge of the electrons in an atom or molecule is spread evenly. For brief periods of time the electrons are concentrated on one side of the atom or molecule more than the other. This gives the atom or molecule

a temporary partial negative charge - a temporary dipole moment. This dipole moment will induce a temporary dipole in a neighbouring atom by attracting/repelling its electron charge cloud. A fraction of a second later the electron distribution changes causing and the temporary dipole-dipole attraction (Van der Waals attraction) to break. This means that the attraction is weak compared to hydrogen bonding or dipole-dipole attractions. As the size of the atoms or molecules increases there are more electrons so the temporary partial charge is bigger resulting in stronger attraction.

These forces, although transient and weak, can provide an important component of protein structure due to their large numbers. Most atoms of a protein are packed sufficiently close to others to be involved in transient Van der Waals attractions.

2.11 Physisorption and Chemisorption

Molecules and atoms can attach to surfaces in two ways. In physisorption, there is a Van der Waals interaction between the absorbate and the surface. Van der Waals interactions have a long range but are weak and the low energy change is insufficient to lead to bond breakage so a physisorbed molecule retains its identity although it may become distorted by the presence of the surface.

In chemisorption the molecules stick to the surface by forming a chemical, usually covalent, bond. The enthalpy of chemisorption is very much greater than physisorption. A chemisorbed molecule may be torn apart by the unbalanced valancies of the surface atoms. Also the existence of molecular fragments on the surface, as a result of chemisorption, is one reason why solid surfaces catalyse reactions.

It is important to note however that proteins are not uniform in charge or hydrophobic group distribution and may have some segments that are predominantly hydrophobic and others that are hydrophilic.

The enthalpy of absorption depends on the extent of surface coverage due to the interaction of the absorbate particles.

2.12 The Langmuir Isotherm

Whenever a gas is in contact with a solid there will be an equilibrium established between the molecules in the gas phase and the corresponding adsorbed species (molecules or atoms) which are bound to the surface of the solid.

As with all chemical equilibria, the position of equilibrium will depend upon a number of factors.

1. The relative stabilities of the adsorbed and gas phase species involved.

2. The temperature of the system (both the gas and surface, although these are normally the same).

3. The pressure of the gas above the surface

In general, factors (2) and (3) exert opposite effects on the concentration of adsorbed species - that is to say that the surface coverage may be increased by raising the gas pressure but will be reduced if the surface temperature is raised.

The Langmuir isotherm was developed by Irving Langmuir in 1916 to describe the dependence of the surface coverage of an adsorbed gas on the pressure of the gas above the surface at a fixed temperature [4].

When considering adsorption isotherms it is conventional to adopt a definition of surface coverage (θ) which defines the maximum surface coverage, or saturation of a particular adsorbate on a given surface, always to be unity, i.e. $\theta_{max} = 1$.

One of the simplest models that describe the interaction between two molecules in solution is the Langmuir adsorption isotherm [4.] This model has been widely used and is based on three basic assumptions: i) Adsorption of molecules produces only a homogenous monolayer; ii) all binding sites are equivalent; iii) all occupied sites do not influence the binding reactions elsewhere.

In order to understand the processes of molecular interactions on a surface it is assumed that only a limited number of binding sites are available.

If one considers a reversible interaction between two molecules, A represents the ligate and B the immobilised ligand:

$$A+B \underset{k_{off}}{\overset{k_{on}}{\rightleftharpoons}} AB$$

The process at the surface is described by the rate constants of adsorption k_{on} and desorption k_{off} from the surface which are related with the association rate of A and B $k_{on}[A][B]$ and the dissociation rate of AB complex $k_{off}[AB]$.

When the two species are present in solution, association and dissociation will occur and with time the rates will become equal. When this occurs it is defined as equilibrium. In equilibrium conditions the concentration of $[A], [B]$ and $[AB]$ are constants and so it can be written:

$$k_{on}[A][B] = k_{off}[AB]$$

Rearranging the equation

$$\frac{[A][B]}{[AB]} = \frac{k_{off}}{k_{on}} = K_D$$

Where K_D is the dissociation equilibrium constant and is the reciprocal of the association equilibrium constant K_A:

$$K_A = \frac{1}{K_D}$$

The association rate constant has units k_{on} of $M^{-1}s^{-1}$ and the dissociation rate constant has units of k_{off} s^{-1}, it follows that the association constant K_A has M^{-1} units and the dissociation constant K_D has M units.

The case described above is the simplest bimolecular interaction where other factors will not influence the interaction between the two species however, as one of the species does not move freely in solution, there are important factors that should be taken in consideration. The most important factor is the transport of the species A from the bulk into the interface where species B is present in very high concentration Therefore, the rate of formation of the complex species (AB) is also influenced by the mass transport rate constant from the bulk to the interface

Where A_b is the concentration of ligate in the bulk solution and A_i is the concentration at the interface.

2.13 Protein electrochemistry and Cytochrome *P*450 enzyme mechanisms.

Electron transfer is fundamental to many biological processes. Direct electron transfer between an electrochemical working electrode and a redox active protein enables important mechanistic information to be determined.

The transfer of electrons between and within proteins is an essential feature for many physiological processes, including biological energy transfer, metabolism and enzymatic catalysis. The mechanism of electron transfer usually involves protein–protein interactions. In the case of a bacterial Cytochrome *P*450 enzyme the electrons are transferred from two other accessory proteins and then to *P*450 itself.

In enzymes an appropriate conformational arrangement is important for the binding of the substrate to the active site and the transfer of charge to the enzyme. The use of electrochemistry allows investigation of the electrochemical properties of redox enzymes and their mechanisms by observing the direct electron transfer in real time.

Cytochrome *P*450 enzymes are a vast family of haem-thiolate proteins with redox properties. They are known as mono-oxygenases because of their ability to activate molecular dioxygen into highly reactive oxygen species (ROS) and then to insert the oxygen into a wide variety of substrates. They are ubiquitous across the biological kingdom and the substrates and reactions of these enzymes are equally ubiquitous, ranging from drug metabolism to the biosynthesis of steroids and fatty acids, metabolic activation of procarcinogens and the generation of damaging ROS [5].

Iron is capable of producing lethal levels of ROS in biological systems and requires careful regulation as a result. *P*450's achieve this by substrate binding which changes the spin state of the haem at the centre of the molecule, thereby enabling stabilisation of bound ROS and oxygenation of the substrate, so in most cases, it is only when a

suitable substrate is bound to the *P*450 protein that oxygen also becomes bound which decreases the likelihood of ROS leaking out in the absence of the substrate [6].

2.13.1 Haem spin state of Cytochrome *P*450 proteins.

Spectrophotometric investigations of the UV spectral changes which occur during substrate binding have enabled a monitoring of the haemoprotein spin sate equilibria in *P*450 systems. However, these investigations also showed that the situation in the microsomal system was not as easily characterised as that which was exhibited in the purified proteins. Microsomal and purified bacterial *P*450 proteins are considered later in more detail.

Purified microsome preparations are routinely used to study the role of cytochrome *P*450s and other enzymes involved in drug metabolism. These preparations are a rich source of membrane-bound, hydrophobic enzymes originating from rough and smooth endoplasmic reticulum. The vesicles, approximately 20 to 200nm, are isolated by differential centrifugation and are composed of three structural features: rough vesicles, smooth vesicles and ribosomes. Numerous enzyme activities are associated with the microsomal fraction [7].

Some microsomal proteins appeared to reside primarily in the high spin state and consequently, may not require substrate binding to modulate their spin and redox equilibria for the initiation of catalytic activity. Even so, the general view is that substrate binding usually has a significant effect on both the spin state and the redox potential of most *P*450 enzymes. The change from predominantly low spin ferric to high spin brings about a lowering of the protein redox potential, thus it becomes less negative in value. This brings about a change to the heam environment, such that the substrate bound protein can be more readily reduced to the ferrous form by the interaction with a relevant redox partner (a reductase). The redox potentials of haemoproteins vary considerably. This may be due to the extent of surface exposure of the haem to the aqueous environment [6].

2.13.2 The Cytochrome *P*450 catalytic cycle.

The *P*450 enzyme system is the major phase 1 biotransforming system in humans, accounting for more than 90% of drug biotransformations [8]. This system has huge catalytic versatility and broad substrate specificity. The basic reaction catalyzed by *P*450 is mono-oxygenation which is the transfer of one oxygen atom from molecular oxygen to a substrate. The other oxygen atom is reduced to water during the reaction with the equivalents coming from the cofactor NADPH. The basic reaction is;

$$\mathbf{RH\ (substrate) + O_2 + NADPH + H^+ = ROH\ (product) + H_2O + NADP^+}$$

The end result of this reaction can be (N-) hydroxylation, epoxidation, heteroatom (N-, S-) oxygenation, heteroatom (N-, S-, O-) dealkylation, ester cleavage, isomerization, dehydrogenation, replacement by oxygen or even reduction under anaerobic conditions. The metabolites produced from these reactions can either be intermediates which have relatively little reactivity towards cellular systems and are readily conjugated; however some intermediates can be disruptive to cellular systems. Inert compounds need to be prepared for conjugation and thus the formation of potentially reactive metabolites is in most cases unavoidable [9]. The active centre is the iron-protoporphyrin IX with an axial thiolate of a cysteine residue as fifth iron ligand. In the absence of a substrate at the beginning of the cycle the protein is in the hexa-coordinated low-spin ferric form with water being the sixth ligand. The resting state of the enzyme is the ferric FeIII complex. That has a water molecule as a distal ligand. This is a low spin species. The entrance of the substrate in to the protein pocket displaces the water molecule resulting in the iron moving out of the plane of the porhyrin which weakens the bond with the ligands which then leads to a high spin state and the complex becomes a good electron acceptor.
This triggers a one electron transfer from the reductase domain that reduces to the high spin ferrous FeII complex.

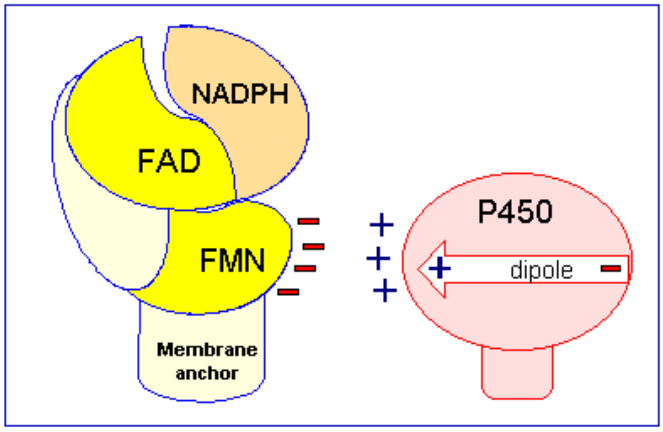

Figure 21. Interpretation of *P*450 and *P*450 reductase domains.
Cytochrome P450 forms a dipole across the molecule, with the positive charge at the proximal face of the protein where the haem makes its closest approach to the surface, shown in Figure 21. (*Adapted from Garrett & Grisham 1998*).

Ferrous porphyrin is an effective dioxygen binder which leads to the binding of molecular oxygen to produce the low spin ferrous dioxygen complex.
The latter species is, again a good electron acceptor which causes another electron transfer from the reductase to give rise to the twice reduced ferric dioxo species.
The distal oxygen atom is transferred to the substrate which is released and replaced by a water molecule to regenerate the resting state of the enzyme.
The *P*450 catalytic cycle in Figure 22 shows the steps involved when a substrate binds to the enzyme.

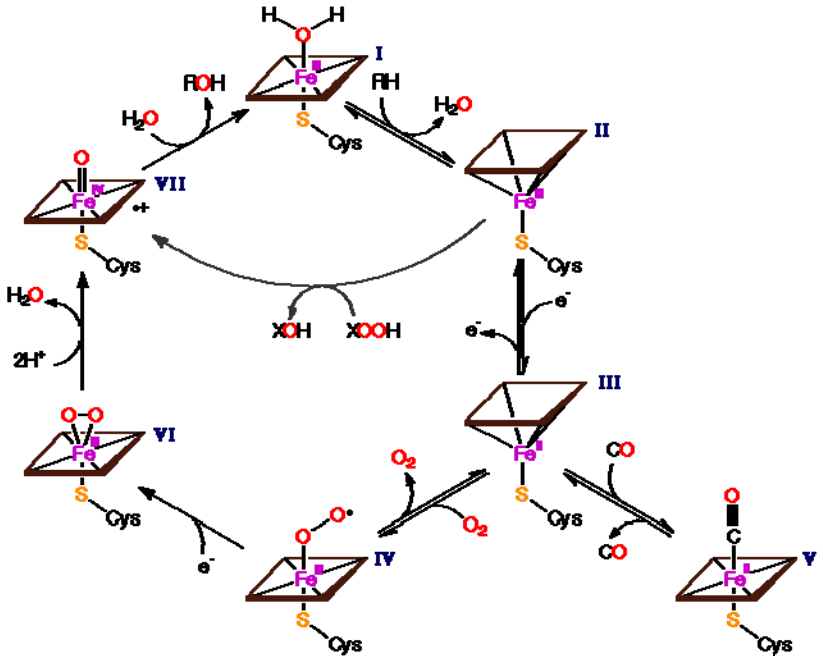

Figure 22. **Schematic interpretation of the *P*450 catalytic cycle and associated haem spin states** [10] *(adapted from Garrett & Grisham 1998)*

(I) The normal state of a *P*450 with the iron in its ferric [Fe^{3+}] state. The cycle is initiated by substrate (RH) binding to the native, predominantly low spin, ferric form

(II) The substrate binds to the enzyme. This then facilitates the high spin ferrous complex.

(III) The enzyme is reduced to the ferrous [Fe^{2+}] state by the addition of an electron from NADPH cytochrome *P*450 reductase. The bound substrate facilitates this process.

(IV, V) Molecular oxygen binds and forms an $Fe^{2+}OOH$ complex with the addition of a proton and a second donation of an electron from either NADPH cytochrome *P*450 reductase or cytochrome b5. A second proton cleaves the $Fe^{2+}OOH$ complex to form water.

(VI) An unstable $[FeO]^{3+}$ complex donates its oxygen to the substrate.

(VII) The oxidised substrate is released and the enzyme returns to its initial state (1)

2.14 Cytochrome *P*450 Protein Model Systems

*P*450s are generally divided into two major classes (class I and class II) according to the different type of electron transfer systems they use. The class I family includes bacterial *P*450s which use a two component shuttle system consisting of an iron – sulphur protein and a reductase. Class II *P*450s are the microsomal *P*450s which receive electrons from a single membrane bound enzyme, NADPH reductase, or Cytochrome *P*450 Reductase (CPR), which contains flavin adenine dinucleotide (FAD) and flavin mononucleotide (FMN) cofactors.

*P*450 proteins or CYPs, in bacteria are generally soluble proteins requiring ferredoxin and ferredoxin reductase for the two electrons required for the CYP catalytic cycle, while CYPs in eukaryotic organisms are typically located in the endoplasmic reticulum with an associated NADPH – CPR complex providing the necessary reducing equivalents.

In this work both systems were used. The bacterial *P*450 protein was produced from the soil dwelling bacteria Pseudomonas Putida and the microsomal proteins were extracted from the fruit fly Drosophila Melanogaster.

2.14.1 Class I Bacterial *P*450 proteins from Pseudomonas Putida. (*P*450cam, Cyp101)

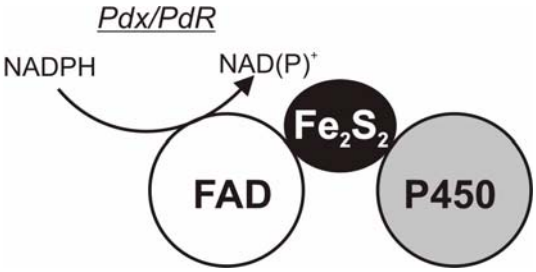

Figure 23. **Schematic diagram of Class 1 *P*450 protein systems.**

In class I systems shown in Figure 23, electrons are shuttled from NADPH through a Flavin Adenine Dinucleotide (FAD) containing ferredoxin reductase and an iron sulphur containing ferredoxin to *P*450. In the bacteria Pseudomonas Putida, these cells are identified as putidoredoxin (*PdX*) and putidoredoxin reductase (*PdR*).

2.14.2 Class II Microsomal *P*450 proteins from Drosophila melanogaster (Cyp6g1).

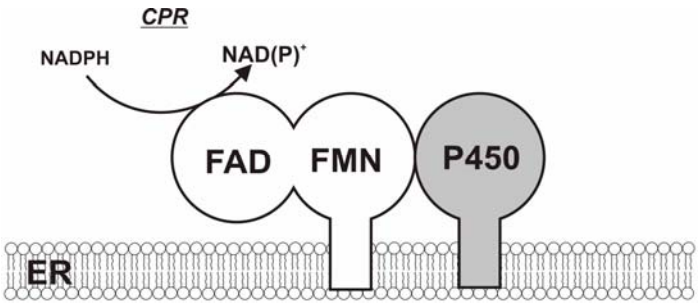

Figure 24. Schematic diagram of a class II *P*450 protein system.

In class II systems shown in Figure 24, electrons are delivered from NADPH through diflavin reductases containing FAD and FMN. In eukaryotes, these are bound to the endoplasmic reticulum (ER). This system is found in microsomal proteins. In cell biology, a microsome is a small vesicle, approximately 20-200nm in diameter, which is derived from fragmented endoplasmic reticulum when cells are homogenised.

Purified microsome preparations are routinely used to study the role of cytochrome *P*450s and other enzymes involved in drug metabolism. These preparations are a rich source of membrane-bound, hydrophobic enzymes originating from smooth endoplasmic reticulum and rough endoplasmic reticulum that catalyze phase I reactions of metabolism. The vesicles are isolated by differential centrifugation and are composed of three structural features: rough vesicles, smooth vesicles and ribosomes. Numerous enzyme activities are associated with the microsomal fraction.

Pseudomonads are globally active in aerobic decomposition and biodegradation, and hence, they play a key role in the carbon cycle. The camC gene in this bacterium encodes the Cytochrome *P*450 monoxygenase protein which protects the organism from chemical attack in its soil environment.

Pseudomonas species are renowned for their abilities to degrade compounds which are highly refractory to other organisms, including aliphatic and aromatic hydrocarbons, fatty acids, insecticides and other environmental pollutants. Apparently, the only organic compounds that these pseudomonads can't attack are Teflon, Styrofoam and one-carbon organic compounds such as methane and formaldehyde. Pseudomonads are also a regular component of microbial food spoilage in the field, in the market place, and in the home [5].

Pseudomonas putida is a fast-growing bacterium found in most temperate soil and water habitats where oxygen is present. It can colonise the root area of crop plants and as a result is a useful tool to researchers in bioengineering to develop biopesticides and plant growth promoters [6]. It is a flagellated rod-shaped bacterium that has the ability to degrade organic solvents. These solvents include toluene which is found in gasoline. This ability has been put to good use in bioremediation, or the use of microorganisms to

biodegrade oil. Pseudomonas Putida is a safe strain of bacteria, compared to the human nosacomial pathogen Pseudomonas Aeruginosa.

In early 2006, researchers from University College, Dublin discovered that P. putida is capable of converting styrene oil into the biodegradable plastic PHA [7]. This may be of use in the effective recycling of Polystyrene foam, otherwise thought to be non-biodegradable. This bacterium is also used as a soil inoculant in agriculture and horticulture.

The genome analysis found P. putida has a single circular chromosome with nearly 6.2 million DNA base pairs [8]. Also, isothermal titration calorimetry (ITC) experiments have shown that the energetics of the *P*450cam and Putidaredoxin association exhibit van der Waals and hydrogen bonding interactions. The study also suggested that the association between Putidaredoxin and Putidaredoxin reductase might be dominated by hydrophobic interactions [9].

In insects Cytochrome *P*450 proteins are encoded by a large multi-gene family and play an important role in the metabolism of both exogenous and endogenous compounds. The *P*450 gene Cyp6g1 is instrumental in the protection of the insect from insecticides. Mechanisms of insecticide resistance caused by the increased capacity of the insect to metabolise insecticides are not very well defined. Although most are believed to be the result of an increased expression of detoxification genes and rarely is the actual mutation identified. It has been shown that broad-spectrum insecticide resistance is widespread in populations of Drosophila melanogaster from around the world and that it is caused by the over-expression of the cytochrome *P*450 gene Cyp6g1[10].

This important fruit fly, an insect about 3mm long, is of the kind that accumulates around spoiled fruit. It is also one of the most valuable of organisms in biological research, particularly in genetics and developmental biology. Drosophila has been used as a model organism for research for almost a century, and today, several thousand scientists are working on many different aspects of the fly. Its importance for human health was recognised by the award of the Nobel Prize in medicine and physiology to Ed Lewis and colleagues [11, 12].

D. melanogaster is undoubtedly the most important model insect for the scientist. Of all the insects, Drosophila is the most understood and widely studied. Because of this work there have been identified a huge number of phenotypic markers for the mapping of resistance which lead to the location of a resistant locus [13]. Almost a century of work

has been carried out turning Drosophila into one of the most important genetic tools available to a scientist studying resistance to insecticides.

D. melanogaster has long been the model organism for geneticists from the early days of genetics at the beginning of the last century. These insects are easy to rear on a diet of treacle, oatmeal and a little yeast. They produce large numbers of offspring and have a simple and short lifecycle of 14 days. They are also very small so large numbers of strains can be kept in a confined space [14]. D. melanogaster has a relatively small number of chromosomes and this makes the mapping of genotypes easier than for species with a large chromosome number [15].

The eukaryotic microsomal *P*450 system contains two components: NADPH: *P*450 reductase (CPR), a flavoprotein containing both FAD and FMN, and *P*450. CPR appears to be a fusion protein consisting of domains which are homologous to flavodoxin (FMN domain) and ferredoxin: NADP+ reductase (FAD domain).

2.14.3 *P*450 substrates and their associated activities.

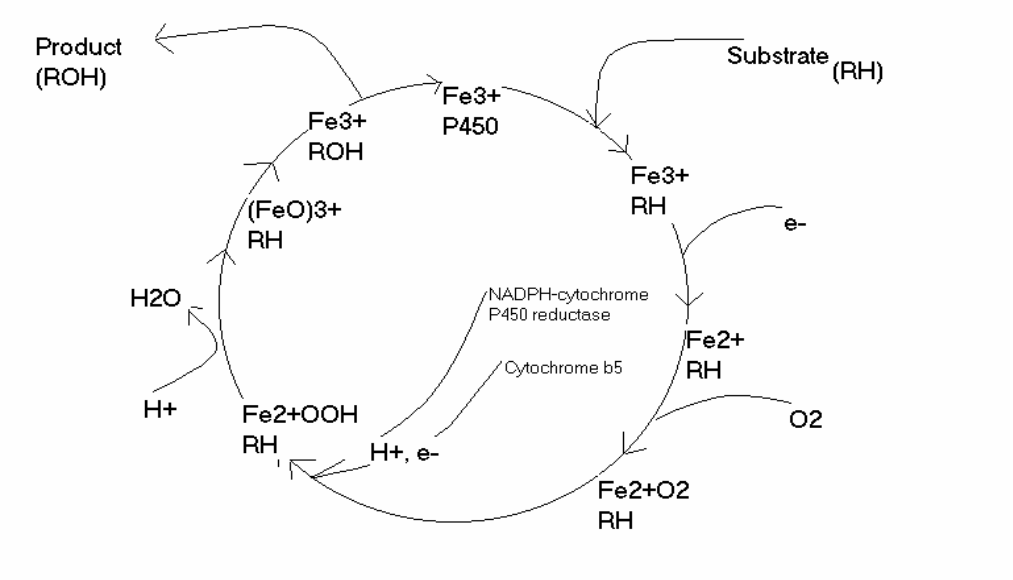

Figure 25. **General interpretation of the catalytic cycle and enzymatic intermediates in *P*450 reactions** (*adapted from Alberts & Bray 1998*).

2.14.4 Nicotinamide Adenine Dinucleotide (NADPH) as an indicator for *P*450cam activity.

Cytochrome *P*450cams' natural substrate is camphor. This white transparent waxy crystalline solid with a strong penetrating pungent aromatic odour, is also highly insoluble.

Nicotinamide adenine dinucleotide (NAD) and nicotinamide adenine dinucleotide phosphate (NADP) are two important coenzymes found in cells. NADH is the reduced form of NAD, and NAD+ is the oxidized form of NAD. It forms NADP with the addition of a phosphate group. NAD is used extensively in glycolysis and the citric acid cycle of cellular respiration. The reducing potential stored in NADH can be converted to adenosine tri phosphate (ATP) through the electron transport chain or used for anabolic metabolism. ATP energy is necessary for an organism to live. Green plants obtain ATP through photosynthesis, while other organisms obtain it by cellular respiration. NADP is used in anabolic reactions, such as fatty acid and nucleic acid synthesis that require NADPH as a reducing agent. This reducing power is also intrinsic in the *P*450 cycle shown in Figure 25.

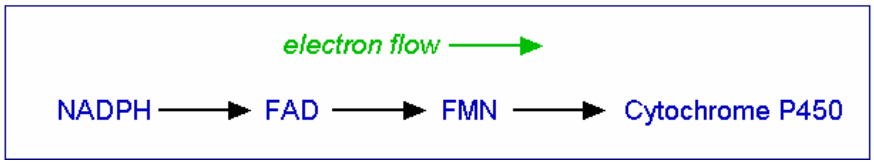

Figure 26. **Scheme showing the electron flow from the reduced electron donor NADPH, through the flavoproteins and then onto *P*450 itself.**

This pathway, shown in Figure 26, would typically be found in Class II *P*450's.

Cytochrome *P*450cam catalyses the 5-exo hydroxylation of camphor in the first step of camphor catabolism, shown in Figure 27, by the bacteria Pseudomonas putida. Cyp101 forms a specific electron transfer complex with its physiological reductant, the Cys(4) Fe(2) S(2) ferredoxin putidaredoxin (Pdx) shown earlier.

With camphor bound at the active site, *P*450cam acts as the terminal monooxygenase in the d-camphor monooxygenase system. Under anaerobic conditions, this enzyme reduces the compounds bound at the camphor-binding site. Additionally, it is the only cytochrome *P*450 enzyme with a known crystal structure. Much of what is known about the molecular level structure/function relationships in *P*450 protein is based on studies with the camphor momooxygenase system from the bacterium Pseudomonas Puitda. *P*450cam was the first *P*450 to be purified and the first crystal structure to be solved. This work was published in 1987[16].

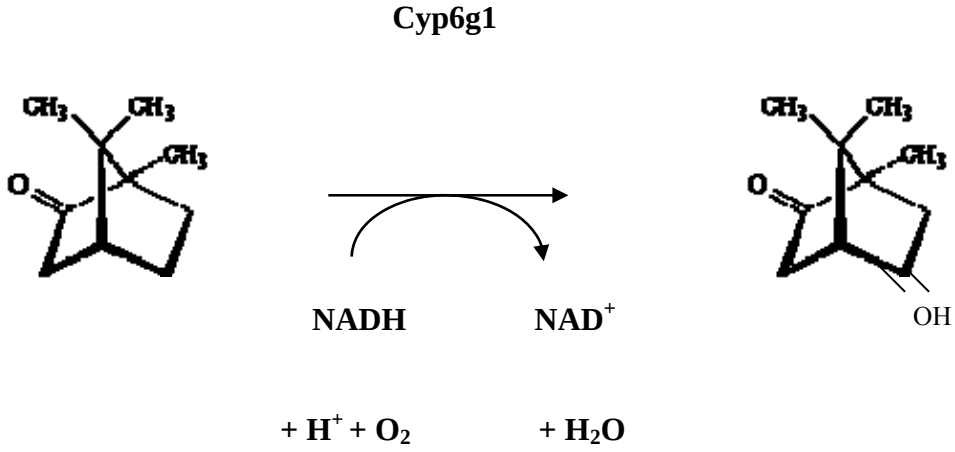

Figure 27. Scheme showing the 5-exo hydroxylation of camphor by *P*450cam and the involvement of NADH in substrate turnover.

2.14.5 Resorufin Methyl Ether (MRES) as an indicator for the detection of microsomal *P*450 activity.

Resorufin methyl ether is a bright red fluorescent dye that serves as the basis for enzyme substrates. It is a versatile model substrate for the Cyp6g1 protein. This compound exhibits an absorption maximum of around 571nm and emission spectra of around 585nm, which provides a useful platform for the detection of the molecules turnover by an enzyme [17].

Resorufin methyl ether and the sodium salt Resorufin are both water soluble and exhibit reversible electron transfer behaviour [18]. The Cyp6g1 enzyme mediated reduction of

MRES in the presence of NADPH, shown in Figure 28, could therefore be followed in real time by following the decrease in reduction current.

It was possible to follow the rate of reduction of MRES by protein microsomes extracted from the insecticide resistant strain of Drosophila melanogaster which over express the Cyp6g1 protein. Experiments in the absence of NADPH, and measurements on insecticide susceptible strains which comparatively under express the protein were also carried out.

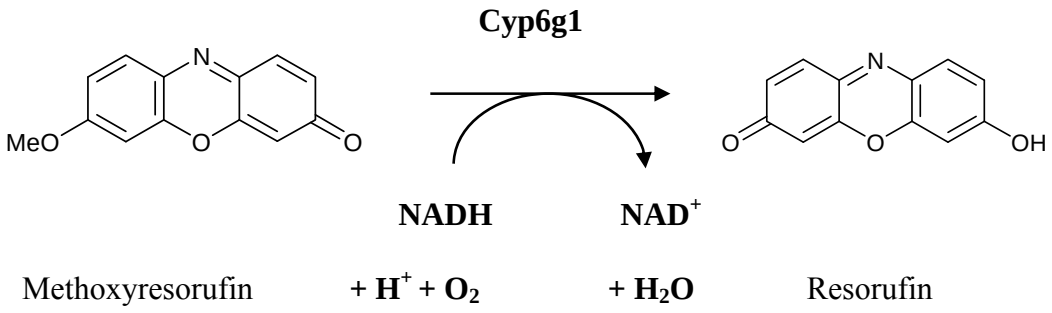

Figure 28. **Scheme showing the Cyp6g1 enzyme mediated demethylation of the substrate methoxy resorufin ether resulting in the product resorufin.**

2.14.6 Inhibition of Cytochrome *P*450 enzyme activity.

It is important to note that these enzymes can be inhibited by various gases, chemicals and antibodies both in the body and experimentally. In drug therapy, this inhibition can result in an increase or decrease in pharmacological effects or toxicity from a drug. Therefore, *P*450 inhibition is an important consideration for the development of novel therapeutic agents and devices. Knowledge of the potential for a therapeutic agent to decrease *P*450 activity at an early stage reduces the risk of therapeutic failure.

Inhibiting the enzymes activity in an experimental set up provides evidence of protein activity and active substrate turnover.

In this work, the non-selective *P*450 inhibitor Carbon Monoxide (CO) was used. The gas was easy to handle in the experimental set up and the crystal structure of *P*450cam

with bound CO in the presence of substrate shows that the CO molecule ligates the haem iron and thus prevents access for the oxygen molecule and so inhibits substrate turnover [19]. CO has also been shown to inhibit microsomal *P*450 activity [23].

2.15 Chapter Summary.

Here, the electrochemical mechanisms observed in this project were considered and the theory which supports them. Also, the complex interactions and forces between a protein and an electrode surface were looked at. The two model protein systems employed in this work were then introduced as well as their corresponding substrates and associated biotransformation mechanisms. Next, the significant body of work which resulted in an expressed and purified bacterial protein is described.

2.16 References

1. Garrett, R.H. & Grisham, C.M. *Biochemistry.* Thompsom Learning. 1998.

2. Bard, E & Faulkener, L. *Electrochemical Methods. Fundamentals and Applications.* Wiley & Sons. 2001.

3. A.C. Fisher. Electrode Dynamics**,** Oxford Chemistry Primer. Oxford Press **2003**

4. I. Langmuir. Phys. Rev. 8, 48–51 (**1916**) Issue 1

5. Liao, C., Ukuku, D.O. **2005.** Role of fluorescent pseudomonads and their pectolytic enzymes in spoilage of fresh and fresh-cut produce. Book Chapter. CRC Press. 483-504.

6. Bacterial Pathogenesis. Abigail A. Salyers (Editor), Dixie D. Whitt (Editor) American Society for Microbiology. **2000**

7. B. Booth. American Chemical Society journal *Environmental Science & Technology*. Vol.40. Iss 7 pp. 2074-2075 **2005**

8. Nelson KE et al: Environ Microbiol. **2002** Dec;4 (12):799-808

9. Aoki, M.K. Ishimori., H. Fukada., K. Takahashi and I. Morishima (**1998)**. Biochim. Biophys. Acta. 1384. 180-188.)

10. Le Goff et al. Insect Biochemistry & Molecular Biology, 33 **2003,** 701-708

11. Lewis, E. B. A Gene Complex Controlling Segmentation in Drosophila. Nature 276: 565-570. **1978**

12. Lewis, E. B. Knafels, J.D., Mathog, D.R. and Celniker, S.E. Sequence Analysis of the *Cis* – regulatory regions of the Bithorax complex of Drosophila. Proc. Natl. Acad. Sci. 92: 8403-8407. **1995.**

13. Wilson, T.G. 1988. Drosophila melanogaster (Diptera: Drosophilidae): a model insect for insecticide resistance studies. Journal of Economic Entomology. 81:22-27.

14. Ashburner, M. 1989. Drosophila: a Laboratory Handbook. Cold Spring Harbor Laboratory Press. 434 pp.

15. ffrench-Constant, R.H., and T. Rocheleau. 1992. Drosophila cyclodiene resistance gene shows conserved genomic organization with vertebrate γ-aminobutyric $acid_A$ receptors. *Journal of Neurochemistry*. 59:1562-1565.

16. Poulos, T.L., Finzel, B.C. and Howard, A.J. (1987). High- resolution crystal structure of cytochrome *P*450cam. *J. Mol.Biol.* 195, 687-700.)

17. . Dabron, P.J., Yen, J.L., Bogwitz, M.R., LeGoff. G., Feil, E., Jeffers.S. Tijet, N., Perry, T., Heckel, D., Batterham, P., Feyereisen,R., Wilson, T.G. & ffrench-Constant R.H. *Science*, **2002**, 297, 2253-2256.

18. Jenkins, A. T. A., Bushby, R.J., Evans, S.D., Knoll, W., Offenhausser, A., Ogier, S.D. *J.Am.Chem.Soc.* **2002**.

19. Raag, R and Poulos, T.L. *Biochemistry*, **1989**, 28, 7586-7592.

20. Layne, E. Spectrophotometric and Turbidimetric Methods for Measuring Proteins. *Methods in Enzymology 3:* 447-455. **1957**

21. Stoscheck , C. M. Quantitation of Protein. *Methods in Enzymology 182:* 50-69. **1990**

22. Bradford, M.M. A rapid and sensitive test for the quantitation of microgram quantities of protein utilizing the principle of protein dye binding. *Analytical Biochemistry 72:* 248-254. **1976**

23. Suk-Jung Choi et al: Microplate Assay Measurement of Cytochrome *P*450-Carbon Monoxide Complexes. *Journal of Biochemistry and Molecular Biology,* Vol. 36, 332-335, **2003.**

3 Expression and purification of Cytochrome *P*450cam Cyp101

3.1. Introduction

3.1.1 Protein Separation.

3.1.2. Plasmid DNA extraction.

3.1.3. Transformation by heat shock.

3.1.4. Heat shock.

3.1.5. Growth of *P*450cam (Cyp101) gene.

3.1.6. Harvest and lysis of cells.

3.2. Separation and purification of proteins by Fast Protein Liquid Chromatography (FPLC)

3.2.1. Gradifrac DEAE Sepharose Ion Exchange Chromatography.

3.2.2. Equlibration of protein for FPLC.

3.2.3. Final protein purification by FPLC.

3.2.4. Equilibration and storage of protein.

3.2.5. Investigation of protein purity by gel electrophoresis.

3.2.6. Investigation of Protein Activity and Concentration.

3.2.7. NADPH consumption activity assay via UV vis absorption spectroscopy.

3.1 Introduction

Protein expression is the process by which a gene's DNA sequence is converted into the structures and functions of a cell. Protein purification is a series of processes intended to isolate a single type of protein from a complex mixture. The starting material is, in this case, a microbial culture. The various steps in the purification process may free the protein from a matrix that confines it, separate the protein and non-protein parts of the mixture, and finally separate the desired protein from all other proteins. Separation of one protein from all others is typically the most laborious aspect of protein purification. Separation steps exploit differences in protein size, physico-chemical properties and binding affinity [1].

Purification may be preparative or analytical. Examples include the preparation of commercial products such as enzymes. Analytical purification produces a relatively small amount of protein for a variety of research or analytical purposes, including identification, quantification, and studies of the protein's structure, post-translational modifications and function [2].

The choice of a starting material is key to the design of a purification process. In a plant or animal, a particular protein usually isn't distributed homogeneously throughout the organism. Different tissues have higher or lower concentrations of the target protein. Use of only the tissues with the highest concentration decreases the volumes needed to produce a given amount of purified protein. If the protein is present in low abundance, or if it has a high value, recombinant DNA technology may be employed to develop cells that will produce large quantities of the desired protein (this is known as an expression system). Recombinant expression allows the protein to be tagged, e.g. by a His-tag, to facilitate purification, which means that the purification can be done in fewer steps. In addition to this, recombinant expression usually starts with a higher fraction of the desired protein than is present in its natural source.

An analytical purification generally utilises three properties to separate proteins. Firstly, proteins may be purified according to their isoelectric points by running them through a pH graded gel or an ion exchange column. Secondly, proteins can be separated according to their size or molecular weight via size exclusion chromatography or by SDS-PAGE (sodium dodecyl sulfate-polyacrylamide gel electrophoresis) analysis [3, 4].

Cytochrome P450 enzymes are about 500amino acid residues in length, including an N-terminal endoplasmic reticulum (ER) retention signal. Removal of the N-terminal ER retention signal has been shown to markedly increase expression of cytochrome *P*450 in bacterial cells without altering catalytic activity. In addition, co-expression of the electron supplying NADPH-cytochrome reductase increases cytochrome P450 activity in *E. coli* by a large factor [5], allowing recombinant *P*450 enzymes to be expressed at levels up to hundreds of nmol of protein per L of bacterial culture[6].

The most general method to monitor the purification process is by running an SDS-PAGE of each of the different steps. This method was employed in this work and the results of this are shown later. This method only gives a rough measure of the amounts of different proteins in the mixture, and it does not distinguish between proteins with similar molecular weights.

If the protein has a distinguishing spectroscopic feature or an enzymatic activity, this property can be exploited to detect and quantify the specific protein, and thus to select the fractions of the separation which contain the target protein.

In order to evaluate the process of multistep purification, the amount of the specific protein has to be compared to the amount of total protein. The latter can be determined by the Bradford total protein assay and by absorbance of light at 280 nm which identifies the proteins peptide backbone. The results of these two methods are shown later.

Depending on the source, the protein has to be brought into solution by breaking the tissue or cells containing it. There are several methods to achieve this. In this case sonication was used. The method of choice depends on how fragile the protein is and how sturdy the cells are. After this extraction process, soluble proteins will be in the solvent and can be separated from cell membranes, DNA and other cellular fractions by centrifugation. The extraction process also extracts proteases, which will start to digest the proteins in solution. As the protein used in this work was sensitive to proteolysis, it was desirable to proceed quickly, and keep the extract cooled in order to slow this process down.

Usually a protein purification protocol contains one or more chromatographic steps. The basic procedure in chromatography is to flow the solution containing the protein through a column packed with various materials. Different proteins interact differently with the column material, and can thus be separated by passing the solution through the

column. The proteins are then detected as they are eluted from the column by their absorbance at 280 nm.

Ion exchange chromatography separates compounds according to the nature and degree of their ionic charge. The column to be used is selected according to its type and strength of charge. Anion exchange resins have a positive charge and are used to retain and separate negatively charged compounds, while cation exchange resins have a negative charge and are used to separate positively charged molecules.

Before the separation begins, a buffer is pumped through the column to equilibrate the opposing charged ions. Upon injection of the sample, solute molecules will exchange with the buffer ions as each competes for the binding sites on the resin. The length of retention for each solute depends upon the strength of its charge. The most weakly charged compounds will elute first, followed by those with successively stronger charges. Because of the nature of the separating mechanism, pH, buffer type, buffer concentration, and temperature all play important rolls in controlling the separation.

Ion exchange chromatography is a very powerful tool for use in protein purification and is frequently used in both analytical and preparative separations.

3.1.1 Protein Separation

Ion exchange chromatography (IEC) is applicable to the separation of almost any type of charged molecule, from large proteins to small nucleotides and amino acids.

It is very frequently used for proteins and peptides, under widely varying conditions. Desorption is then brought about by increasing the salt concentration, shown in Figure 29, or by altering the pH of the mobile phase. Ion exchange containing diethyl aminoethyl (DEAE) groups are most frequently used in biochemistry.

The property of a protein that governs its adsorption to an ion exchanger is the net surface charge. Since surface charge is the result of weak acidic and basic groups of protein; separation is highly pH dependent. Going from low to high pH values the surface charge of proteins shifts from a positive to a negative surface charge At a pH value below its isoelectric point a protein (+ surface charge) will adsorb to a cation exchanger (-). Above the isoelectric point protein (-surface charge) will adsorb to an anion exchanger (+), such as one containing DEAE-groups [7].

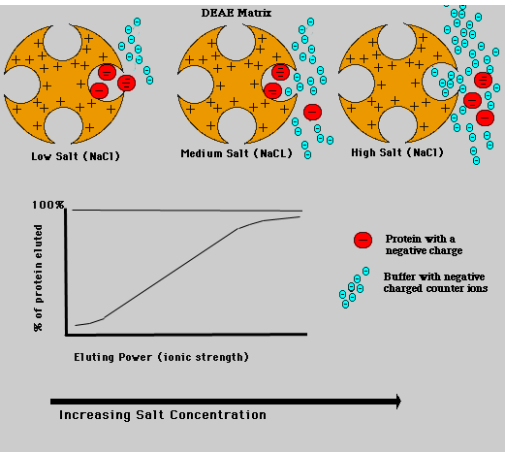

Figure 29. Schematic interpretation of elution of proteins with increasing salt concentration (*adapted from Alberts 1998*).

3.1.2 Plasmid DNA extraction

Plasmids used in genetic engineering are called vectors. They are used to transfer genes from one organism to another, and typically contain a genetic marker conferring a phenotype that can be selected for or against, shown in Figure 30. Most also contain a polylinker or multiple cloning site (MCS), which is a short region containing several commonly used restriction sites allowing the easy insertion of DNA fragments at this location [9].

Plasmids are often used to purify a specific sequence, since they can easily be purified away from the rest of the genome. For their use as vectors and for molecular cloning, plasmids often need to be isolated.

There are several methods to isolate plasmid DNA from bacteria. For this work the Novagen SpinPrep™ Plasmid miniprep method was used. This method can be used to quickly find out whether the plasmid is correct in any of several bacterial clones. The yield is a small amount of impure plasmid DNA, which is sufficient for analysis by cloning techniques.

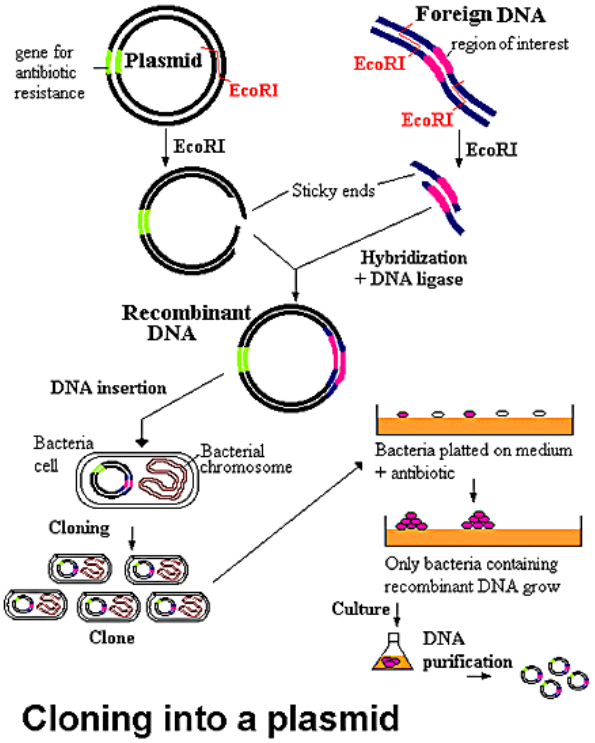

Figure 30. Scheme indicating steps involved in inserting gene of interest into a plasmid to produce a clone.

EcoR1 are the restriction endonucleases, which cleave DNA at specific sites.
The cells containing the plasmid of interest were then grown to provide a supply of protein (*adapted from T.A.Brown, 2006*).

3.1.3 Transformation by heat shock

Heat shock proteins (HSPs), also called stress proteins, are a group of proteins that are present in all cells in all life forms. They are induced when a cell undergoes various environmental stresses like heat, cold and oxygen deprivation [10].
The process of transformation changes the bacteria from being susceptible to resistant to an antibiotic. The resistant gene is inserted into the bacteria via this process. This enables the bacteria to acquire foreign DNA, which results in the transformation or alteration of the bacteria's characteristics.

Freshly prepared cells were used for the transformation procedure. 2-5ul of the chosen vector was added to 100ul of frozen competent cells which had previously been primed to take up DNA.

3.1.4 Heat shock

The cell preparation was kept at 0°C for forty five minutes on ice followed by 45seconds in a water bath at 42°C. The process was then repeated at 0°C for but for two minutes. The whole protein solution volume was then added to 1ml Luria-Bertani (LB) nutrient growth media, and then shaken at 180rpm for 50min at 30°C.

250ul were then spread onto LB agar containing 34ug/mL of the antibiotic Chloramphenicol and grown for thirty hours at 30°C. The two most viable colonies were picked with a toothpick and grown in 2mL of LB media containing Cloramphenicol and incubated overnight at 30°C.

3.1.5 Growth of *P*450cam (Cyp101) gene.

A supply of DNA was produced which coded for *P*450cam as previously described. The growth characteristics of the *E. Coli* JM109 strain containing the pAW7292 plasmid were determined by producing a growth profile of the organism.
In order to determine the optimum conditions for growth and induction, a growth profile of the organism was required. This was achieved by measuring the optical density (OD_{600}) of the culture at determined time intervals, producing a growth curve. This confirms the viability of the cells as well as providing an estimation of how long the cells should be allowed to grow before induction.
The *E. coli* JM109 strain competent cells containing the camC gene of interest, pRH1091, were plated onto LB growth media. This gene codes for antibiotic resistance. A promoter region was also present. (JM109 cells are standard for routine cloning applications). High selective pressure was maintained by including a high concentration of the antibiotic, Chloramphenicol. 2ul of a 34mg per ml stock was added to 20ul of cells in the starter culture. The cells were then grown at 30ºC for thirty hours.
A single colony was then inoculated into 5ml LBcm and grown at 30ºC overnight.

This preparation was then inoculated into 500ml LBcm and, again grown at 30ºC overnight.
30mls per litre were then inoculated into 12 x 1L LBcm, with 4ml glycerol added, and grown for 4 to 6 hours at 30ºC to an optical density at 600nm of 1.0 AU.
The incubation temperature was then increased to 37ºC and camphor was added to 1mM. Although camphor is the proteins natural substrate, it also provided a structural framework enabling the protein to fold. The preparation was then left to grow for a further 6 to 8 hours, shown in Figure 31.
The 30ºC preparations promoted cell division as the promoter region was not active below this temperature, but the proteins of interest were not expressed until the culture temperature was increased to 37ºC.

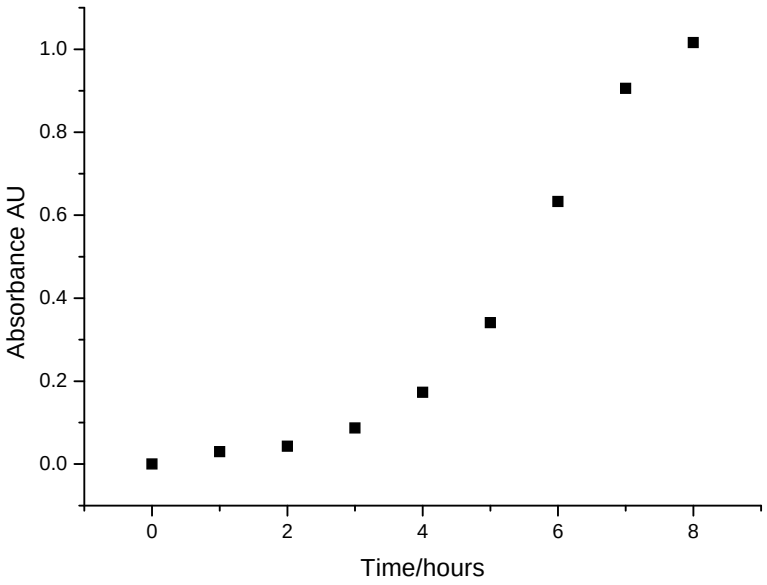

Figure 31. Cell growth curve at OD_{600}. *E Coli* JM109 competent cells containing the camC gene of interest pRH1091 in the plasmid pAW7292,.
The cells were grown in LB broth at 30°C for 9 hours. At 6 hours the media was inoculated with camphor and the temperature increased to 37°C to promote protein production.

3.1.6 Harvest and lysis of cells

The cells were then harvested by centrifugation in a 600 x 500ml rotor for 5minutes at 5000rpm at 4ºC. Each cell pellet was then resuspended and combined in 20mls of buffer P (buffer P consisted of 40mM potassium phosphate and 1mM camphor, at pH7.4).
The cells were then lysed by sonication for 1 minute. This was carried out using a 200ml beaker of sample kept on ice at all times. The suspension was then left to cool for 1 minute and the sonication process repeated 9 times.
1ml of the suspension was spun down for 1min and the pellet examined by eye to check for any red colouration. If any red was seen, the sonication process was repeated. The red colour indicated whole cells in the solution.

The lysed cells were then transferred to 50ml Oak Ridge tubes and the cell debris removed by centrifugation using an 8 x 50ml rotor for 20 minutes at 18000rpm at 4ºC. The resulting cell free supernatant was removed and combined.

3.2 Separation and purification of proteins by Fast Protein Liquid Chromatography (FPLC)

3.2.1 Gradifrac DEAE Sepharose Ion Exchange Chromatography

All protein separation was carried out on an ÄKTA™ design system from Amersham Pharmacia Biotech Ltd.
The ion exchange column was a HiTrap™ 16/10 Sepharose™ FF IEX from Amersham Biosciences, UK.
The G25 de salting column was a HiPrep™ 26/10 from Amersham Biosciences, UK.
All filters were Amicom from The Millipore Corporation.
PD10 columns were from Amersham Biosciences, UK.

Firstly, the column was equilibrated using 1L of buffer P ran on programme 1(column wash at 6mls per minute) twice.
The cell free extract was then loaded onto the column using programme 9 (monomer-dimer separation at 6mls per minute) followed by a manual programme (purification standard programme at 6mls per minute)
The protein was then eluted with a gradient of 80mM to 230mM KCL in buffer P over 4 litres using programme 2. The coloured fractions were collected. The column was then washed with 500ml of 2 mol dm^{-3} NaCl followed by 1L of Milli Q.
The G25 column was then equilibrated using 1L of buffer P.

3.2.2 Equilibration of protein for FPLC.

The protein was concentrated using a 200ml Amicon and YM-30 membrane into 30mls of buffer P.
The protein was then loaded onto a G25 de-salting column and eluted with buffer P.
The protein solution was then filtered using a 0.22um Amicom filter. Shown in Figures 32 and 33.

3.2.3 Final protein purification by FPLC

2L of buffer P and 1L of buffer P with 1M KCL was prepared, filtered and degassed. The FPLC pumps were washed and the column equilibrated.
The fractions were collected and all fractions with an absorbance A392/A280 ratio of > 1.6AU were combined. As these proteins have an iron centre, they absorb strongly at around 400nm.

3.2.4 Equilibration and storage of protein

At the end of protein purification, the protein usually has to be concentrated. Ultrafiltration concentrates a protein solution using selective permeable membranes. The function of the membrane is to let the water and small molecules pass through while retaining the protein. The solution is forced against the membrane by centrifugation.
The protein was concentrated using a 200ml Amicon with a YM-30 membrane to approximately 100um. The protein solution was then filtered through a 0.22um filter into a fresh 50ml tube. An equal volume of glycerol was then added, mixed and stored in 1.5ml aliquots at -20ºC. The addition of the glycerol helped to prevent freezer damage. Prior to analysis, the protein solution was passed through a PD10 column to remove the glycerol.

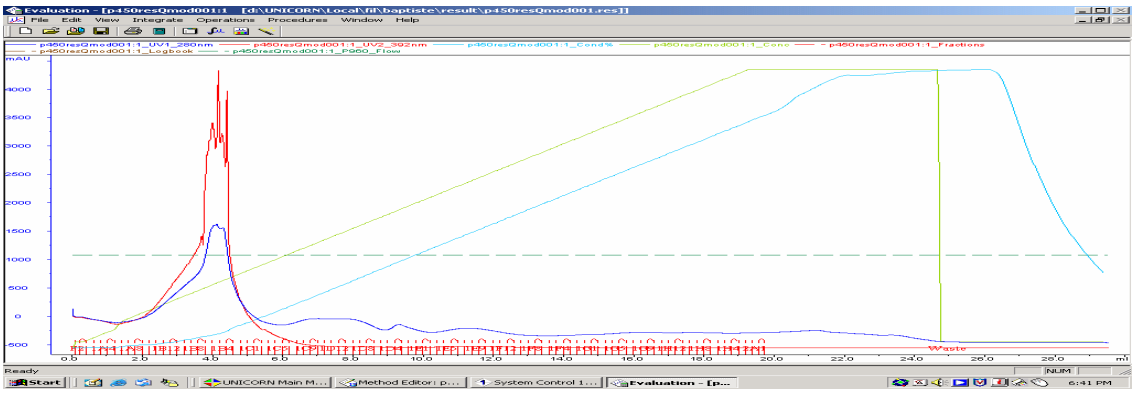

Figure 32. **Chromatogram of evaluation of purified *P*450 protein run via FPLC.**

The chromatogram shows the haem peak in red from the proteins iron centre at 392nm and the protein peptide backbone peak in blue at 280nm. The later peak denotes the conductivity of the salt. The jagged peaks are typical of the first purification run and is indicative of an impure sample.

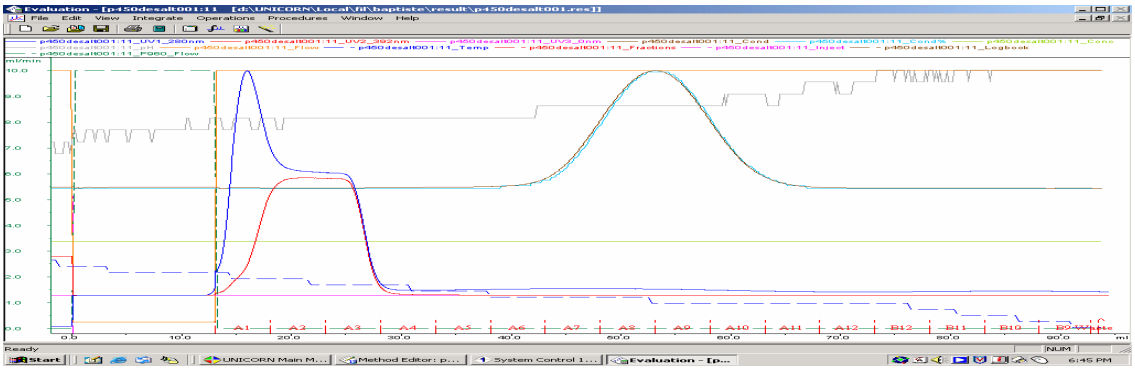

Figure 33. **Chromatogram of evaluation of purified *P*450 protein run via FPLC.**

The second run following desalting indicates a purer sample. The heam and peptide backbone peaks are more clearly resolved.

3.2.5 Investigation of protein purity by gel electrophoresis

Gel electrophoresis is a method that separates macromolecules on the basis of size, electric charge, and other physical properties. The gel is a colloid in a solid form and 'electrophoresis' describes the migration of charged particles under the influence of an electric field. Activated electrodes at either end of the gel provide the driving force. A molecule's properties determine how rapidly an electric field can move the molecule through the gelatinous medium.

Proteins are usually denatured in the presence of a detergent such as sodium dodecyl sulfate (SDS) which coats the proteins with a negative charge. Generally, the amount of SDS bound is relative to the size of the protein, so that the resulting denatured proteins have an overall negative charge, and all the proteins have a similar charge to mass ratio. Since denatured proteins are rod shaped instead of having a complex tertiary shape, the rate at which the resulting SDS coated proteins migrate in the gel is relative only to its size and not its charge or shape. The protein *P*450cam had a weight of 46.9 kiladaltons (kDa).

After the electrophoresis run, the molecules in the gel can be stained to make them visible, shown in Figure 34. Coomassie blue dye was used in these experiments.

Protein samples were collected at each step of purification. 10ul of each sample was added to a NuPAGE® Bis-Tris Gel, from Invitrogen, UK, prior to the electrophoresis run.

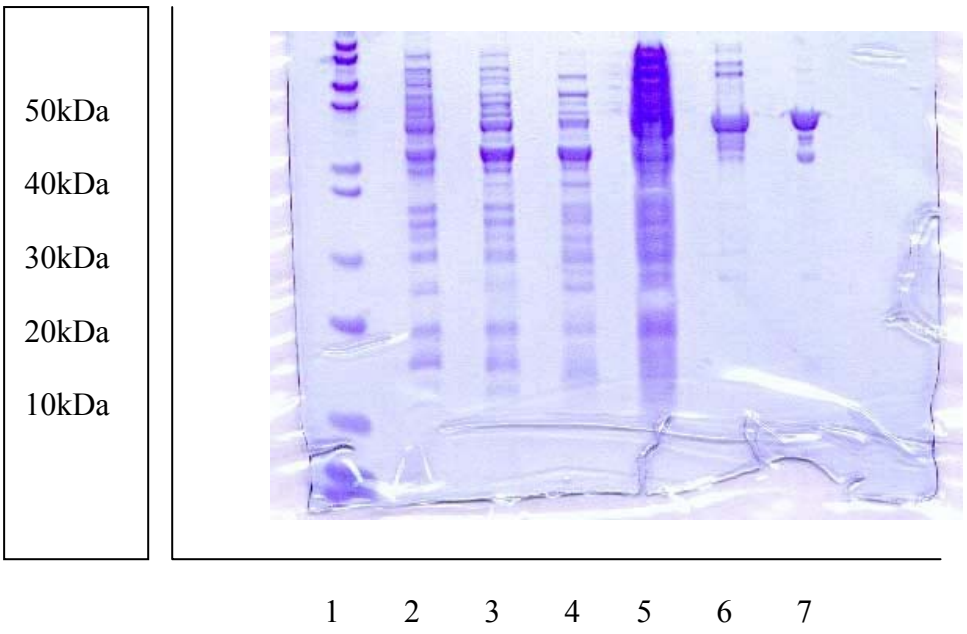

Figure 34. **NuPAGE® Bis-Tris Gel showing increasing purity of *P*450cam.**

From left

Track 1. Protein molecular weight standard.

Track 2. 30°C cell growth stage.

Track 3. 37°C cell growth stage.

Track 4. Following cell lysis by sonication.

Track 5. Following centrifugation.

Track 6. After the de-salting purification step by FPLC.

Track 7. The final pure protein sample, which has a molecular weight of 46.9kDa.

3.2.6 Investigation of Protein Activity and Concentration

In order to investigate an enzyme, two properties must be accounted for; the total amount of protein present and the total amount of activity. This is true for studies on the purification of the enzyme and almost any characterization study that is to be performed. Over time many enzymes lose their activity, even though the total protein present in a sample may remain constant.

Absorbance assays are fast and convenient, since no additional reagents or incubations are required. No protein standard need be prepared and the assay does not consume the protein. The relationship of absorbance to protein concentration is linear. However, different proteins and nucleic acids have widely varying absorption characteristics. Any non-protein component of the solution that absorbs ultraviolet light could also interfere with the assay. The most common use for the absorbance assay is to monitor fractions from chromatography columns as in this case.

Proteins in solution absorb ultraviolet light with absorbance maxima at 280 and 200 nm. Amino acids with aromatic rings are the primary reason for the absorbance peak at 280 nm. Peptide bonds are primarily responsible for the peak at 200 nm. Secondary, tertiary, and quaternary structure all affect absorbance, therefore factors such as pH, ionic strength, etc. can alter the absorbance spectrum [11].

Absorbance Assay at 280nm

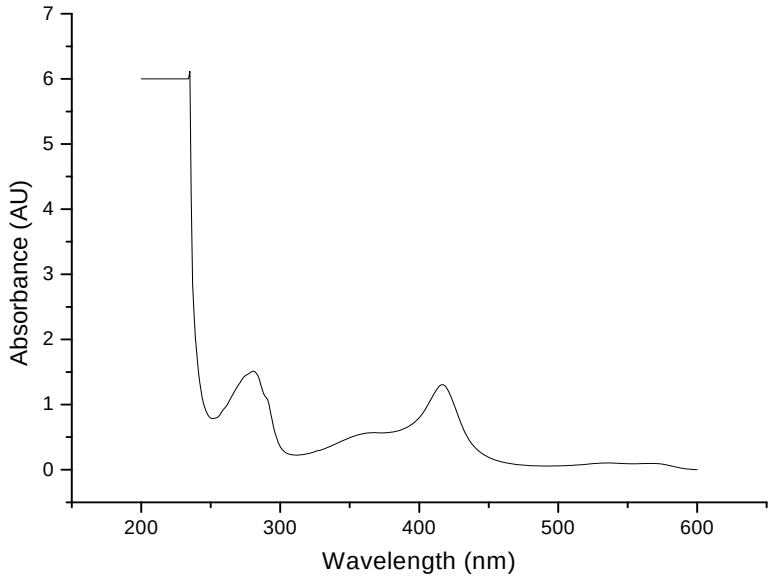

Figure 35. **Absorbance spectra of Cyp101 *P*450 protein in phosphate buffered saline (pH7.4).**

Figure 35 shows an absorbance peak at approximately 400nm (haem peak) and at approximately 280nm (protein peptide backbone peak). This confirmed that the expressed and purified protein had an intact structural conformation.

3.2.7 NADPH consumption activity assay via UV vis absorption spectroscopy

This time, the proteins activity was investigated and the loss of co enzyme, shown in Figure 36, was observed in the assay. The enzyme under investigation was at low concentrations compared with the other two, putidaredoxin and putidaredoxin reductase, which were in excess.

These two additional enzymes enable a flow of electrons down a potential gradient from NADPH to putidaredoxin reductase to putidaredoxin itself which needs to be present in order for this particular *P*450 protein to be active.

A 2x reaction buffer was prepared, which consisted of buffer P with 200mM KCL and 2mM camphor.

The three enzymes, P redoxin, P reductase and *P*450cam, were then added. The reaction solution mixture was then placed into a 1ml cuvette and positioned in a spectrophotometer which was set at 340 nanometres. The NADPH was then added, the cell was inverted to mix and measurements were taken.

Concentrations of original stock solutions.

*P*450cam 29.6µM
Putidaredoxin 80µM
Putidaredoxin reductase 37.4µM
NADH 156mM

In final reaction of 1ml

*P*450cam 0.1µM (3.38µl)
Pd 10uM (125µl)
PdR 1uM (26.6µl)
NADH 250uM (1.6µl)
Reaction buffer (50mM Tris pH7.4 with 2mM camphor) (480µl)
Buffer T (50mM Tris pH 7.4)

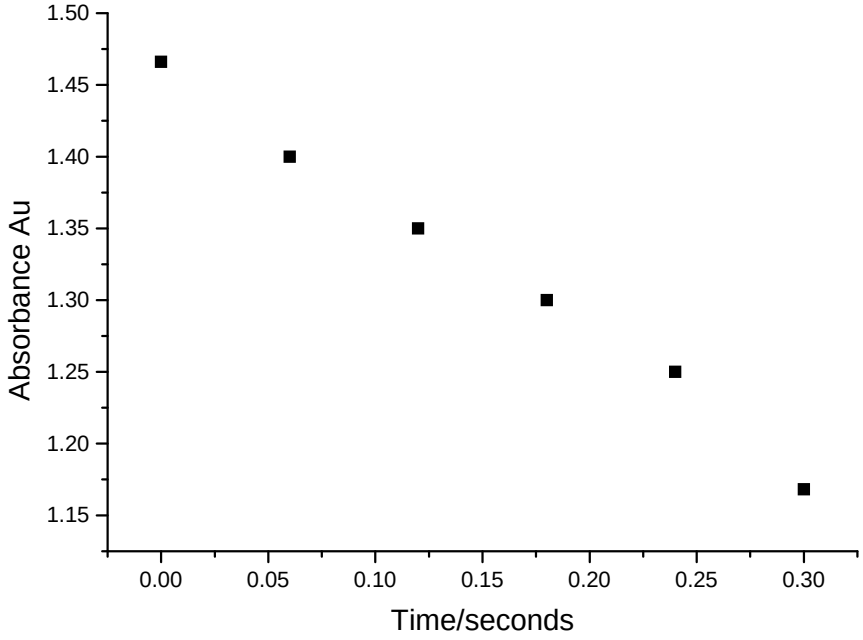

Figure 36. **NADPH consumption activity assay via UV vis absorption spectroscopy of Cyp101 *P*450 protein, P. redoxin and reductase in reaction buffer at 340nm.**

The activity number was calculated as follows;

Where

ΔA_{340} = change in absorbance at 340 nanometres divided by:

Δt = time of linear decrease in absorbance.

[E] = concentration of enzyme in μM.

6.22×10^{-3} = extinction coefficient of NADPH

Activity number = number of mols NADPH consumed per mol of enzyme per second.

$N = \Delta A340 / (\Delta t \times 6.22 \times 10^{-3} \times [E])$

Beers law was used to calculate the proteins activity number.

Five runs produced an average activity of N/Sec^{-1} 24.85 which compared favourably to published results [3, 9.]

The Beer-Lambert law (or Beer's law) is the linear relationship between absorbance and concentration of an absorbing species. When working in concentration units of molarity, the Beer-Lambert law is written as:

$$A = \varepsilon \cdot b \cdot c \qquad \textbf{Equation 9}$$

Where :

A is absorbance

ε is the wavelength-dependent molar absorptivity coefficient with units of M^{-1} cm^{-1}.

b is the light path length in cm

c is the concentration of the absorbing compound

These experiments showed that the expressed and purified Cyp101 *P*450 protein had intact structural conformation as well as enzymatic activity.

3.3 The extraction of microsomal *P*450 protein from *Drosophila Melanogaster.*

Microsomes can be concentrated and separated from other cellular organelles by using a centrifuge to produce differential centrifugation. Unbroken cells, nuclei, and mitochondria sediment out at 10,000g, whereas soluble enzyme and fragmented ER, which contains the *P*450s, remain in solution. At 100,000g, achieved by faster centrifuge rotation, ER sediments out of solution as a pellet but the soluble enzymes remain in the supernatant. In this way, *P*450s in microsomes are concentrated and isolated.

3.3.1 Microsome preparation

Drosophila Melanogaster flies were collected at less than seven days old and snap frozen in liquid nitrogen. They were then stored at -80°C for use in future assays.

All buffers were kept at 4ºC
100 mM phosphate buffer pH 7.2 (K_2HPO_4/KH_2PO_4)
1 mM EDTA (ethylenediaminetetraacetic acid)
0.1 mM DTT (dithiothreitol)
0.4 mM PMSF (phenylmethylsulphonylfluoride)

All work was carried out on ice. The heads were removed from the flies by placing them in liquid nitrogen then transferring to a brass sieve (850 μm aperture, Fisher cat no. SIH-400-150B) and running fingers over the flies. The flies were crushed in 5 ml phosphate buffer in a 5ml hand homogenizer, then filtered through muslin and transferred back to the homogenizer with another 5 ml phosphate buffer added and the flies crushed and filtered again. The solution was then centrifuged at 10000g for 15 min at 4˚C. The supernatant was then centrifuged at 100,000g for 1h15mins at 4˚C. The pellet was then resuspended in 1ml of 100 mM phosphate buffer and 20% glycerol in a 2 ml hand homogenizer. The preparation was then frozen in liquid nitrogen in 200 μl aliquots.

3.3.2 Bradford dye binding protein assay for the detection of protein concentration.

This assay is based on the observation that the absorbance maximum for an acidic solution of Coomassie Brilliant Blue G-250 shifts from 465nm to 595nm when protein binding occurs. Both hydrophobic and ionic interactions stabilize the anionic form of the dye, causing a visible colour change. The assay is useful since the extinction

coefficient of a dye-albumin complex solution is constant over a higher protein concentration range[12].

1 µl of microsomes were added to 99 µl water and 900 µl of Bradford Reagent (Sigma B6916) and left to stand for 10 minutes. The solution was then inverted once to mix and then analysed in a spectrophotometer at 595nm.

The experiment was then repeated with more or less microsome solution until an adequate number of data points were gathered. The results shown in Table 1 were then compared to a standard curve constructed using know amounts of bovine serum albumin (BSA, Sigma A7517), to calculate the total protein present.

0.5µl each	µg/ml/sample	mg/ml
CS4	15051.395	15.051
CS5	17356.828	17.357
CS6	15242.291	15.242
HR4	14111.601	14.112
HR5	13406.755	13.407
HR6	20983.847	20.984

Table 1. **Table showing the amount of protein in mg/ml of each HR (HikonR) resistant and CS (CantonS) susceptible, microsomal protein samples.**

3.3.3 Microsomal *P*450 protein oxygen consumption activity assay using a Clark electrode.

Next, the activity of the microsomal protein was investigated. The monitoring of oxygen loss in this assay, shown in Figure 38, indicated substrate turnover and measurable enzyme activity.

Leland C. Clark developed an enzyme electrode in 1962 which made this kind of investigation possible [13]. In his electrode glucose oxidase, which reacts with oxygen, was trapped on the surface of a platinum electrode and this made it possible to follow the enzymes activity by measuring oxygen concentration changes due the reduction of oxygen in the presence of the enzyme. The electrochemical reaction at the surface of the platinum electrode produced a change in current that was measurable. Rosenthal, Cooper, and Estabrook went on to study the metabolism of codeine, monomethyl-4-aminopyrine, and acetanilide, and found them to be inhibited by carbon monoxide. This CO inhibition went on to demonstrate that cytochrome *P*450 is the oxygen-activating enzyme in xenobiotic metabolism [14].

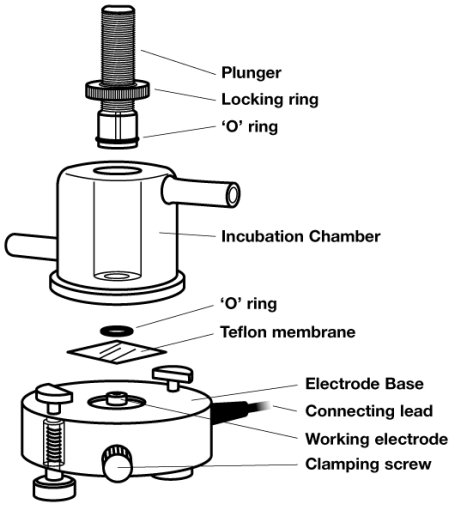

Figure 37. **Glass Clark Oxygen electrode** *(Adapted from Severinghaus 1986)*

A Clark oxygen electrode, shown in Figure 37, is composed of two half cells separated by a salt bridge. A platinum electrode is separated from a solid silver electrode by insulating material. A concentrated potassium chloride solution is held in place over the surfaces of the electrodes by a Teflon membrane which is attached by an O-ring that surrounds the electrodes. The oxygen monitor holds a constant voltage difference across the two electrodes so that the platinum electrode is negatively charged with respect to the silver electrode.

Platinum is a strong catalyst for the covalent dissociation or re-association of water. In the Clark electrode, electrons combine with dissolved molecular oxygen and hydrogen

ions to produce water. The rate of electron movement is proportional to the concentration of oxygen that is available to react with them. The movement of electrons is an electrical current which is then converted to a voltage by the oxygen monitor circuitry [15, 16].

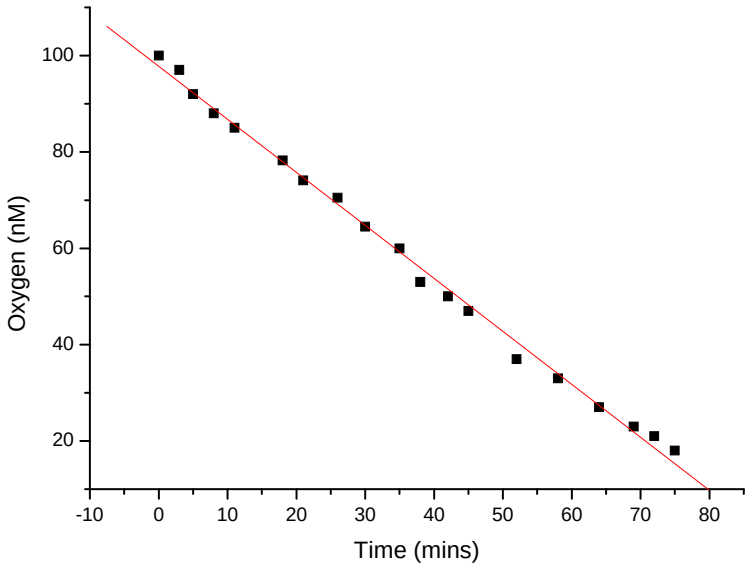

Figure 38. **The detection of oxygen consumption by microsomal *P*450 enzymes Hikon R (resistant strain).**

The water bath was kept at a constant 26ºC and stirred. The reaction chamber contained 50µl of microsomal *P*450 together with 3µl of 1mM MRES substrate and 100µl of 0.079mol dm^{-3} NADPH. The final volume in the reaction chamber was made up to 3.5mls with phosphate buffer at pH7.4.

9.628nM oxygen per min was consumed in the assay which compared favourably with the literature [3, 4.]

3.4 Chapter Summary

The work in this chapter produced two functional Cytochrome *P*450 proteins. Firstly, Cyp101 from the bacteria Pseudomonas Putida by a somewhat labour intensive and time consuming process of extraction and purification. Secondly, Cyp6g1 from the fruit fly Drosophila Melanogaster by an extraction method which yielded functional microsomal proteins. It was crucial to determine the purity of the extraction and purification processes at each step and most importantly, that both processes yielded functionally active proteins with structural integrity. The success of this protein production process allowed the following two experimental stages to go ahead.

Next, the investigation of microsomal *P*450 proteins from the fruit fly *Drosophila Melanogaster* and their associated substrate biotransformation mechanisms are presented. This particular proteins' activity was probed using both electrochemical and fluorescent methods and focused on the *P*450 gene intrinsic in metabolic resistance in the fly.

3.5 References

1. Garrett, R.H. & Grisham, C.M. **1998.** *Biochemistry.* Thompsom Learning, UK.

2. Alberts B. **2001** *Molecular Biology of the Cell.* Garland Science, UK.

3. Ehle H and Horn A **1990** *Bioseparation. Immunoaffinity chromatography of enzymes.*. 1(2) pp97-110.

4. Regnier FE **1993.** *Science. High-performance liquid chromatography of biopolymers* 222 (4) pp245-52

5. Lewis, D.F.V. **2001**. *Cytochromes P450. Structure and Function.* Taylor and Francis. London, UK.

6. Ortiz de Montellano **1995** *Cytochrome P450. Structure, Mechanism and Biochemistry.* Kulwer Academic, USA.

7. Lebart, M.C **1993**, *Journal of Biol. Chem*. 268 (8) pp5642.

8. Tietz **2005** *Textbook of Clinical Chemistry and Molecular Diagnostics*. Saunders (W.B.) Co Ltd, UK.

9. Corthier, G J. **1994** *Immunol. Meth*. 66 (1) pp75.

10. Dawson JH. **1988** *Science. Probing structure-function relations in heme-containing oxygenases and peroxidases.* 240(4851) pp433-9.

11. Stoscheck C. M. **1990** *Quantitation of Protein. Methods in Enzymology* 182 pp50-69.

12. Bradford, M.M. **1976** *A rapid and sensitive test for the quantitation of microgram quantities of protein utilizing the principle of protein dye binding. Analytical Biochemistry* 77 pp 248-254.

13. Clark L.C and Gollan F **2002** *Ann Thorac Surg. bubble oxygenators and perfusion hypothermia* 74(2) pp612-4.

14. Cooper, D. Y., Levin, S., Narasimhulu, S., Rosenthal, O., and Estabrook, R. W. **1965** *Science Photochemical action spectrum of the terminal oxidase of mixed function oxidase system.* 147 pp400–402

15. Clark L.C **1953** *J Appl Physiol Continuous Recording of Blood Oxygen Tensions by Polarography* 6 pp189-193.

16. Severinghaus, J.W., and Astrup, B.P. **1986.** *J Clin Monit History of Blood Gas Analysis IV. Leyland Clark's Oxygen Eelctrode* 2 pp125-139.

4 Methoxy-resorufin ether as an electrochemically active biological probe for Cytochrome *P*450 *O*-demethylation

4.1 Introduction and Aims

This chapter describes the utilization of the substrate methoxy resorufin ether (MRES) as an electrochemical probe for investigating the activity of the specific microsomal *P*450 protein, Cyp6g1, found in the fruit fly *Drosphila melanogaster* which is intrinsic in providing metabolic resistance.

MRES has been used extensively as a versatile substrate for *P*450 proteins and its demethylated product, Resorufin, has fluorescent properties. Recent work has shown the utilization of MRES in detecting the activity of the *P*450 protein Cyp1B1. The study investigated this protein, which is found in renal cell carcinoma, and its activity was observed by the fluorescent detection of the substrates product [1]. Also, xenobiotic metabolism in rat and human liver microsomes has been assessed spectrofluorometrically by following the demethylation of the substrate MRES in another recent study [2].

In this work however, it has been shown that in addition to the established fluorescent properties, MRES also exhibits reversible electron transfer characteristics. Cyclic voltammetry and differential pulse voltammetry measurements have shown that the substrate can be detected easily at low concentrations in a conventional three electrode electrochemical cell.

When in contact with the *P*450 protein Cyp6g1, the enzyme mediated demethylation of MRES took place and was probed using electrochemical techniques.

Figure 39 shows the *P*450 mediated de-methylation of the substrate which results in the end product resorufin. By observing this mechanism, it was possible to investigate the activity of the microsomal *P*450 protein in the fruit fly by using both fluorescent and electrochemical techniques. This work went on to show that these electrochemical measurements could discriminate between the activities of proteins from flies of two different strains.

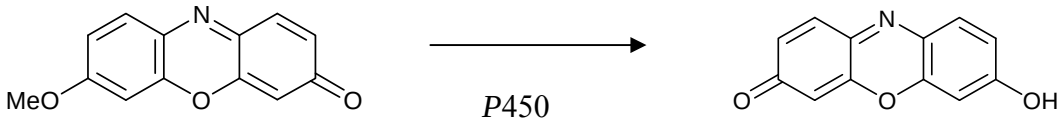

Methoxy resorufin ether (MRES) Resorufin

Figure 39. **The Cyp6g1 enzyme mediated demethylation of the substrate methoxy resorufin ether resulting in the product resorufin.**

MRES is water soluble and electrochemically active with a reduction potential of approximately -0.19 V vs Ag/AgCl shown in Figures 40 and 41. The substrate product, resorufin, is electrochemically reduced at more negative potentials and also exhibits fluorescent properties.

These important features facilitated parallel methods of probing the activity of the *P*450 enzyme, the fluorescent response of the demethylated product and the electrochemical properties of the MRES substrate.

The fruit fly used in this work provided a useful and significant model for the investigation into the mechanisms underpinning *P*450 mediated drug and pesticide biotransformation within a whole organism. All of the *P*450 genes in Drosophila have been identified [3] and the mutation within one of these genes, Cyp6g1, has been shown to be responsible for the over expression of its corresponding enzyme.

Direct electrochemical measurements of *P*450s have been performed using varied methods and this has facilitated the observation of the reduction of haem centres within the protein [4, 5.] A number of *P*450 proteins have been found to exhibit MRES *O*-dealkylase activity, including the Cyp1A2 and Cyp3A6 enzymes found in the human liver [6].

This work has demonstrated that it was possible to discriminate between two different protein microsomes extracted from insecticide resistant and insecticide susceptible *Drosophila* by following the rate of *O*-demethylation of the MRES substrate electrochemically.

A fluorometric assay was also carried out which showed the rate of production of the substrate product, resorufin. These results confirmed the dependence on fly strain on substrate turnover rate.

The involvement of *P*450 in substrate turnover was confirmed by arresting the proteins' haem activity. Previous work has shown that Carbon Monoxide (CO) in the presence of substrate ligates the haem iron centre of the protein and thus prevents access for the oxygen molecule and so prevents substrate turnover [7].

The introduction of CO and the omission of the electron donor NADPH in the experimental set up, confirmed that substrate metabolism was indeed *P*450 mediated. The study went on to show that both the electrochemical and the fluorometric results showed corresponding effects of substrate turnover arrest by two different methods.

4.2 Metabolic resistance in the fruit fly *D. melanogaster*

There are several classes of enzymes that have, in the past, been implicated in insecticide resistance. These are Glutathione S-transferases (GSTs), esterases and Cytochrome *P*450s [8]. In some cases, one type of enzyme is used in an insect almost exclusively for all its metabolic resistance mechanisms, such as *D. melanogaster* using *P*450s [9]. However, other classes of insect will make use of a wide range of mechanisms to confer resistance to a variety of insecticides such as *M. domestica*[10].

Dichloro-Diphenyl-Trichloroethane (DDT) was the first modern pesticide and is arguably the best known organic pesticide. It is a highly hydrophobic, colorless solid with a weak chemical odor and is almost insoluble in water but has a good solubility in most organic solvents, fats and oils [11].

D. melanogaster has been shown to have DDT resistance caused by over-expression of a specific *P*450 protein and organophosphate resistance can be conferred by amino acid substitutions in an esterase gene [12].

Metabolic resistance works by an enzyme being altered; either its amino acid sequence is mutated making it better able to metabolise an insecticide or an enzyme can be over-transcribed and so it takes a higher dose of insecticide to kill the resistant insect.

With enzymes such as *P*450, it has been shown that a single amino acid substitution is sufficient to cause a large change in substrate specificity. An example of this is in the human *P*450 CYP2C2, which is a lauric acid hydrogenase, but a single amino acid substitution of S473V changes the substrate specificity to accept the hormone

progesterone [12]. In this way we can see that a small change in sequence can have large consequences for substrate specificity and therefore either cause a genetic disease in mammals or as in the this case, cause insecticide resistance.

The genome of *D. melanogaster* contains 87 genes predicted to encode functional *P*450 enzymes. This would appear to be about the average for complex animals, with humans, mice and *C. elegans* all having around 50 to 90 *P*450s [13]. However, research in this area continues and new *P*450 proteins are being discovered continually.

Many of these enzymes will be involved in endogenous processes and will therefore be necessary for the development of the insect. It is almost certain that a large number will have evolved to metabolise plant xenobiotics and so increase the range of environments in which the fruit fly can survive [14].

In the brief history of insecticide resistance there have been many published cases and the majority of the examples of metabolic resistance are due to changes in the *P*450 profile. In some cases *P*450 proteins are induced in the presence of plant xenobiotics such as nicotine, and this has lead to the insect being able to feed on a previously toxic plant [15]. It is not difficult to see how insecticide resistance could evolve in an analogous way. Instead of evolution over millions of years to tolerate a plant xenobiotic, it has been shown that new cases of insecticide resistance have evolved in just 50 years or less [16].

In many cases the up-regulation of a *P*450 would be deleterious to an organism. The organism would show a decreased fitness under normal conditions but in the presence of an insecticide, the insect with the mutant form of *P*450 would thrive and so pass on its genes [17]. There are many laboratory cases where resistance has been induced by a gradual increase of toxin concentration over many generations and this has led to the organism showing a slightly higher expression of one particular enzyme [18.] However, in many of these cases the up-regulation is not permanent and when the toxin is removed from the diet the enzyme profile returns to that of a susceptible insect. Subsequently the same numbers of generations are again needed to reselect for the up-regulation of the gene, and therefore resistance [19].

Work carried out in the 1960s employed the simple method of collecting strains from areas thathad been heavily sprayed with DDT which lead to fly strains being collected from around Hikone City in Japan.

4.3 DDT resistance and the Cyp6g1 gene

Insecticide resistance is one of the most widespread genetic changes caused by human activity, but little is understand about the origins and spread of resistant alleles in global populations of insects. Transgenic analysis of Cyp6g1 shows that over transcription of this gene alone is both necessary and sufficient for insecticide resistance [20].

Insecticide resistance in laboratory selected *Drosophila* strains has been associated with up regulation of a range of different cytochrome *P*450s. *D. melanogaster* resistance to DDT and other compounds, is conferred by one *P*450 gene, Cyp6g1, so DDT resistance in Drosophila is associated with the over-expression of this particular protein coded for by the Cyp6g1 gene [21].

The fly strains used in these experiments were 'Hikone-R', a resistant strain established from field collections in the early 1960s [22,23]. This work showed that only Cyp6g1 was over transcribed relative to Canton-S, a susceptible reference strain.

The genes for the cytochrome *P*450s are a large family involved in a wide variety of metabolic functions. In insects, these enzymes play roles in key processes ranging from host plant utilization to xenobiotic resistance [24]. Within the complete genome sequence of *D. melanogaster*, some 90 individual *P*450 genes have been identified [25].

4.4 Experimental

4.4.1 Protein Microsome preparation

Drosophila Melanogaster flies were collected at less than seven days old and snap frozen in liquid nitrogen. They were then stored at -80°C for use in future assays.

All buffers were kept at 4ºC

100 mM phosphate buffer pH 7.2 (K_2HPO_4/KH_2PO_4)
1 mM EDTA (ethylenediaminetetraacetic acid)
0.1 mM DTT (dithiothreitol)
0.4 mM PMSF (phenylmethylsulphonylfluoride)

All work was carried out on ice. The heads were removed from the flies by placing them in liquid nitrogen then transferring to a brass sieve (850 μm aperture, Fisher cat no. SIH-400-150B) and running fingers over the flies. The flies were crushed in 5 ml phosphate buffer in a 5ml hand homogenizer, then filtered through muslin and transferred back to the homogenizer with another 5 ml phosphate buffer added and the flies crushed and filtered again. The solution was then centrifuged at 10000g for 15 min at 4˚C. The supernatant was then centrifuged at 10,0000g for 1h15mins at 4˚C. The pellet was then resuspended in 1ml of 100 mM phosphate buffer and 20% glycerol in a 2 ml hand homogenizer. The preparation was then frozen in liquid nitrogen in 200 μl aliquots.

4.4.2 Determination of protein preparation concentration.

1 μl of microsomes was added to 99 μl water and 900 μl of Bradford Reagent (Sigma B6916) and left to stand for 10 minutes. The solution was then inverted once to mix and then analysed in a spectrophotometer at 595 nm. The theoretical considerations of this method are explained in chapter 3. The experiment was then repeated with more or less microsome solution until an adequate number of data points were gathered. The results from Table 2 were then compared to a standard curve constructed using know amounts of bovine serum albumin (BSA, Sigma A7517), to calculate the total protein present.

0.5µl each **S = susceptible** **R = resistant**	**mg/ml microsomal protein**
Canton S sample 4	15.051
Canton S sample 5	17.357
Canton S sample 6	15.242
Hikon R sample 4	14.112
Hikon R sample 5	13.407
Hikon R sample 6	20.984

Table 2. The results of the Bradford Dye binding assay to determine the protein concentration in mg/ml for each fly strain sample.

4.4.3 Electrochemical Cell Set-Up.

An Autolab12 potentiostat was used in conjunction with General Purpose Electrochemical Software (GPES) version 4.9. The differential pulse mode was selected and the voltage swept from zero to –0.04volts. The step potential was 0.00105 volts and the modulation amplitude 0.04495 volts. A current range of 100uA to 100nA was selected.

Differential pulse Voltammetry (DPV) parameters were; start potential 00V, end potential -0.4 V vs Ag/AgCl. Step potential was 1mv and the modulation potential was 50mV. The modulation time was 40ms and the interval time, 100ms. The scan rate was $10mV^{-1.}$

A protein microsome concentration of 2mg ml^{-1} in phosphate buffered saline (pH7.4) was used with an initial MRES concentration of 1µmol dm^{-3} in the electrochemical cell which made a total cell volume of 400µl.

For the experiments which employed the cofactor NADPH, a final concentration of 2.5 mmol dm^{-3} was achieved. For the experiments which used CO, the gas was bubbled through the solution for ca. 10ml^{-1} for 20 minutes.

A BAS MF-2031 low volume cell was used and placed in a glass vessel containing phosphate buffer adjusted to pH 7.4. Argon gas was bubbled through the buffer for ca.

30 minutes prior to any measurements to exclude oxygen. An edge plane graphite working electrode and a Ag/AgCl reference electrode, together with a gold counter electrode were used in the set-up.

A baseline measurement was firstly recorded using the electrochemical cell set-up in phosphate buffer only. The microsomal protein and MRES (Sigma M1544) were then added and another measurement taken.

The volume of each protein sample solution added to the electrochemical cell was calculated to give a final concentration of 2mg per ml. The same volume of substrate was dissolved in phosphate buffer and then added at a final concentration of 1μM. 2μl of a 4 mol dm^{-3} solution of NADPH in phosphate buffer was then added and differential pulse measurements were taken immediately every ten minutes over 200 minutes for each separate protein sample.

A corresponding experiment was run in tandem for each protein preparation following the above protocol with the electron donor NADPH omitted.

The properties of MRES as an electrochemical probe were investigated using cyclic voltammetry (CV). An MRES solution of 5mmol dm^{-3} was made by adding a small amount of ethanol and then dispersing in 50mM phosphate buffered saline (pH 7.4) to produce a 0.1 mmol dm^{-3} final MRES solution. This solution was then degassed under Argon. A freshly polished glassy carbon or edge plane graphite electrode of 3mm diameter was used as the working electrode.

The cyclic voltammetry measurements were made by cycling between +0.1 V and -0.4 V vs Ag/AgCl at scan rates between 10mV s^{-1} and 600mV s^{-1}.

The experiments were repeated with carbon monoxide (Aldrich 295116) bubbled through the protein solution for ten minutes immediately prior to adding MRES and NADPH.

All electrochemical measurements were performed a minimum of three times and all trends were found to be reproducible.

4.5 Results and Discussion

4.5.1 Electrochemical Properties of the substrate Methoxy Resorufin Ether (MRES).

Cyclic voltammetry and differential pulse voltammetry measurements of MRES only, showed that the substrate was clearly electrochemically active and the peak separation suggested a two electron transfer process. The electrochemical properties of this substrate went on to provide an indicator of protein activity and demonstrated a clear difference in the activity of protein from both susceptible and resistant fly stains.

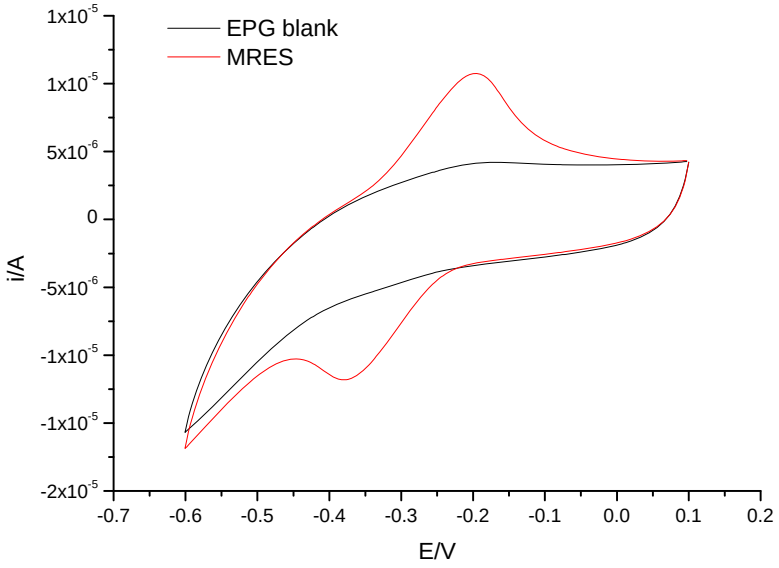

Figure 40. Cyclic voltammograms (scan rate 0.1Vs^{-1}) from edge plane graphite (EPG)

The working electrode was immersed in 50mM phosphate buffered saline (pH 7.4) with 0.1mmol dm^{-3} MRES showing peak reduction and oxidation. The reference electrode was Ag/AgCl and the buffer was bubbled with Argon prior to measuring.

Next, increasing concentrations of MRES only were measured using differential pulse voltammetry (DPV).

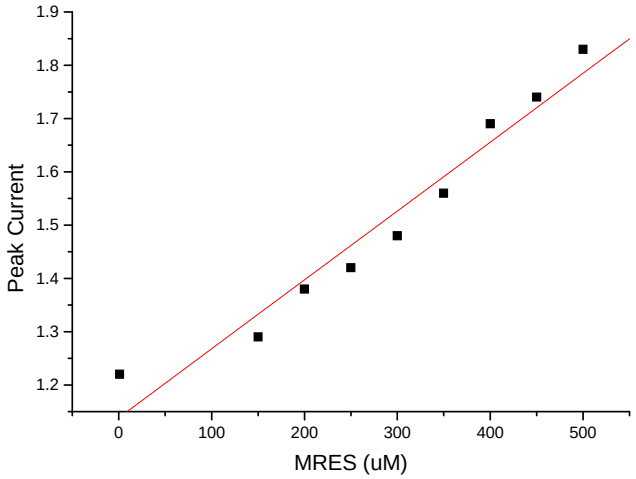

Figure 41. Plot showing peak current/scan rate^{½} of Voltammogram (DPV) from glassy carbon working electrode.

The electrode was immersed in 50mM phosphate buffered saline (pH 7.4) with increasing concentrations of MRES. The reference electrode was Ag/AgCl and the buffer was bubbled with Argon prior to measuring.

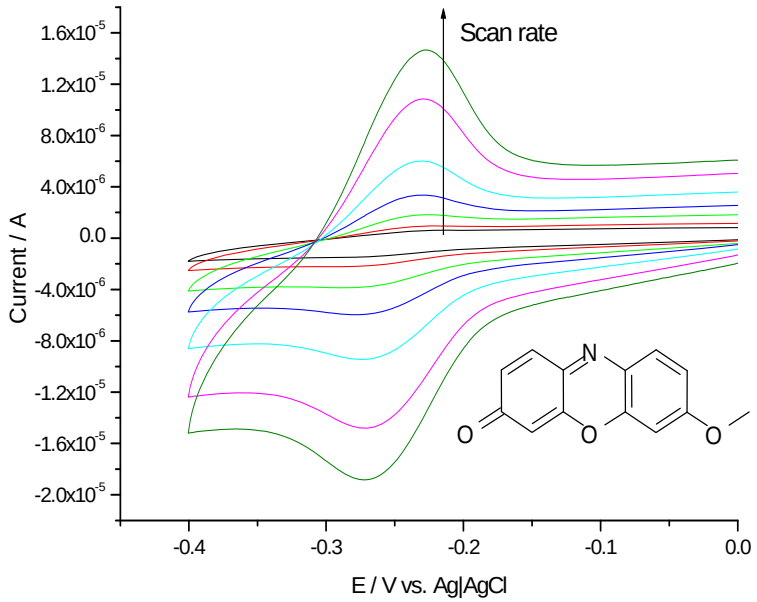

Figure 42. Cyclic voltammograms of 0.1mmol dm^{-3} MRES showing peak reduction at increasing scan rates.

Sweep rates were at 10, 20, 50, 100, 200, 400 and 600 mV s $^{-1}$. The peak reduction current of the substrate MRES was measured at – 265 V vs Ag/AgCl. In these experiments, results shown on Figure 42, the peak current was proportional to the concentration of MRES. The substrate had a more cathodic reduction potential at -0.32 V vs Ag/AgCl. This allowed electrochemical detection of substrate concentration in real time [25].

The separation between the oxidation and reduction peaks for scan rates at 100 to 600mV s $^{-1}$ gave an average value of 37mV shown in the figure below. Although somewhat higher than the theoretically predicted 29.5mV, it was still much lower than the theoretical value for 1 electron transfer of 59mV [29]

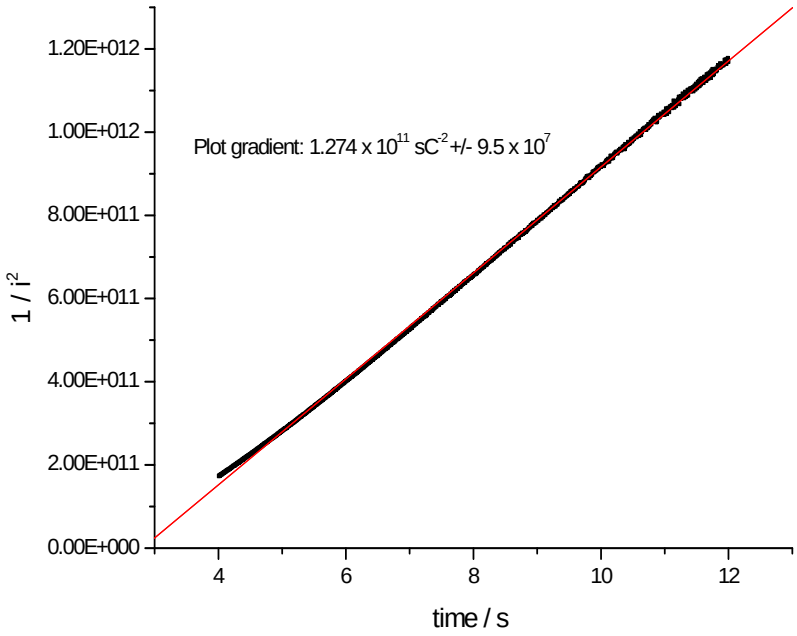

Figure 43. **Cotrell plot ($1/i^2$ vs t) for 0.1 mmoldm^{-3} MRES for the determination of the diffusion coefficient.**

A plot,shown in Figure 43, of the square root of scan rate vs. peak anodic current was linear, suggesting diffusion controlled mass transport of MRES to the electrode. Chronoamperometry measurements were performed in order to estimate a value of the diffusion constant of MRES. The current time response was re-plotted as $1 / i^2$ vs. time, but with all data in the first two seconds after the pulse being disregarded as this current contains a significant contribution from the capacitive charging of the electrode. A linear fit of the data, shown below, revealed a diffusion coefficient for MRES to be 1.3 x 10^{-9} m^2s^{-1}.

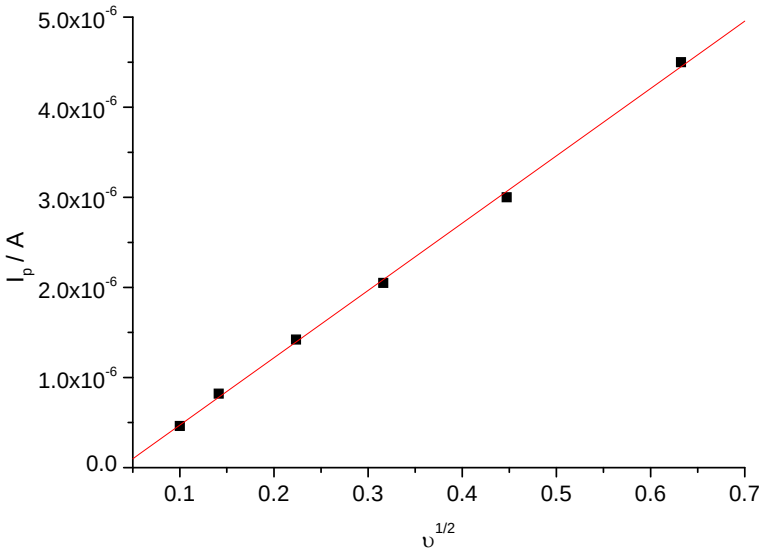

Figure 44. Plot showing peak current vs scan rate^{½} for 0.1mmol dm^{-3} Methoxy Resorufin Ether.

The plot in Figure 44 shows the linear relationship between square root of sweep rate and the peak anodic current indicating that the overall process was diffusion controlled.

4.5.2 Electrochemical study of methoxy-resorufin ether *O*-demethylation by the microsomal protein CYP6G1.

Firstly, the microsomal protein activity from the resistant fly strain Hikon R was investigated. The resistant strain of fly had increased levels of *P*450 protein due to the over transcription of the Cyp6g1 gene and so maintained its ability to readily turnover substrate. Two experiments were carried out in tandem. Both electrochemical cells contained aqueous protein in de gassed buffer and MRES substrate. The enzyme co factor NADPH was added to one cell but omitted from the other and the measurement start times synchronized.

For these experiments it was necessary to have a low concentration of MRES in order that substrate depletion might be observed. The concentration was calculated and adjusted from the results of the Hikone-R fluorescence study, shown later in this chapter, made in the presence of NADPH. The problem with working with low

concentrations of MRES is that the charging current of the electrode obscures the Faradaic electrochemical response of the substrate itself. For this reason it was necessary to use differential pulse voltammetry (DPV), which effectively subtracted the charging current contribution from the total measured current, thus allowing voltammetric resolution of low concentration electroactive species. Further electrochemical measurements were performed to study substrate metabolism in the presence and absence of both the electron donating co-factor NADPH and *P*450 inhibitor carbon monoxide, thus confirming that MRES biotransformation was both NADPH dependent and CO inhibited.

The following figures showed the change in cathodic current of MRES as it was boitransformed by the protein. A clear difference in rate of substrate metabolism was observed.

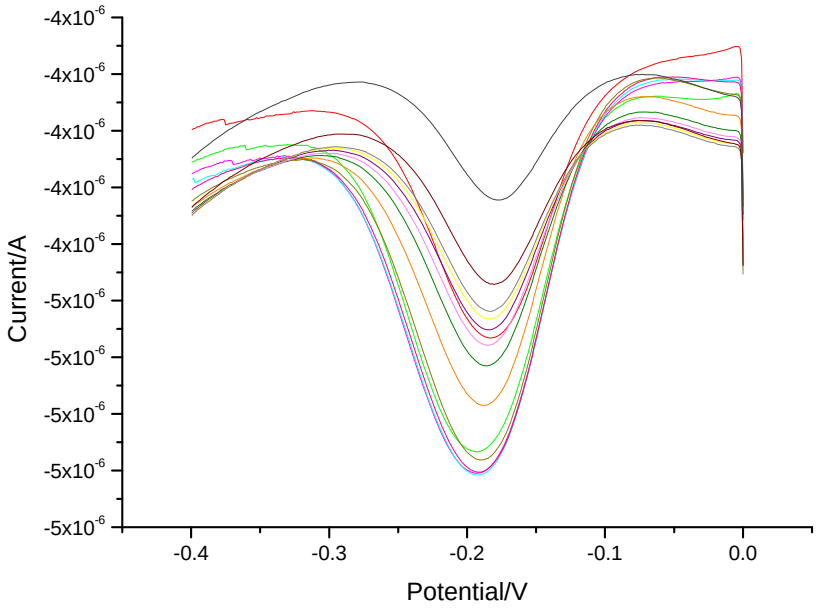

Figure 45. **Differential Pulse Voltammogram showing the biotransformation of the substrate MRES by Cyp6g1 microsomal protein from the** resistant **fly strain** Hikon R **over time.**

In Figure 45 measurements were recorded every ten minutes from zero to eighty minutes. The cell contained an aqueous solution of 2mg/ml of protein & 1µM substrate all in phosphate buffered saline (pH 7.4) degassed with argon. 2µl of

4mol dm $^{-3}$ NADPH was added prior to measuring. The reference electrode was Ag/AgCl.

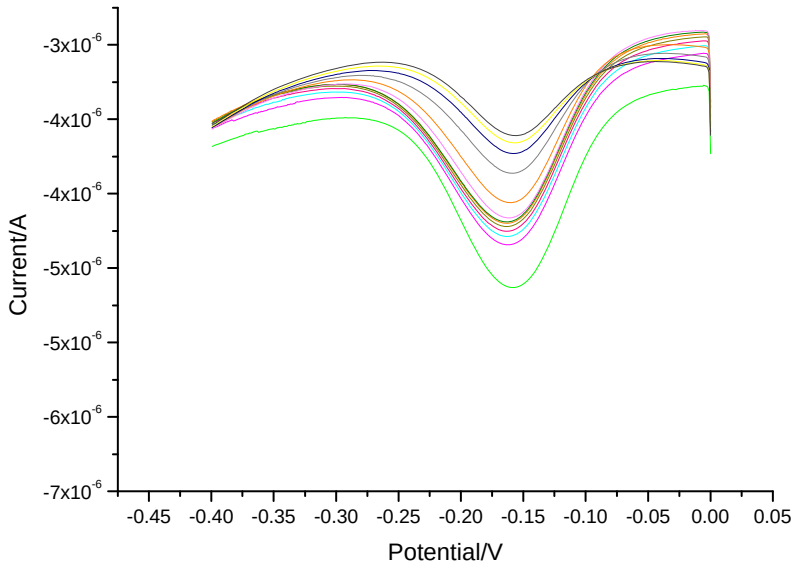

Figure 46. **Differential Pulse Voltammogram showing the biotransformation of the substrate MRES by Cyp6g1 microsomal protein from the** resistant **fly strain** Hikon R **over time.**

In Figure 46 measurements were recorded every ten minutes from zero to eighty minutes. The cell contained an aqueous solution of 2mg/ml of protein & 1μM substrate all in phosphate buffered saline (pH 7.4) degassed with argon. The reference electrode was Ag/AgCl.

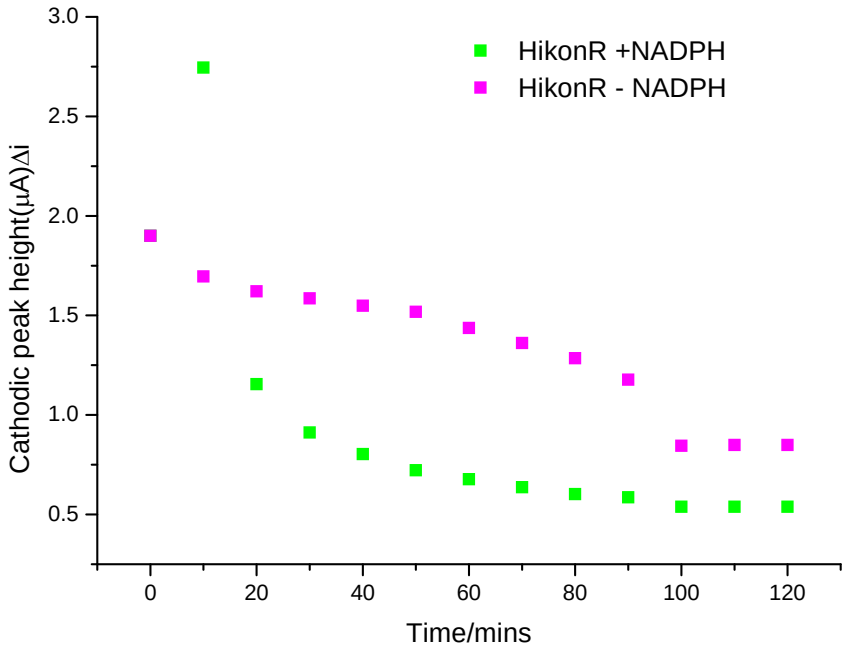

Figure 47. **Electrochemical determination of MRES substrate concentration measured as a function of time for protein microsomes from Hikone-R fly strain in the presence and absence of NADPH co-factor.**

The difference in the substrate turnover rates by proteins from the two different fly strains, shown in Figure 48 were, then investigated. These experiments were carried out in the absence and presence of the co enzyme NADPH and with and without carbon monoxide which prevented substrate binding.

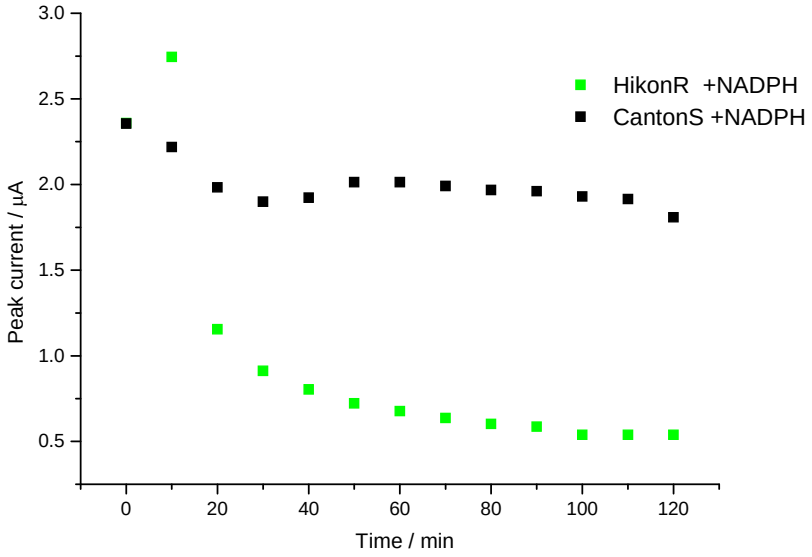

Figure 48. **Electrochemical determination of MRES substrate concentration measured as a function of time for protein microsomes from *Hikone-R* (resistant) and *Canton-S* (susceptible) fly strains.**
Note the increased rate of substrate biotransformation for the resistant strain. NADPH co-factor was present in both experiments.

Figure 49 shows the results of the same experiment was then carried out but this time carbon monoxide was bubbled through the aqueous protein sample from the resistant strain Hikon. The co factor NADPH was present and the substrate was then added immediately prior to measuring. CO in the presence of substrate ligates the haem iron of the protein and prevents access for the oxygen molecule and so inhibits substrate turnover [28]. This provided a clear indication that the protein was indeed active and biotransforming its substrate within the experimental set up.

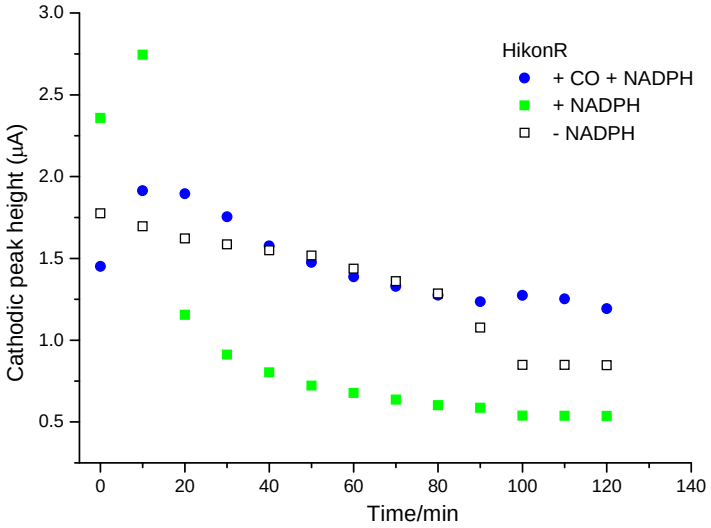

Figure 49. Electrochemical determination of NADPH dependence and CO inhibition of MRES biotransformation by *Hikone-R* (resistant) fly strain protein microsomes.

The reason for the increase in cathodic current observed at around 20 minutes was not clear, but may correspond to the enzymatic metabolism of methoxy-resorufin ether being more efficient at the start of the reaction. In this case an enhanced cathodic current would be expected, via an *EC* type reaction mechanism. The overall decrease in peak current with time for the two control systems may have been due to electrode fouling by the protein microsomes.

4.6 Fluorescent determination of *O* demethylation Methoxy Resorufin Ether by the microsomal *P*450 protein Cyp6g1

To further validate the electrochemical measurements, a fluorometric assay was performed to determine the concentration of resorufin which is the product of Cyp6g1 biotransformation of methoxy-resorufin ether. Although fluorescence is inherently more sensitive than electrochemistry, this technique measured the metabolite concentration rather than the starting material Methoxy Resorufin concentration.

A 200µl reaction solution was prepared in a Sterilin flat bottomed 96 well plate containing 250µg of Drosophila protein microsomes in 100mmol dm^{-3} sodium phosphate buffer (pH 7.8) together with 2.5 mmol dm^{-3} NADPH. The reaction was induced by the addition of the substrate at 0.25 mmol dm^{-3}. The plate reader (Labsystems Fluorocan Ascent, Thermo, UK) was set to 530nm excitation wavelength and 590nm emission wavelength and the reaction was read for 10 minutes. The results were then compared to a substrate standard curve which allowed the concentration of the metabolic product to be determined. Measurements were made using both the susceptible Canton S and the resistant Hikon R strains in the presence and absence of the co enzyme NADPH and with the addition of the *P*450 inhibitor carbon monoxide.

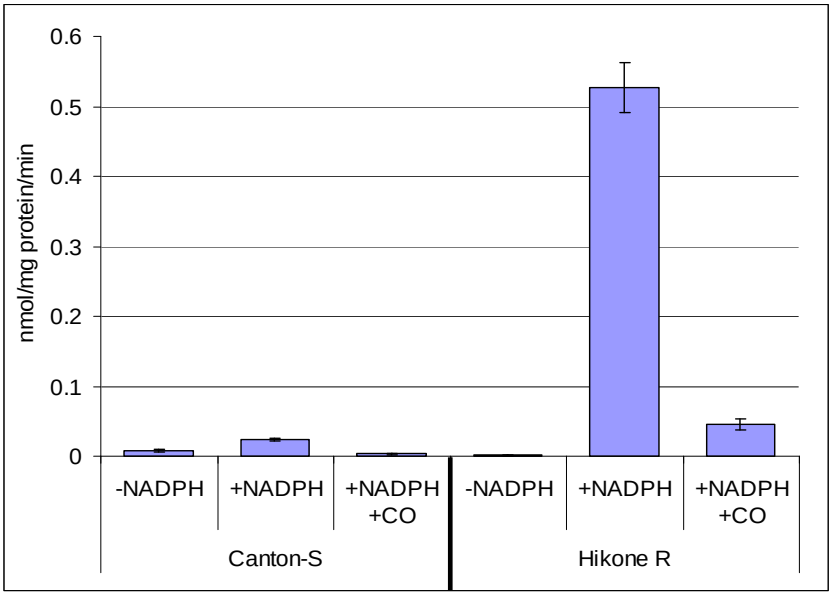

Figure 50. Fluorescence determination of the metabolic product resorufin by protein microsomes from Canton-S (susceptible) and Hikone-R (resistant) fly strains.

This shows moles of metabolic product being produced per minute / mg of protein. Metabolism of the MRES substrate was both NADPH dependent and CO inhibited.

These results in Figure 50 show the change in fluorescence for microsomes from insecticide resistant and susceptible fly strains. In order to determine the NADPH co factor dependence of the fluorometric response, two further measurements were carried out. Measurements were made in the absence and presence of NADPH and with the addition of the inhibitor CO. The resistant microsomes, which contain more Cyp6g1 showed greater rates of substrate metabolism than those from susceptible flies under these conditions. These results confirmed earlier gene analysis of insecticide resistant Drosophila, that a single gene, Cyp6g1, is over transcribed.

4.7 Chapter Summary

This work presented the first electrochemical study of the microsomal Cytochrome *P*450 protein Cyp6g1 from the fruit fly *Drosophila Melanogaster*. The extraction of microsomes containing this protein from two different fly strains has been described. The electrochemical measurements of the biotransformation of substrate methoxy-resorufin ether allowed the effects of the over transcription of a single gene Cyp6g1 to be investigated. This proved to be an effective way of directly following substrate metabolism and compared well with what is already known about the genetic differences in the two strains of *Drosophila* from which the protein microsomes were extracted. The results reinforced the findings from the fluorescence study of the substrate metabolic product. Similar electrochemical approaches in tandem with fluorescent measurements will therefore be useful in further investigations of other xenobiotic metabolising *P*450s. This technique would be particularly significant where electrochemically active drug related substrates are available or can be designed, for example, *P*450 mediated metabolism of the well known, but liver toxic pain killer, paracetamol (*N*-acetyl-*p*-aminophenol) which is electrochemically active.

The next chapter investigates microsomal *P*450 proteins from the fruit fly on an electrode surface.

4.8 References

1. Mc Fayden M.C, Melvin W.T, Murray G.I. **2004** *Br. J. Cancer Cytochrome P450 Cyp1B1 activity in renal cell carcinoma.* 91 pp966-971.

2. Day B J and Kariya C, **2005** *Toxicological Sciences* 85(1) pp713-719;

3. Daborn P J, Yen J.L, Bogwitz L.R, Le Goff G, Feil E, Jeffers F, Tijet N, Perry T, Heckel D, Batterham P, Feyereisen T, Wilson T and ffrench-Constant **2002** R, *Science A single P450 allele associated with insecticide resistance in Drosophila*, 297 pp 2253–2256.

4. Honeychurch M J, Hill H A O and Wong L L, **1999** *FEBS Lett The thermodynamics and kinetics of electron transfer in the cytochrome P450$_{cam}$ enzyme system*. 451 pp. 351–353.

5. Fantuzzi A, Fairhead M and Gilardi G, **2004** *J. Am. Chem. Soc Direct electrochemistry of immobilized human cytochrome P450 2E1* 126 , pp. 5040–5041.

6. Teel R.W and Huynh H, **1999** *Cancer Lett Modulation by phytochemicals of cytochrome P450-linked enzyme activity* 133 pp. 135–141.

7. Lewis D.F, **2001** *Guide to Cytochromes P450, Structure and Function* 1st Ed. Taylor and Francis, New York pp. 132–134.

8. Ranson, H., C. Claudianos, F. Ortelli, C. Abgrall, J. Hemingway, M.V. Sharakhova, M.F. Unger, F.H. Collins, and R. Feyereisen. **2002** *Science Evolution of supergene families associated with insecticide resistance.* 298 pp179-181.

9. Feyereisen, R. **1995** *Toxicology Letters*. *Molecular biology of insecticide resistance.* 82/83 pp83-90.

10. Feyereisen, R. **1999** *Ann. Rev. Entomol Insect P450 Enzymes*.. 44 pp507-533.

11. Carson R **2000** *Silent Spring* Penguin Books Ltd, UK.

12. Sabourault, C., V.M. Guzov, J.F. Koener, C. Claudianos, F.W. Plapp, Jr., and R. Feyereisen. **2001**. *Insect Mol Biol Overproduction of a P450 that metabolizes diazinon is linked to a loss-of-function in the chromosome 2 ali-esterase (MdalphaE7) gene in resistant house flies.*. 10 pp 609-18.

13. Nelson, D.R. **1999.** *Arch Biochem Biophys*. *Cytochrome P450 and the individuality of species.* 369 pp1-10.

14. Stevens, J.L., M.J. Snyder, J.F. Koener, and R. Feyereisen. **2000**. Inducible *P*450s of the CYP9 family from larval Manduca sexta midgut. *Insect Biochem Mol Biol*. 30:559-68.

15. Snyder, M.J, Stevens L, Andersen J.F, and Feyereisen R. **1995.** *Arch Biochem Biophys* Expression of cytochrome *P*450 genes of the CYP4 family in midgut and fat body of the tobacco hornworm, Manduca sexta.. 321 pp13-20.

16. Denholm, I., M. Cahill, T.J. Dennehy, and A.R. Horowitz. **1998.** Challenges with managing insecticide resistance in agricultural pests, exemplified by the whitefly *Bemisia tabaci*. *Philosophical Transactions of the Royal Society of London*. 353:1757-1767.

17. Le Goff, G., S. Boundy, P.J. Daborn, J.L. Yen, L. Sofer, R. Lind, C. Sabourault, L. Madi-Ravazzi, and ffrench-Constant R.H. **2003**. *Insect Biochem Mol Biol*. *Microarray analysis of cytochrome P450 mediated insecticide resistance in Drosophila*. 33 pp701-8.

18. Fogleman, J.C. **2000.** *Chem Biol Interact Response of Drosophila melanogaster to selection for P450-mediated resistance to isoquinoline alkaloids* 125 pp93-105.

19. Roush, R.T., and J.A. McKenzie **1987** *Annu Rev Entomol Ecological genetics of insecticide and acaricide resistance* 32 pp361-80.

20. Kikkawa, H. **1961**. *Ann. Rep. Sci. Works Fac. Sci Genetical studies on the resistance to parathion in Drosophila melanogaster . I. Gene analyses* 9 pp1-20.

21. Hallstrom I and Blanck A, **1985** *Chem Biol. Interact.* 56 pp157.

22. H. Kikkawa, *Botyu-Kagaku* **1964**. *Science Single P450 Allele Associated with Insecticide Resistance in Drosophila* 29 pp37.

23. H. Kikkawa, **1961** *Ann. Rep. Sci. Works Fac. Sci. Osaka Univ.* The Genetic Basis of Resistance to Diazinon in Natural Populations of Drosophila melanogaster 9 pp1

24. R. Feyereisen, *Ann. Rev. Entomol.* **1999** Insect cytochromes P450: diversity, insecticide resistance and tolerance to plant toxins 44 pp507.

25. Tijet N, Helvig C, Feyereisen R, **1999** *Gene The genomics of insecticide resistance.* 4 (1) pp202

26. A.J. Bard and L.R. Faulkner, **2001** *Electrochemical Methods* (2nd Ed), Wiley, Danvers, US, pp. 226–231.

27. A.C. Fisher. **1996** *Electrode Dynamics*. Oxford Science Publications, UK pp. 30-31.

28. Raag, R and Poulos, T.L. *Biochemistry*, **1989**, 28 pp7586-7592

5 Investigation of Microsomal Cytochrome *P*450 protein (*Cyp6g1*) on an edge plane graphite electrode.

5.1 Introduction and Aims

The fundamental structural element of all biomembranes is a phospholipid bilayer shown in Figure 51. The most crucial function of this layer is that it separates the inner and outer parts of the cell by a permeable membrane and facilitates the uptake of nutrients, receptor binding, enzymatic activity and the control of cell-cell interactions. The lipid bilayer is unique in that it not only provides a physical barrier for separating the cells cytoplasm from its extracellular surroundings but also separates organelles inside the cell.

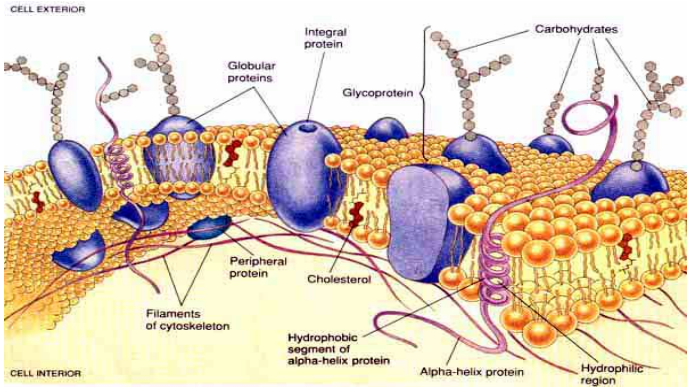

Figure 51. An interpretation of the structure of a lipid bilayer showing the integration of membrane bound proteins *(Adapted from Banks 2005)*

Biomembranes are made up of different combinations and quantities of phospholipids and glycoproteins. There are numerous different kinds of lipid molecules but they all share the feature that they are 'amphipathic', or one region of the molecule is polar and hydrophilic whilst the other is non-polar and hydrophobic. When dispersed in water these molecules tend to self-assemble to form aggregates or vesicles.

The electrical properties of these layers have provided useful information regarding the thickness and dielectric activity of model membranes as well as the organisation and

orientation of the ions and molecules in the bilayers. Simplified models of these cell membranes have been the subject of intense study.

The model bilayer lipid membrane or BLM was introduced approximately forty years ago by Donald Rudin and his collegues. The BLM was about 5nm thick and interposed between two aqueous solutions. This model is now the most widely used in biomembrane investigations [1].

Experimental investigations have looked at the most robust and appropriate support for biomembranes. Puu and colleagues compared the differences between a platinum and glass solid support to that of platinum and silicon. The group's work also focused on layer formation and discovered that lipid layers fused more readily onto surfaces when proteins were incorporated [2]. Ann Plant showed that the use of a metal support, such as gold, permits the application of electrochemical techniques for examining the insulating characteristics of the lipid layers and for assessing the activity of membrane bound proteins within the layers [3].

Various electrochemical and optical techniques have been employed in studies to investigate the architecture and activity of artificial bilayer lipid membranes. Bockrin and Diniz studied the electron transfer phenomena by potentiometric measurements [4]. Extensive studies have been carried out using amperometric methods[5] and impedance spectroscopy has also been employed due to its provision of refined information on the mechanism of interfacial electron transfer [6]. Plant also considered the effects of forming bilayers using alkanethiol tethering chemistry. These layers were found to permit a degree membrane protein activity[3].

Meuse and collegues investigated the driving force for the formation of the bilayers. The results of the work highlighted the role and effects of surface free energy in bilayer formation [7].

It would seem that the important question here is how well do model membranes mimic biological membranes and facilitate the true enzyme activity of the proteins inserted in them?

The electrochemistry of cytochrome *c* has been studied at numerous types of electrode surfaces with the aim of understanding the interfacial interactions that accompany direct electron transfer between redox proteins and electrodes. It wasn't until 1977 that Eddowes and Hill discovered that a modified gold electrode allowed the observation of well defined and reversible electrochemistry[11].

Salamon and Tollin went on to investigate direct electron transfer between bacterial ferredoxins with a gold electrode modified with a self assembled lipid bilayer. These results suggested a theory that deposition of lipid bilayers on a gold electrode produces, under certain experimental conditions, non-uniform electro-active micro sites on the electrode surface where both positively and negatively charged redox proteins are able to exchange electrons with the electrode [12]. These studies are examples of the potential usefulness of electrochemical techniques to investigate the mechanism of action in membrane bound proteins.

Further work went on to establish whether mediated diffusion or direct electron tunnelling was the mechanism of transport across the phospholipid layers [13].

Lymar and Hurst had previously considered the significance of discriminating between electron tunnelling and mediator transport. Their work on ubiquinone concluded that due to the considerable distance across the lipid membrane, the potential dependence of the observed current could not simply be accounted for by electron transfer [14]. Laval and Majda once again looked at bilayer assemblies to investigate electron transfer and the possible lateral mobility of ubiquinone. The ubiquinone molecule appeared to be immobile when deposited directly onto an octadecanethiol monolayer but exhibited lateral mobility when incorporated with the monolayer and a 1-Palmitoyl-2-sn-Glycero-3-Phosphocholine (DPPC) bilayer assembly. It seemed that pinhole defects in the layers affected the behaviour of the ubiquinone when measured electrochemically [16]. This work highlighted the significant effect of holes and defects in the layers on the interpretation of electrochemical results.

Another area of research interest was the understanding of the forces that direct and drive the self assembly of phospholipid molecules. Earlier work had found that supported lipid bilayers could be formed from vesicles fusing with various metal, glass and silica surfaces [17].

In general, the researches found that the osmotic pressure and lateral tension of the phospholipid vesicles together with the concentration of vesicles and the adhesion free energy of the surface all influenced the formation of the phospholipid bilayer on a hydrophilic surface. It was also found that lipid vesicles interact with hydrophobic surfaces, however the exact processes were poorly understood [18,19].

Silin and colleagues found that the kinetics of bilayer formation strongly depended on the concentration of the lipid vesicles. The work concluded that the success of bilayer formation at a hydrophobic surface was dependent on the extent of the polar component

of the surface free energy of that surface [20]. Hill and co workers had used bare EPG electrodes to characterize the electrochemistry of recombinant CYP101 *P*450 [21]. In this work, cyclic voltammetric measurements were carried out in the presence and in the absence of the substrate camphor. Anaerobic conditions were used to prevent formation of the binding of oxygen to Fe^{2+} and the possibility of second electron transfer. The results indicated reversible oxidation and reduction. The interaction of the CYP101 with the bare EPG had been proposed by the authors to be possible via the positively charged amino acid residues on the surface of CYP101.

In the light of recent studies indicating the possibility of protein denaturation [22], the following chapter investigates possible enzyme activity of the microsomal *P*450 from *Drosophila Melanogaster*.

In this system the enzyme is already embedded in a microsomal unit, thus more likely to mimic a biologically active system as the orientation of the active protein site is less likely to be in direct contact with the electrode surface which may lead to protein denaturation. Edege plane graphite electrodes have been shown to be highly advantageous in electroanalysis due to the highly reactive edge plane sites which allow high sensitivity and low detection limits [23]. Graphitic edge planes are attractive surfaces for chemical coupling and modification procedures. Edge planes are also polar and thus hydrophilic implying that aqueous coupling reactions can be used with a good degree of success [24]. Immobilisation is an important aspect in the production of nano devices, as sensitivity may strongly depend on both concentration at the surface and specific orientation. Control over these two requirements can be difficult to address, however, the introduction of a microsomal unit onto the electrode surface can provide a stable environment for the protein to interact with the electrode and thus less likely to denature.

5.2 Experimental

5.2.1 Assembly of microsomal *P*450 *Cyp6g1* films on an Edge Plane Graphite (EPG) electrode

Instrumentation

Electrochemical experiments were carried out on a PGSTAT 30 Autolab system (Eco Chemie, Netherlands) in a standard three electrode cell set up as described in detail in chapter 3. The reference electrode was silver / silver chloride saturated with potassium chloride electrolyte. The counter electrode was gold wire.

Reagents

Protein solutions were prepared in aqueous 50mM phosphate buffer at pH 7.4. All solutions were prepared using deionised water. All chemical reagents were obtained commercially from Aldrich and were used without any further purification. All experiments were carried out at room temperature.

Procedures and protein absorption

An EPG (Le Carbone Ltd, Sussex, UK) electrode was thoroughly cleaned by polishing with 0.3um aluminium powder, sonnicated and rinsed. This process was repeated three times or until the electrode surface appeared smooth and clean on inspection. The electrode was then placed into a small volume cell containing 50mM PBS at pH 7.4 which had been degassed with argon for thirty minutes. A cyclic voltammetry measurement was performed in order to obtain a baseline or blank.

Scan conditions were:

+0.1v start potential
-0.6v finish potential
5 cycles @ 100mv per second
First conditioning potential = 0.1v

The electrode was then removed and rinsed in water and dried under a stream of argon gas. The Hikon R (resistant) protein samples were used in all experiments due to them having a higher concentration of *P*450. 20µl of microsomal protein solution was then dropped onto the electrode surface and allowed to dry for two hours at 4ºC. For the films which had substrate added, 0.4µl of 0.05mM Methoxy Resorufin Ether (MRES) was added to the film at this stage.
20µl of salmon sperm DNA obtained from Sigma, at 1mg per ml in PBS was also added to the film to serve as 'glue'. The film was then allowed to dry for thirty minutes in air at 4ºC. The electrode with the film attached was then placed back into the cell containing 50mM PBS at pH 7.4 and further measurements taken.

5.3 Results and discussion

Firstly, microsomal protein only was introduced onto edge plane graphite (EPG) electrode surface shown in Figure 52.

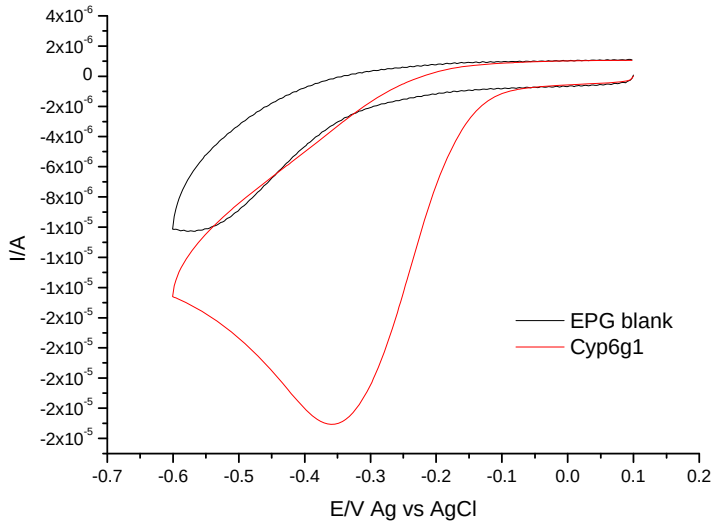

Figure 52. Cyclic voltammogram for EPG working electrode only followed by the addition of 20.9mg/ml microsomal Cyptochrome *P*450 Cyp6g1 in 50mM PBS, pH 7.4. Potential scan rate 50mV s^{-1}. Area of working electrode 0.25cm^2

Next, the substrate MRES was added to the film following the application of the protein layer, shown in Figure 53.

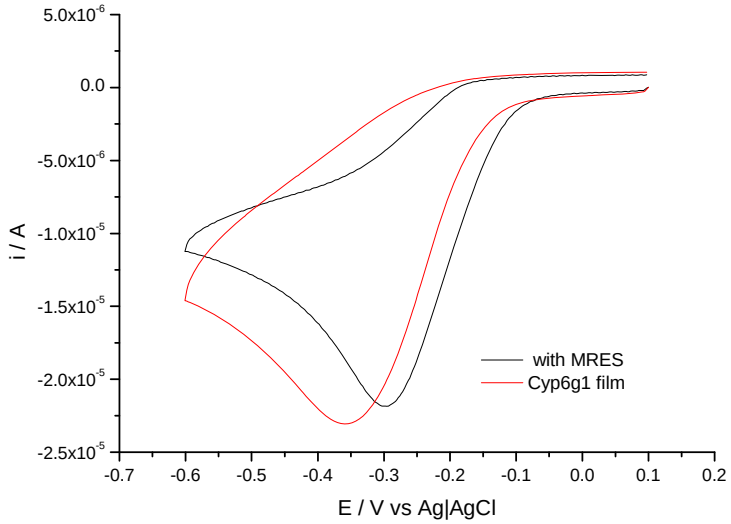

Figure 53. Cyclic voltammogram for 20.9mg/ml microsomal Cyptochrome *P*450 Cyp6g1 in 50mM PBS, pH 7.4 with the addition of 0.4ul of 0.05mM MRES on an EPG working electrode, pH 7.4. Potential scan rate 50mV s^{-1}. Area of working electrode 0.25cm^2

There was no back peak observed in this particular experiment thus suugesting limited reduction of dioxygen catalysed by the haem. The susbstrate free reaction would require greater rorganisation energy than the bound protein. A mass transport limited reaction is observed here.

Note the positive peak shift upon the addition of substrate in Figure 53. This may be due to a shift in spin state of the ferri haem iron from low spin in the absence of substrate to high spin in the substrate bound protein. In addition, a redox potential change has been observed upon substrate binding due to reprganisation energy change. Kazlauskaite *et al* [21] reported a positive potential shift upon binding of camphor substrate in similar experiments but carried out with recombinant Cytochrome P450cam.

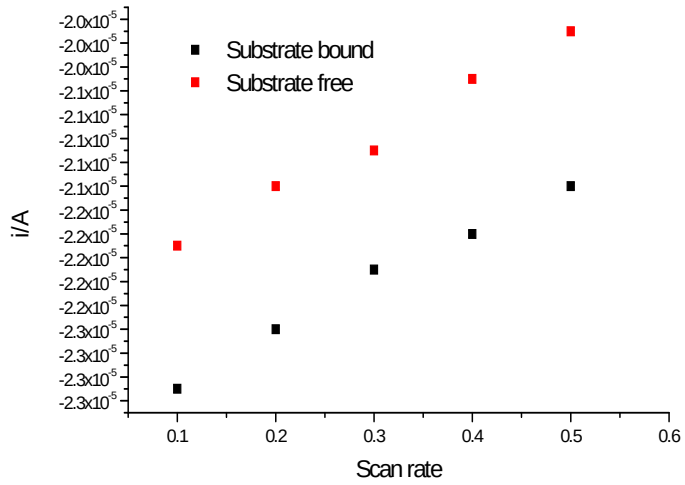

Figure 54. The dependence of cathodic peak current on the potential scan rate for substrate bound and substrate free *P*450 microsomal protein.
Conditions were as for figure 53.

Interestingly, previous work had shown deviation from linearity for the substrate free protein and was considered to be due to adsorption to the electrode surface [21]. Despite repeated experiments, so such deviation was observed in these experiments. This may have been due to the protein being more stable in the microsomal environment. Another important point to consider here is the overall surface charge of the microsomal unit. *P*450 proteins are generally negatively charged overall at pH 7.4 and it was likely that a specific pattern of positively charged amino acid residues favours an interaction between the enzyme and the electrode surface in such a way that electron transfer could take place. However, this can not be confirmed unless further investigation takes place.

5.4 Chapter Summary

This chapter communicates the first stages of experimental work with microsomal protein electrochemistry. The first results have been encouraging but further work needs to be carried out to confirm these findings.

Microsomal *P*450 Cyp6g1 protein from the fruit fly *Drosophila Melanogaster* was introduced to an EPG electrode surface. Experiments were carried out in the presence and absence of substrate. Results showed a positive potential shift upon introduction of substrate which was likely to be a binding event. However, this is difficult to confirm unless further work is carried out.

5.4.1 References

1. Meuller, P., Rudin, D.O., Tien, H.T. and Wescott, W.C. **1962** *Nature*, *Reconstitution of cell membrane structure in vitro and its transformation into an excitable system.* 194 pp979.

2. Puu, G., Gustafson, I., Artursson, E., Ohlsson, P.A. **1995**, *Biosensors and Bioelectronics, Distribution and stability of membrane proteins in lipid membranes on solid supports* 10 pp 463-476.

3. Plant, A.L. *Langmuir Method for fabricating supported bilayer-lipid membranes* **1999,** 15, 5128-8135.

4. Bockrin, J.O'M and Diniz, **1988** F.B. *J. Electrochem. Soc.*, 135, 1947-1954.

5. Tien, H.T. *J.* **1984** *Phys. Chem. A combined AC-DC method for investigating supported bilayer lipid membranes***.** 88 pp3172-3174.

6. Yamanda H, Shiku H, Matsue T, and Uchida. **1993** *The Journal of Physical Chemistry, Membrane Biophysics* 97 pp 9547-9549.

7. Meuse, C.W., Niaura, G., Lewis, G. and Plant, A.L. **1998** *Langmuir*, *Spectroscopy of Flavoproteins* 14 pp 1604.

8. Florin, E.L. and Gaub, H.E. **1993** *Biophys.J. Measurement of membrane binding between recoverin, a calcium-myristoyl switch protein, and lipid bilayers by AFM-based force spectroscopy* 64 pp 375-383.

9. Torchut, E., Bourdillon, C. and Laval, J. **1994**, *Biosens. Bioelectron. Reconstitution of functional electron transfer between membrane biological elements in a two-dimensional lipidic structure at the electrode interface* 9 pp 719-723.

10. Gordillo, G.J. & Schiffrin, D.J. **2000** *Faraday Discussions. The electrochemistry of ubiquinone-10 in a phospholipid model membrane*, 116 pp 89-107.

11. Eddowes, M.J. and Hill, H.A.O. **1977** *J.Chem. Soc Chem. Commun, Direct Electrochemistry of Redox Proteins* 771 pp 417 - 423

12. Salamon, Z. & Tollin, G. **1991** *Bioelectrochemistry and Bioenergetics,Optical anisotropy in lipid bilayer membranes,* 26 pp321-334.

13.Cheng, Y., Cunnane, V.J., Kontturi, A.K., Schiffrin, D.J. **1996** *J. Phys. Chem, Potential Dependence of Transmembrane Electron Transfer across Phospholipid Bilayers Mediated by Ubiquinone 10,* 100, pp15470-15477.

14. Lymar, S.V. and Hurst, J.K. **1994**, *J. Phys, Chem. Peroxynitrite Rapidly Permeates Phospholipid Membranes* 98 pp 898.

15. Marchal, D., Boireau, W., Laval, J.M., Moiroux, J., Bourdillon, C. **1997** *Biophysical Journal An electrochemical approach of the redox behavior of water insoluble ubiquinones or plastoquinones incorporated in supported phospholipid layers* 72 pp 2679-2687.

16. Laval, J.M & Majda, M. **1994**, *Thin Solid Films. Electrochemical Measurement of Lateral Diffusion Coefficients of Ubiquinones and Plastoquinones of Various Isoprenoid Chain Lengths Incorporated in Model Bilayers* 24 pp836-840.

17. Brian, A.A. and McConnell, H.M. **1994** *Proc. Natl. Acad. Sci. USA.*, *Electrical manipulation of glycan-phosphatidyl inositol-tethered proteins in planar supported bilayers.* 81 pp 6159-6163.

18. Whitesides, G.M., Laibinis, P.E. **1989** *Langmuir*, *Self-Assembled Monolayers: Alkanethiols on Gold and Alkane Carboxylic Acids on Alumina*" 6 pp 87-96.

19. Kalb, E., Frey, S. and Tamm, L.K. **1992** *Biophys. Biochim. Acta. Lipid vesicle adsorption versus formation of planar bilayers on solid surfaces* 1103 pp307-316.

20. Silin, V. I., Weider, H., Woodward, J.T., Valincius, G., Offenhausser, A., Plant, A.L. **2002** *J. Am.Chem.Soc*, 124 pp1476-1483.

21. Kazlauskaite, J., Westlake, A.C.G., Wong, L.L. and Hill, H.A.O. **1996** *Chem. Comm.*, 18, 2189-2190.

22. Milsom, E.V., Dash, H.A., Thetford, A., Bligh, N., Wojciech, N., Opallo, M & Marken F. **2007** *Journal of Elecroanalytical Chemistry* 610 (1), 15 pp 28-36

23. Banks, C.E, and Compton, R.G. **2005** *Anal. Sci. The electrochemical ion-transfer reactivity of porphyrinato metal complexes in 4-(3-phenylpropyl) pyridine21* pp1263

24. Honeychurch, M.J., Hill, H.A.O. & Wong, L.L. **1999** *FEBS Letters*, *The thermodynamics and kinetics of electron transfer in the cytochrome P450cam enzyme system* 451 pp351-353

6 Putative Immobilisation of Cytochrome *P*450 (CYP101) into Nanoparticulate TiO_2 Films

6.1. Introduction and Aims

6.2. Haem Proteins in TiO_2 nanoparticulate films.

6.3. Nanoparticulate Titanium dioxide (TiO_2) as a host electrode material.

6.4. Method for the construction of ITO/TiO_2 films incorporating Cytochrome *P*450.

6.5. Results and discussion

6.5.1. Deposition and Characterisation of Nanoparticulate TiO_2 Film Electrodes.

6.5.2. Imaging of Nanoparticulate TiO_2 Film Electrodes by Scanning Electron Microscopy (SEM).

6.5.3. Immobilisation and Reactivity of Cytochrome *P*450 in TiO_2 Film Electrodes.

6.5.4. Investigations of reduction responses of Cytochrome *P*450 adsorbed into multi layer TiO_2 host films.

6.5.5. Reduction Process 1.

6.5.6. Reduction Process 2.

6.5.7. The effects of increasing scan rate on peak potential of *P*450 protein adsorbed onto TiO_2 host electrodes.

6.5.8. Effects of time and layer thickness on the peak reduction currents of *P*450 protein in TiO_2 nanoparticle host electrode material.

6.6 Chapter Summary

6.7. References

6.1 Introduction

The incorporation of biological redox systems into mesoporous films has generated interest due to the possibility of direct electron exchange between the redox active sites in proteins and the porous host electrode. Direct electrochemistry of redox proteins or enzymes can provide biomimetic environments for fundamental studies together with a basis for designing devices without the need for electron transfer mediators [1]. There has been a variety of approaches for the immobilisation of biological redox systems. These include adsorption [2], the binding of molecules into lipid structures [3], covalent binding and electrostatic binding [4, 5]. Haemoglobin (Hb) and methaemoglobin immobilised at electrode surfaces have been previously employed as model redox systems. Earlier work focused on the reduction of Hb on dropping mercury electrodes [6] but because of slow rates of electron transfer between Hb and the electrode surface, attempts have been made to facilitate the electron transfer by using mediators and special electrode materials. Previously, surfactant films have provided a biomembrane mimic for the study of redox proteins [7]. Although Hb does not function physiologically as an electron carrier, it is a useful model for the study of electron reactions for other haem proteins like *P*450, mainly due to the fact that it is readily available and inexpensive and its structure is well known. It is also important to note that Hb has reductive and oxidative characteristics very similar to the enzyme activity of Cytochrome P450 [8].

It is also interesting to note that the haem protein cytochrome *c* has been coupled successfully to electrode surfaces by Hill et al [9]. Over the past two decades, this redox protein of 12 kD mass and approximately 3.7 nM size has also been considered as a model system for biological electron transfer and for bioelectrocatalysis. The most prominent feature of the almost spherical cytochrome *c* structure is a strongly positively charged lysine rich region on the outer shell of the protein, which is responsible for docking to electron donor and acceptor sites with complementary negative surface charge[10]. A wide range of films with negative surface functionalities, e.g. carboxylate functionalised surfaces, polysulfonates, polyphosphate (DNA) modified surfaces and dialysis membranes have been proposed for reversibly docking cytochrome *c* and related haem proteins for applications in bioelectrochemistry and in biosensing [11,12,13].

6.2 Haem Proteins in TiO_2 nanoparticulate films.

It has been shown that Hb and cytochrome *c* have both been successfully adsorbed from aqueous solutions into thin films of TiO_2 nanoparticles [14, 15]. After immersion of the TiO_2 film coated onto tin-doped indium oxide (ITO) electrode surfaces, high concentrations of these redox proteins in a stable and active state were immobilised. Increasing the film thickness in a layer-by-layer manner increased the amount of adsorbed redox active protein and therefore improved the electrochemical responses. This three-dimensional binding of a redox protein to the electrode surface was rationalised by a transport process similar to diffusion with either protein diffusion, electron hopping from site to site within the mesoporous film, or both occurring simultaneously. This mechanism is looked at in more detail in this chapter.

Interfacial protein electron transfer has received wide and significant research interest. In particular, there is a strong interest in developing novel bioelectronic interfaces that are suitable for the probing of protein electrochemistry. This kind of study may deepen the understanding of biological protein electron transfer and promote the development of bioelectronic sensors for a variety of applications.

In this work, TiO_2 films on indium tin oxide (ITO) electrode surfaces were combined with bacterial Cytochrome *P*450 and it was shown that in addition to providing a rigid host structure, metal oxides can also contribute to the efficient transport of electrons.

6.3 Nanoparticulate Titanium dioxide (TiO_2) as a host electrode material

Anatase is one of the three mineral forms of titanium dioxide. It is always found as small, isolated and sharply developed crystals and a more commonly occurring modification of titanium dioxide.

Titanium dioxide, particularly in the anatase form, is a photocatalyst under ultraviolet light. Its strong oxidative potential oxidises water to create hydroxyl radicals. It can also oxidise oxygen or organic materials directly. Titanium dioxide is thus added to paints, cements, windows, tiles, or other products for sterilising, deodorising and anti-fouling properties and is also used as a hydrolysis catalyst.

Nanosized titanium oxide is a useful and diverse biocompatible material widely used in paint, toothpaste and cosmetics also. Due to its unique physiochemical properties and its tendency to selectively combine with some biomolecules, it is now regarded as a promising interface for the immobilisation of a range of haem and metalloproteins.

Electrochemical studies of these proteins have been investigated at some length since fundamental studies of their redox behavior can be of considerable use towards understanding the relationship between the proteins structure and function.

Protein electrochemistry can be carried out in protein solutions or with surface confinement of the molecules. There are a number of restrictive elements which inhibit the direct electron transfer between electrodes and proteins. Firstly, electroactive prosthetic groups may be buried deep within the proteins structure. Also denaturation of the protein as it adsorbs onto the electrodes surface may occur. Secondly, the proteins surface charges do not present an organized and symmetrical distribution. These factors combine to produce, in many cases, a low rate of electron transfer. This problem has been challenged in the past by the addition of mediators or promoters. It has been generally demonstrated that the introduction of such molecules is likely to favor the orientation of protein molecules over the surface of the electrode [16].

The electrochemical investigation of proteins in solution can also present interfering factors. Large volumes of protein sample need to be used in this kind of experimental procedure and proteins are costly and time consuming to produce. Also, proteins have a strong tendency to adsorb onto surfaces and it can therefore be problematic in distinguishing between surface adsorbed species and free solution species. So using surface confined techniques to immobilise redox protein molecules onto electrode surfaces whilst retaining their biological and electrochemical integrity has been the main thrust in this area of research [17].

It has been reported that TiO_2 particles may react favorably with some groups on the proteins surface which may facilitate less denaturation. Work continued in this area leading to the investigation of molecules such as cytochrome c, haemoglobin and myoglobin being immobilised onto nanosized $TiO_{2\ films}$ [18, 19].

Mesoporous oxides in the form of thin films are relatively stable in aqueous environments and are versatile for a wide range of applications in sensors. Considerable interest in TiO_2 films exists predominantly due to their application in hydrophilic coatings, and as pigments as previously mentioned.

There have also been several previous reports on the immobilisation of biological redox systems such as oligonucleotides and DNA, haem proteins or redox enzymes in titanium dioxide and other metal oxide hosts such as manganese dioxide and tin dioxide [20]. By combining a rigid host structure, prepared for example from metal oxide nanoparticles of appropriate size, and a more fragile biological system, novel functional composite materials can be obtained.

6.4 Method for the construction of ITO/TiO_2 films incorporating Cytochrome *P*450.

Reagents

A suspension of 40nm diameter TiO_2 particle (TAYCA Corporation Lot No. 6530J AMT-600) was prepared by sonnicating in methanol for 1hour (20 kHz Fisherbrand Ultrasonic bath). Suspensions in methanol were stable for several hours but underwent slow sedimentation which was found to be accelerated in the presence of water.

Protein solutions were prepared in aqueous 50mM phosphate buffer at pH 7.4. All solutions were prepared using deionised water.

All chemical reagents were obtained commercially from Aldrich and were used without any further purification.

Instrumentation

Electrochemical experiments were carried out on a PGSTAT 30 Autolab system (Eco Chemie, Netherlands) in a standard three electrode cell set up as described in detail in chapter 3. The reference electrode was silver / silver chloride saturated with potassium chloride electrolyte. The counter electrode was gold wire.
The working electrodes were prepared from tin doped indium oxide (ITO) coated glass with a resistivity of 15Ohm/square. ITO glass from Image Optics Ltd, Basildon.UK.

The glass was cut approximately 40mm x 10mm. It was then thoroughly rinsed in ethanol and milliQ and calcined at 500ºC for 30mins in a furnace (Elite Tube) to thoroughly clean the electrodes.
For the Scanning Electron Microscopy (SEM), a JEOL JSM6310 system was used. The UV/Vis spectra for the evaluation of solution sample concentrations were obtained with a Helios γ spectrometer from Thermo Electron Corp, UK. The temperature for all experiments was 22 ± 2ºC.

Procedures and electrode design

A suspension of the 40nm TiO_2 particles was achieved by preparing a 3% wt solution on methanol and sonicating as previously described. A clean ITO electrode was then dipped into the suspension for 1 minute. Retracted and the methanol was allowed to evaporate leaving behind a well defined and uniform layer of TiO_2. This deposition process was repeated in order to build up several layers of TiO_2 particles. The required number of layers of particles could be adjusted to allow variation in film thickness.
The resulting film was then calcined in air at 500ºC for 1 hour which aided adhesion and removed impurities and moisture.
The electrodes were then left to cool for about 10mins.

Protein absorption

The films were then soaked in a known concentration of protein in PBS (50mM pH7.4) overnight. After soaking the films were taken out and rinsed in water.
Protein samples were taken from storage at -80ºC following the expression and purification process. Glycerol was added to prevent freezer damage. The protein and glycerol stock were run through a PD10 column packed with Sephadex™ G-25 Medium from Amersham Biosciences, to remove the glycerol.

Protein adsorption involved equilibrating the TiO_2 modified electrode in a solution of protein of a known concentration which was determined during the purification process as previously described in chapter 3.

6.5 Results and discussion

6.5.1 Deposition and Characterisation of Nanoparticulate TiO_2 Film Electrodes

Firstly, the TiO_2 only films were investigated. The homogenous adsorption of the Cyp101 protein was achieved by using TiO_2 films prepared with 40 nm diameter particles. The particle size allowed adsorption of the protein into the large pores and throughout the film and both the redox protein and the TiO_2 substrate contributed to the electrochemical characteristics of the film. After formation of the multi-layer TiO_2 at the electrode surface, a calcination step of 1 hour at 500ºC in air was employed to further improve adhesion. The heat treatment served to remove all organic components, thus reducing the possibility of film contamination. The characteristic electrochemical reduction response of the immobilised TiO_2 nanoparticles immersed in aqueous 50mM phosphate buffered saline is shown in the Figure 55.

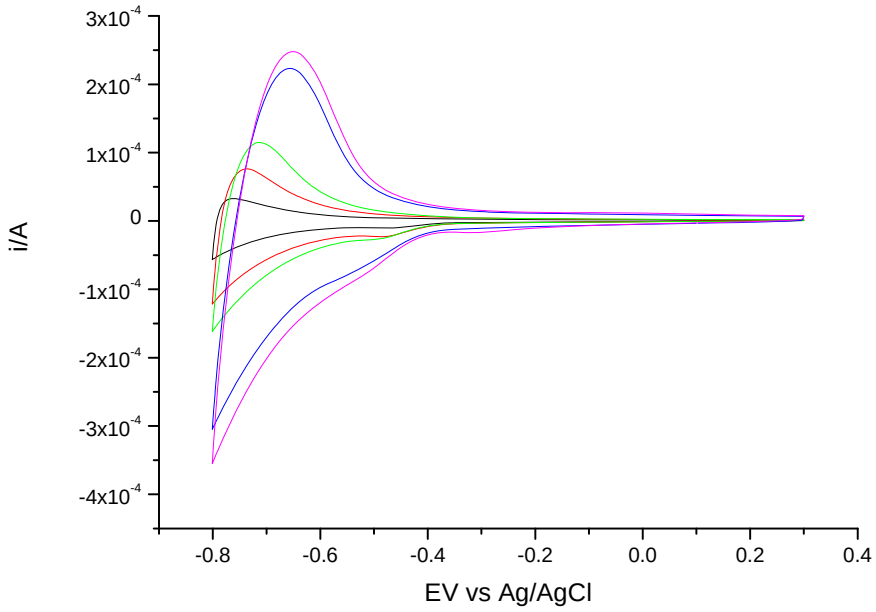

Figure 55. Cyclic Voltammograms (scan rate 0.1 Vs^{-1}) for a 1cm^2 electrode coated with 2 to 40 layer films of 40 nm diameter TiO_2 particles (followed by calcination) immersed in aqueous phosphate buffered saline pH 7.4 and degassed with argon.

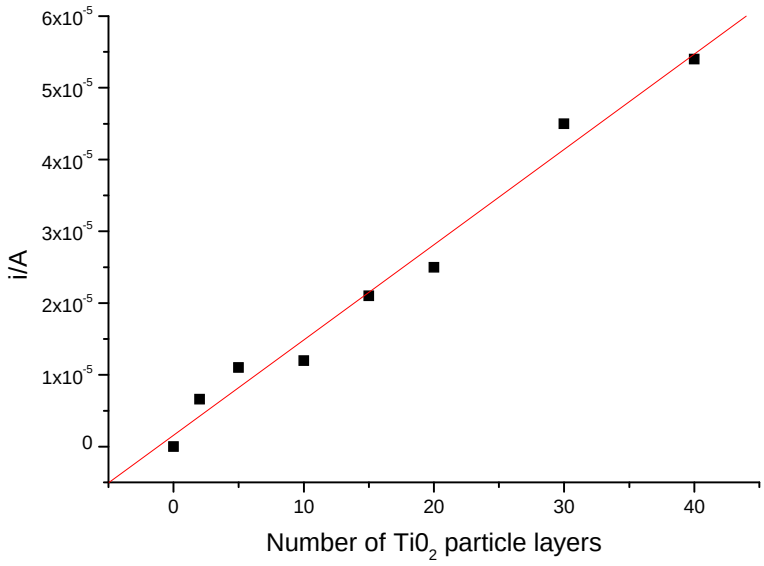

Figure 56. **Plot to show the increase in peak current of increasing layered thicknesses of 40 nm diameter TiO_2 particles (followed by calcination) immersed in aqueous phosphate buffered saline pH 7.4 and degassed with argon.**

The characteristic reduction process was predominantly capacitative in nature, demonstrated in Figure 56. Fabregat-Santiago and co workers suggested that a crucial characteristic of nanoporous semiconductor electrodes is the ability to accumulate a large number of injected electron charges in the solid matrix [21]. This capacatative effect was very marked in 30 and 40 layer films. This may have been due to the large accumulation of TiO_2 nanoparticles aggregating as the layers increased. This is seen more clearly in the following imaging data of Figures 57 to 61.

It was observed that the increase in charge was approximately proportional to the number of depositions or layers of TiO_2 particles on the electrode. The topography of the TiO_2 particle deposits was characterised by scanning electron microscopy (SEM) which clearly showed aggregated deposits of particles as opposed to a thin homogenous film.

6.5.2 Imaging of Nanoparticulate TiO_2 Film Electrodes by Scanning Electron Microscopy (SEM).

The electrodes were prepared as previously described in this chapter. The electrodes were then coated in a thin layer of gold prior to imaging. The surface was scratched in order to image the edge of the TiO_2 nanoparticles in figures 58 and 59.

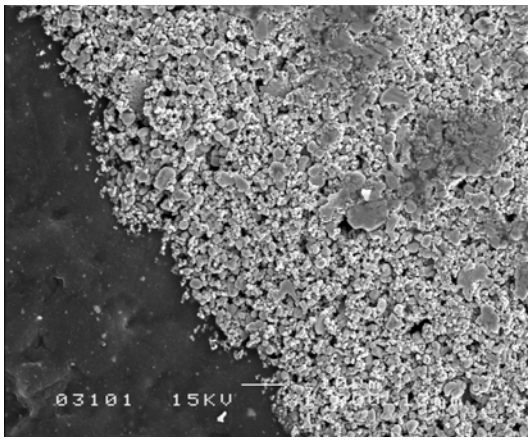

Figure 57. Scanning Electron Microscopy Image (SEM) of a 3 layer deposit of 40nm TiO_2 nanoparticles at an ITO electrode surface. Top view.

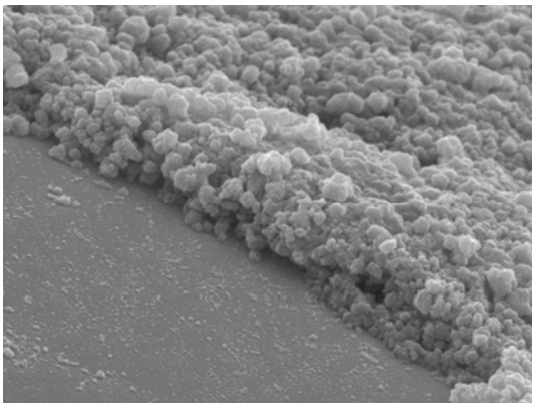

Figure 58. Scanning Electron Microscopy Image (SEM) of a 3 layer deposit of 40nm TiO_2 nanoparticles at an ITO electrode surface. Edge view.

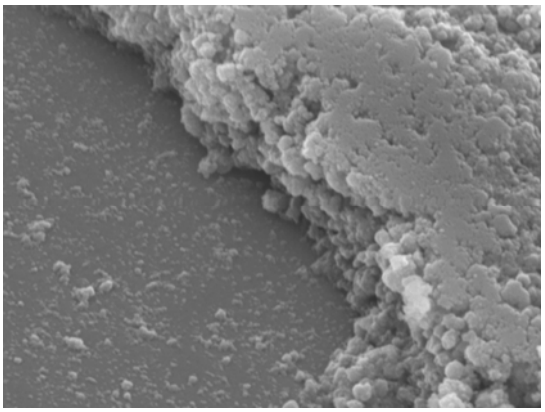

Figure 59. Scanning Electron Microscopy Image (SEM) of a 3 layer deposit of 40nm TiO_2 nanoparticles at an ITO electrode surface. Edge view.

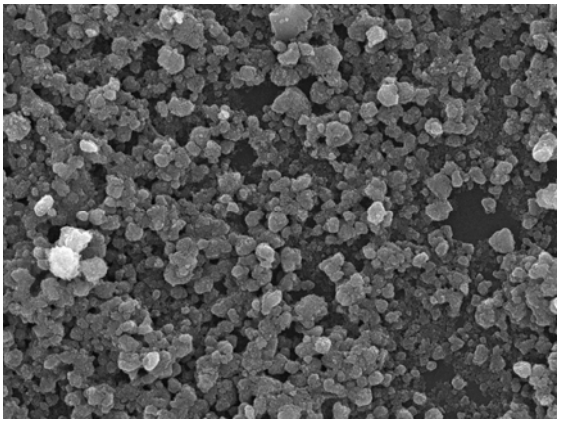

Figure 60. Scanning Electron Microscopy Image (SEM) of a 3 layer deposit of 40nm TiO_2 nanoparticles at an ITO electrode surface. Top view.

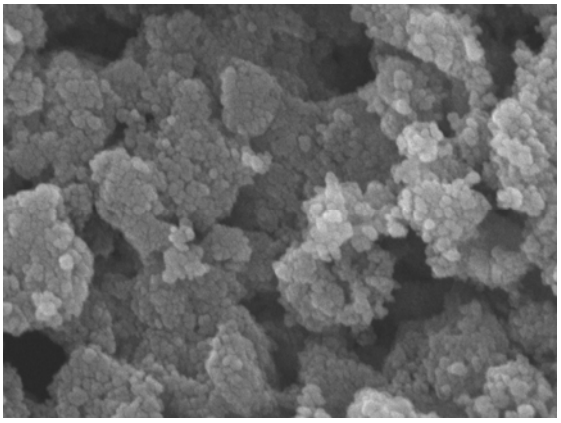

Figure 61. **Scanning Electron Microscopy Image (SEM) of a 3 layer deposit of 40nm TiO_2 nanoparticles at an ITO electrode surface. Top view.**

Figures 57 and 58 clearly show the layer effect of the titanium oxide nanoparticles on the glass surface. The layers are not particularly ordered as would be expected by manually dipping the ITO glass into the TiO_2 nanoparticulate suspension and figures 59 and 60 show the porous structure of the particles on the electrode surface. This is particularly evident from the higher magnification in figure 61. It is likely that the proteins absorbed homogeneously into this porous matrix. This figure also shows the somewhat random deposition of the TiO_2 nanoparticles onto the electrode surface which creates great difficulty in the exact identification of film thickness. This particular film has three depositions of 40 nm particles each which would suggest a thickness of 120 nm. However, due to the action of immersion and withdrawal, the films do not appear to be organised in homogenous 40 nm layers. The lack of order in the layers seemed to increase proportionally with the number of layers deposited. Figure 57, although at a lower magnification, clearly showed the 'wave like' formation of the layers. This may have been due to the slow withdrawal of the electrode from the TiO_2 nanoparticle suspension and the drying of the methanol in air. However, the immobilisation of the TiO_2 nanoparticles onto the electrode surface was permanent although in clusters. The porous clusters enabled successful adsorption of the protein.

6.5.3 Putative Immobilisation and Reactivity of Cytochrome *P*450 in TiO_2 Film Electrodes.

The TiO_2 film electrodes were then immersed overnight in a solution of 1 mg mL^{-1} protein in 50mM phosphate buffered saline at pH 7.4 and kept at 4ºC and covered to prevent any possible evaporation or contamination. Two reduction peaks can clearly be seen in Figure 62.

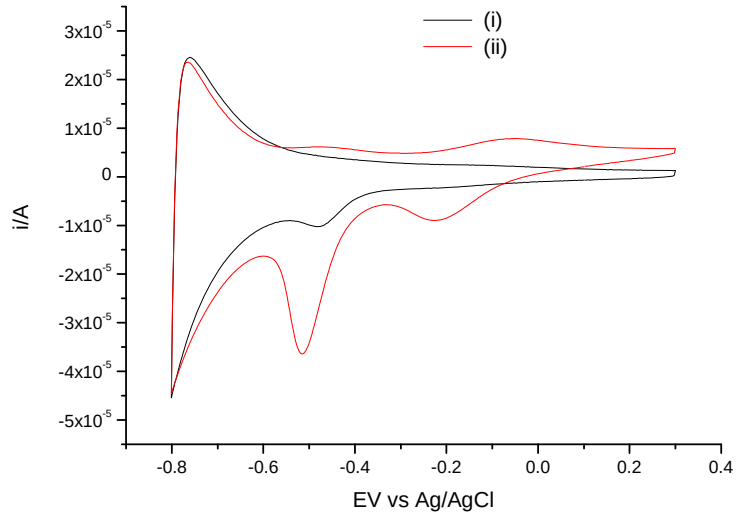

Figure 62. **Cyclic voltammograms obtained (scan rate 0.1Vs^{-1}) from (i) first scan (ii) second scan for the reduction of adsorbed protein on an ITO electrode covered with 3 layers of 40 nm diameter TiO_2 particles.**

The film was immersed overnight in an aqueous solution of 1 mg mL^{-1} *P*450 protein and phosphate buffered saline pH 7.4. The electrode was thoroughly rinsed before the experiments were performed to remove any residual protein.

6.5.4 Investigations of reduction responses of Cytochrome *P*450 adsorbed into multi layer TiO_2 host films.

The reduction response of the protein was then investigated in more detail. The following figures show cyclic voltammograms obtained in phosphate buffered saline solution, pH 7.4 for film electrodes ranging from 2 layers to 20 layers. The cyclic voltammograms showed more than one peak depending on the presence or absence of the protein in the film. The source of the peaks was investigated further. The peaks were identified as likely to be from separate processes.

6.5.5 Reduction Process 1

There were two clear observable reduction peaks (Figure 63) in these experiments which may have arisen from two putative mechanisms. Firstly, process one will be looked at in more detail.

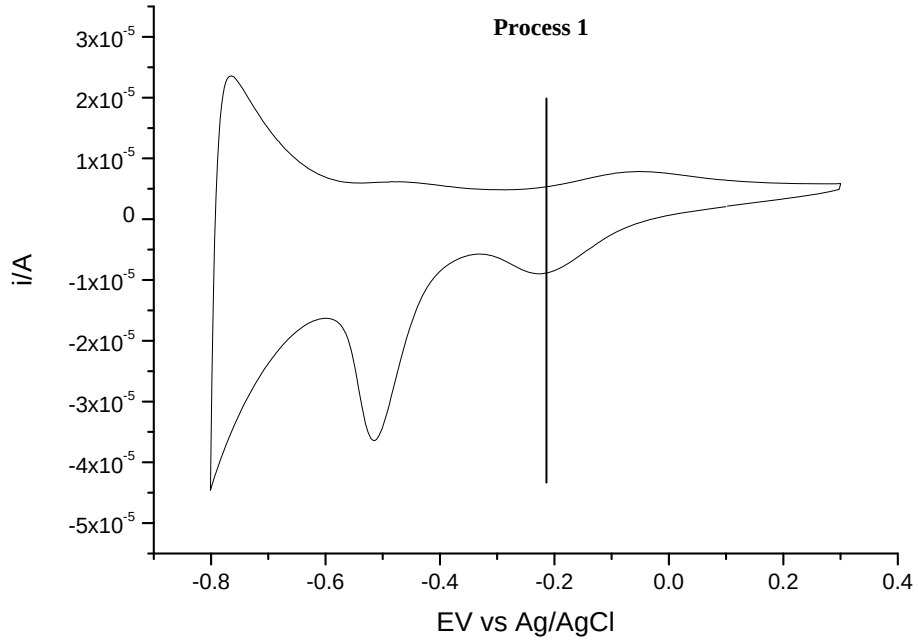

Figure 63. Reduction process 1. Scan 2 of 10 scans for a 10 layer TiO_2 film electrode. Cyclic voltammograms (scan rate 0.1 V s^{-1}) obtained for the reduction of protein immobilised in a 3 layer TiO_2 on ITO electrode.
Voltammograms were obtained in aqueous 50mM phosphate buffered saline pH 7.4 prior to voltammetric experiments, electrodes were immersed in a solution of 1mg mL^{-1} of protein overnight.

This process was absent during the first excursion as shown in Figure 64, but became apparent on the second and subsequent cycles during cyclic voltammetry.

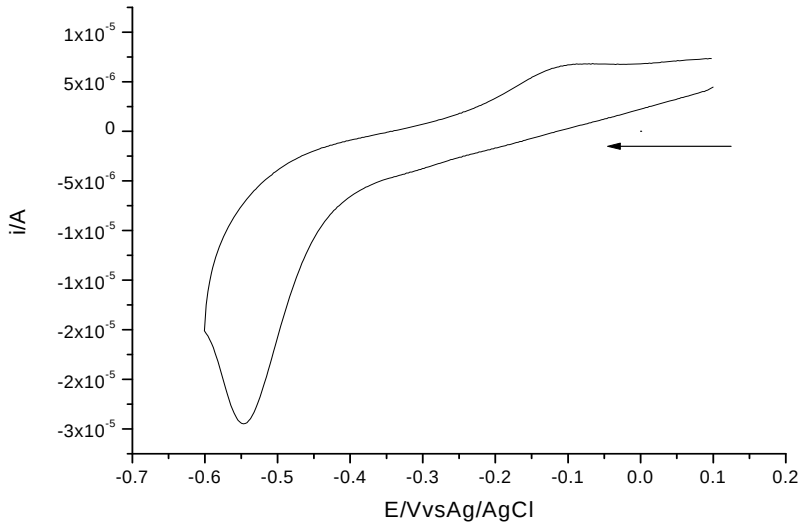

Figure 64. Scan 1 of 10 scans for a 10 layer **TiO_2 film electrode. Cyclic voltammograms (scan rate 0.1 V s^{-1}) obtained for the reduction of protein immobilised in a 10 layer TiO_2 on ITO electrode.**

Voltammograms were obtained in aqueous 50mM phosphate buffered saline pH 7.4 prior to voltammetric experiments, electrodes were immersed in a solution of 1mg mL^{-1} of protein overnight.

On the second cycle, process 1 became apparent and this was followed by a very strong enhancement in cycle 2 which was followed by a decay of the signal during subsequent cycles as observed from scans 2 to 10 shown in Figure 65.

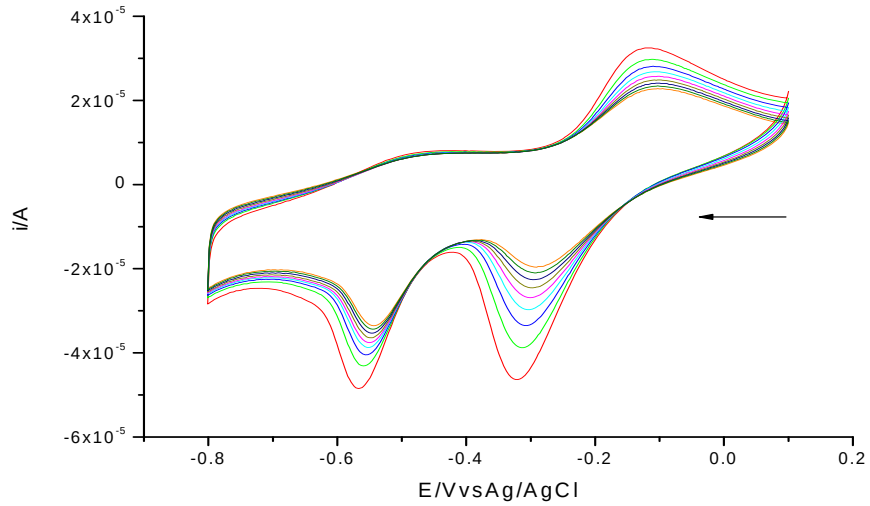

Figure 65. **Scans 2 to 10 for a** 10 layer **TiO_2 film electrode. Cyclic voltammograms (scan rate 0.1 V $s^{-1)}$ obtained for the reduction of protein immobilised in a 10 layer TiO_2 on ITO electrodes.**
Voltammograms were obtained in aqueous 50mM phosphate buffered saline pH 7.4 prior to voltammetric experiments, electrodes were immersed in a solution of 1mg mL^{-1} of protein overnight.

This strongly suggested that the protein was indeed adsorbed within the matrix of the TiO_2 films and further suggests that the protein was likely to have been accessed after the first reduction cycle. The reactivity of the redox protein immobilised within the TiO_2 electrode appeared to be effected by the conductivity of the host matrix. It seemed that only the first reduction process was associated with the direct transfer of electrons from the ITO electrode surface to the immobilised *P*450 protein. The second reduction process seemed to require conduction of electrons from within the TiO_2 matrix. Figure 66 shows a schematic interpretation explaining the possible pathway for the reduction current during process 1. This may also explain the difference in the effect of film thickness on the voltammetric responses for processes 1 and 2 which are considered later in this chapter.

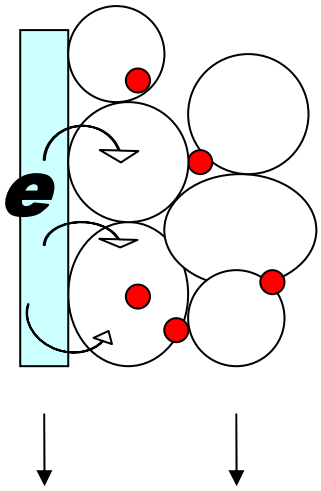

ITO electrode TiO_2 nanoparticle matrix incorporating protein.

Figure 66. Schematic drawing of the electron transport via direct transfer from the ITO electrode which may take place in process 1.

This process may be considered as a 'short range' electron transport mechanism, shown in Figure 66.

This process may be identified as:

Process 1 short range:

Fe (III) (Haem) + e^- (ITO) $\rightleftharpoons$ Fe (II) (Haem)

It is important to remember here that this process does not take place during the first excursion during cyclic voltammetry. Next, process 2 will be looked at in more detail.

6.5.6 Reduction Process 2

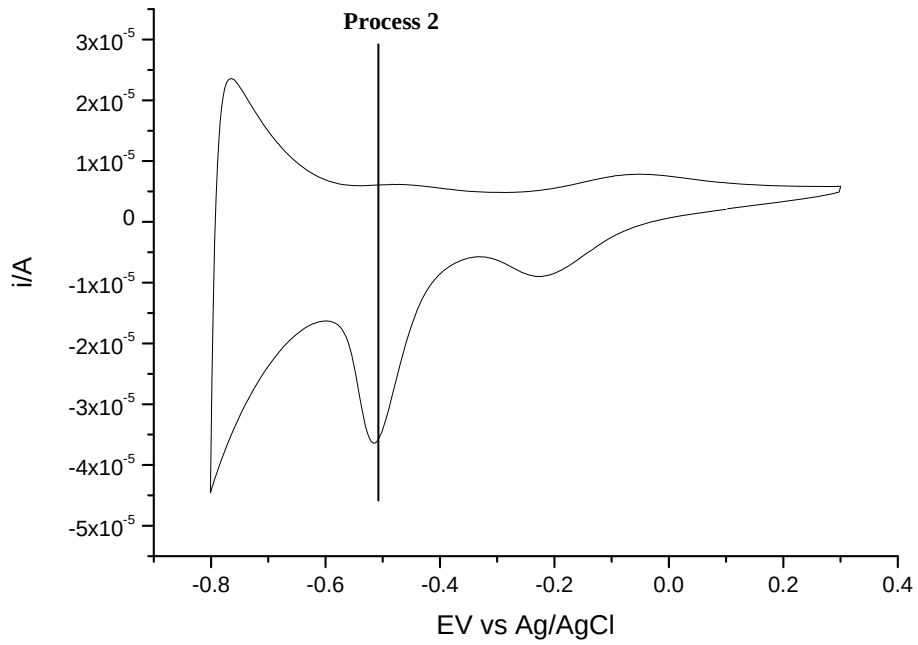

Figure 67. **A second reduction process was observed at an approximate potential of between -0.5 and -0.6 V vs Ag/AgCl.**

This reduction was comparatively small for a 3 layer TiO_2 film but enhanced for a 10 layer film. This is shown in more detail later in this chapter.

This second reduction process may be identified as the Fe (III/II) process associated with electron conduction through the bulk TiO_2 film or 'long range' electron transport mechanism shown in Figure 68.

This second reduction process requires the transport of electrons through the porous TiO_2 matrix and therefore occurs at a more negative potential at which a sufficient concentration of electrons is available in the TiO_2 matrix.

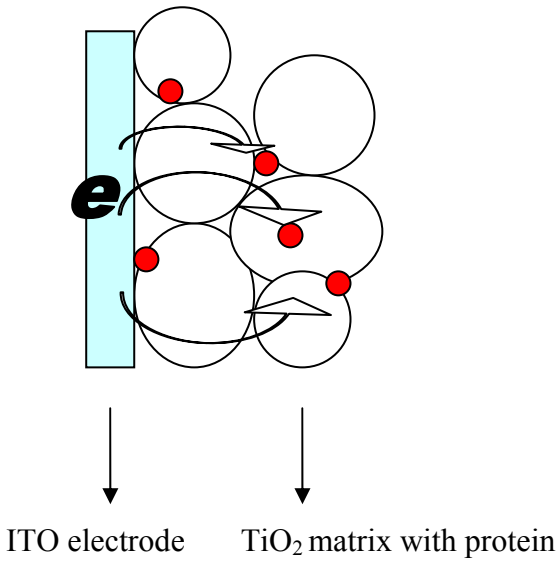

Figure 68. Schematic drawing of the electron transport via the conduction through the TiO_2 host material matrix containing the haem centered protein.

Process 2 long range:

Fe (III) (Haem) + e^- (TiO_2) $\rightleftharpoons$ Fe (II) (Haem)

For both 3 layer and 10 layer TiO_2 film electrodes, the second reduction process is pronounced only during the first potential cycle and then gradually disappears during subsequent cycles. This loss of signal is unlikely to be associated with the loss of protein from the porous TiO_2 structure but more likely to be associated with the irreversibility of electron transfer in the system.

Figure 69 shows an electrode exposed to several potential cycles displays essentially full recovery of the electrochemical activity when stored in aqueous phosphate buffered saline (pH 7.4) for a number of days. This shows typical voltammograms before and after recovery. A 10 layer TiO_2 film immersed in protein was stored overnight in buffer at 4ºC following a series of experiments and allowed to recover. The electrode was then thoroughly rinsed. The results were then compared with the same scanning conditions for a freshly prepared 10 layer electrode.

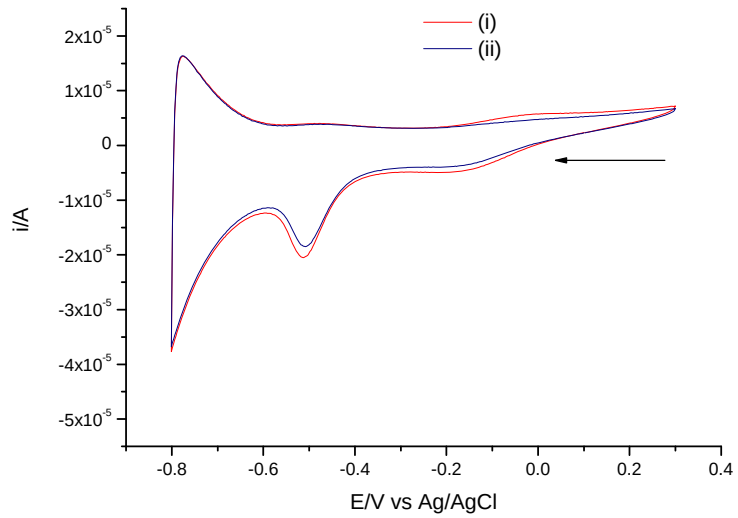

Figure 69. Cyclic Voltammogram (scan rate 0.1Vs $^{-1}$) showing scan 1 for the reduction of protein in a TiO_2 film immersed in 50mM phosphate buffered saline (pH 7.4).

(i) With a freshly prepared electrode and (ii) with a used electrode following recovery.

This strongly suggested that the protein was permanently bound and any observed loss of electrochemical activity seemed to be temporary and more likely to be linked to conductivity effects in the TiO_2 host material. It is also important to consider the electron transfer processes in the native state of *P*450 proteins here. The protein must be highly inert towards oxygen in order to prevent dangerous radical species from being formed in vivo and to prevent loss of native activity, so the observed irreversibility would be expected.

Next, the effects of scan in this system were considered.

6.5.7 The effects of increasing scan rate on peak potential of *P*450 protein adsorbed onto TiO_2 host electrodes.

The observed processes for protein immobilised in TiO_2 host films were dependent on the scan rate applied in the voltammetric set up. Figure 70 shows voltammograms obtained from the reduction of protein immobilised in a 5 layer film. The peak currents for all the observed processes increased approximately linearly with the scan rate.

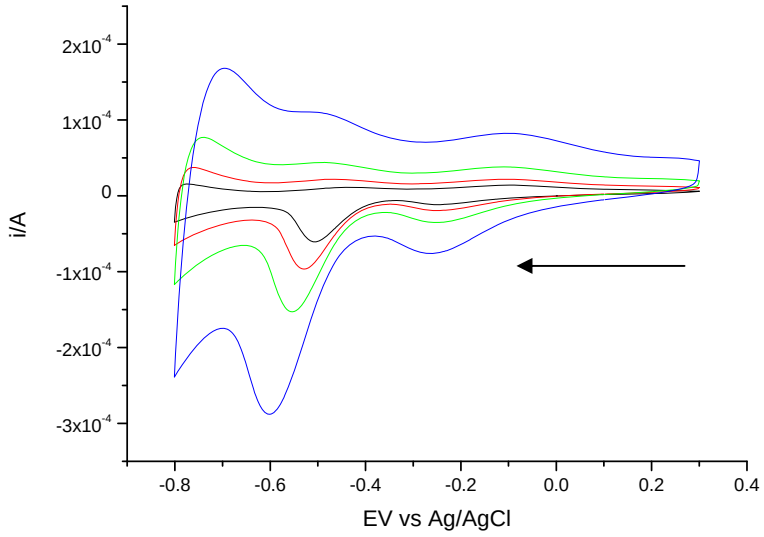

Figure 70. **Cyclic voltammograms at increasing scan rates for the reduction of protein immobilised in a 5 layer TiO_2 film electrode immersed in 50mM phosphate buffered saline (pH 7.4).**
The film was 24 hours old.

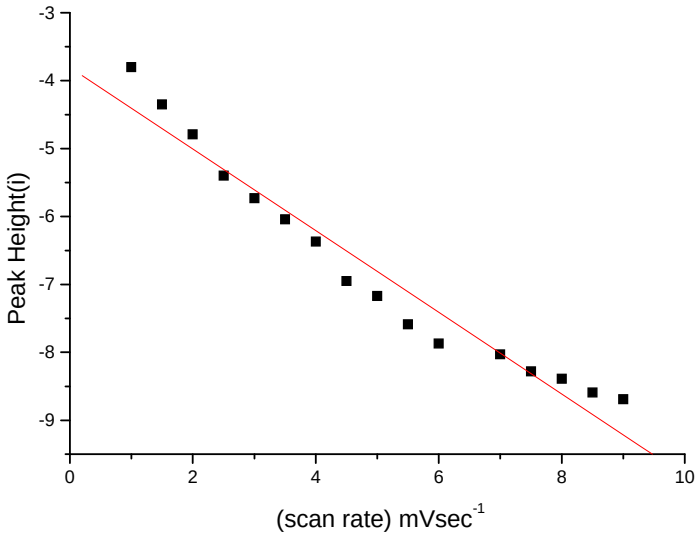

Figure 71. **Peak current at increasing scan rates for the reduction of protein immobilised in a 5 layer TiO_2 film electrode immersed in 50mM phosphate buffered saline (pH 7.4).**

These results tell us that the proteins may have been immobilised onto the surface of the 40nm TiO_2 nanoparticles matrix, this may suggest that the newer films (24 hours) had some residual protein which was exposed to electrochemical reduction; however the older films appeared to have protein buried deep inside the TiO_2 matrix which was more likely to be immobilised. It was also likely that process 1 reduction took place close to the top layers of the TiO_2 matrix.

Next, the effects of how long the protein was exposed to the films and the thickness of the films were considered.

6.5.8 Effects of time and layer thickness on the peak reduction currents of *P*450 protein in TiO_2 nanoparticle host electrode material.

The observed redox processes for protein immobilised in a TiO_2 host film appeared to be dependent on film layer thickness so the observed effect of how long the protein stayed in the film was examined.

The following figures show the effects on both processes and the resulting effects due to film layer thickness and the number of days the protein stayed active in the film.

All films were immersed in a solution of protein in phosphate buffered saline (pH 7.4) overnight at 4ºC. The films were then removed from the protein solution and thoroughly rinsed to remove any residual surface protein. An increase in peak reduction current in processes 1 and 2 with the addition of TiO_2 nanoparticle layers was observed. As was an increase in peak reduction current with the number of days the protein stayed in the films. This was particularly marked in process 1.

The 24hour film showed significantly smaller reduction peaks in all layered thicknesses from 2 to 50 layers (figure 6.21). However, a significant increase in reduction peak current was observed in process 1 after 13 days in all thicknesses of film (figure 6.22).

Firstly, the effects of the first and second scans, shown in Figures 72 and 73, with regard to increasing layered thicknesses were looked at.

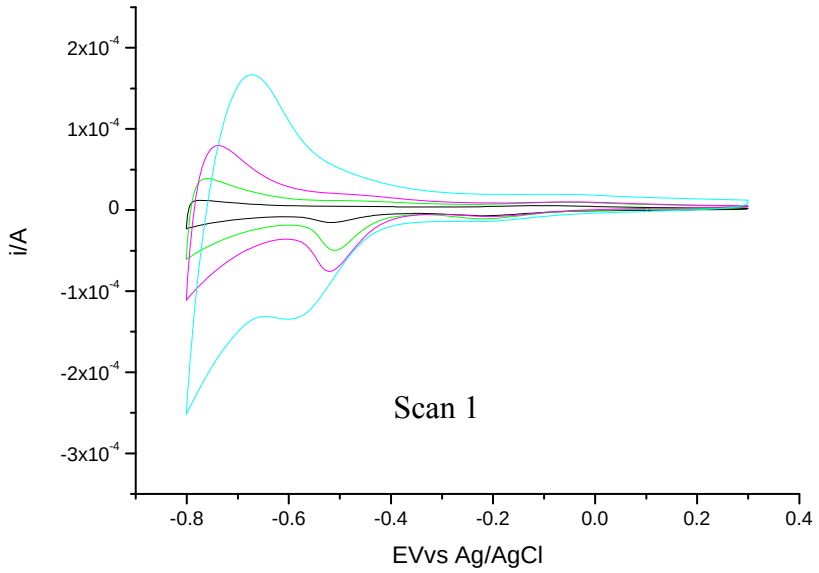

Figure 72. Cyclic voltammograms showing the reduction of protein immobilised in 40nm TiO_2 particle film electrodes from the first scan at increasing layer thickness, 3, 10, 30 and 50 layers.

Scan rate100 mVs^{-1}.

The films were immersed in de gassed 50mM phosphate buffered saline (pH 7.4). The experiments were carried out 24hours after immersion in the protein solution.

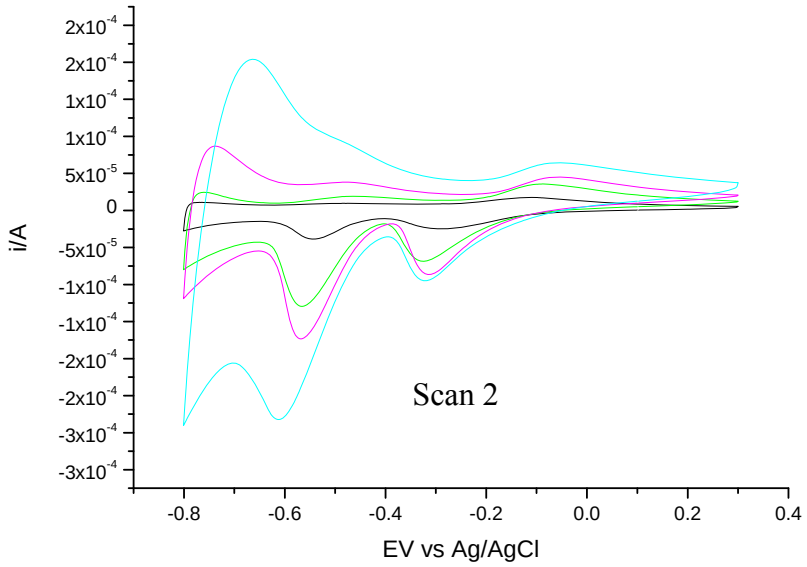

Figure 73. Cyclic voltammograms showing the reduction of protein immobilised in 40nm TiO_2 particle film electrodes at increasing layer thickness, 3, 10, 30 and 50.

Scan rate100 mVs^{-1}.

The films were immersed in de gassed 50mM phosphate buffered saline (pH 7.4). The experiments were carried out 13 days after immersion in the protein solution.

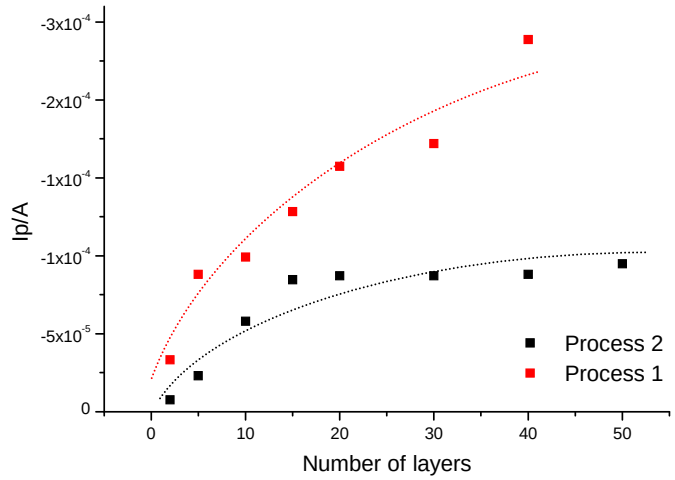

Figure 74. **Plot to determine peak height of process 1 and 2 from the reduction of protein immobilised in 40nm TiO_2 nanoparticle films at increasing layer thickness.**

Scan rate 100mVs^{-1}. The films were immersed in de gassed 50mM phosphate buffered saline (pH 7.4). The experiments were carried out 13 days after immersion in the protein solution.

It is interesting to note from Figure 74, that the magnitude of the voltammetric response for process 1 increases upon increasing the number of TiO_2 layers and that the increase in process 2 is considerably less.

Below is a plot to determine the increase of reduction peak for process 1 on increasing the number of days the protein has been in the TiO_2 matrix.

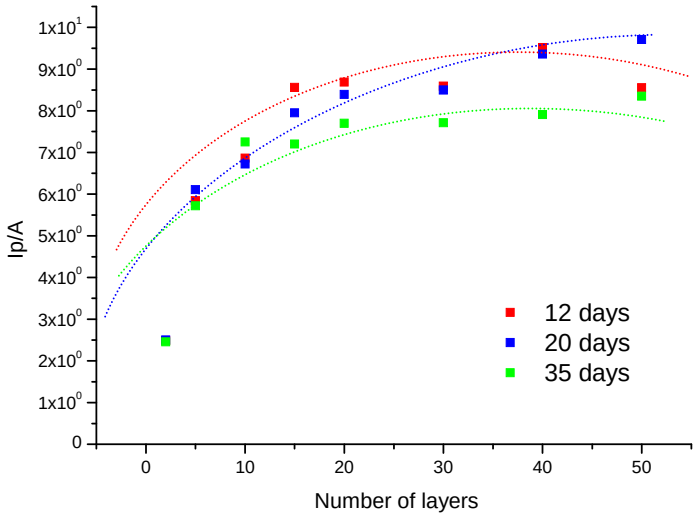

Figure 75. Plot to determine peak height of process 1 from the reduction of protein immobilised in 40nm TiO_2 nanoparticle films at increasing number of days old.

The 24 hour 40nm TiO_2 particle film with immobilised *P*450 protein (data not shown) did not exhibit any linearity in any of the different layered thicknesses. However, the 12, 20 and 35 day old films demonstrated an approximate linear relationship between peak reduction height and layered thickness as shown in Figure 75. The peak reduction current for process 1 increased with the number of layers and the number of days the protein stayed immobilised within the TiO_2 matrix, however, there was little correlation between increased reduction peak and number of days old after 10 days.

These results illustrated that this process was essentially irreversible and left the protein intact for electron transfer processes to occur some considerable time after the ITO/TiO_2 film electrode was exposed to the protein. It was therefore likely that the protein migrated through the TiO_2 matrix and became embedded, but more importantly, was still redox active.

The immobilisation of cytochrome *P*450 proteins in 40nm diameter TiO_2 nanoparticle films resulted in reproducible and stable electrodes which displayed characteristic Fe (III/II) reduction responses. The immobilisation process may have occurred due to the electrostatic interaction between the phosphate coated (negatively charged) TiO_2 matrix and the positively charged patches on the surface of the *P*450 protein. Previous work has shown that *P*450 CYP101 protein has an equal number of acidic and basic residues. However, there is an inequality in the surface distribution of the charged residues, such that the side distal to the haem group is heavily anionic and the proximal side has a few cationic clusters amongst the anionic residues [23]. So in reality, it would be extremely difficult to identify the precise orientation of the protein as it lies within the TiO_2 host material.

6.6 Chapter Summary

The reactivity of redox systems immobilised in TiO_2 films was shown to be strongly associated with and affected by the conductivity of the host matrix. It would appear that only process 1 was associated with the direct electron transfer of electrons from the ITO electrode surface into the TiO_2 matrix and eventually to the immobilised protein. Process 2 appeared to require conduction of electrons within and from the TiO_2 matrix which was capacitative in nature.

It has been shown that *P*450 protein was electrostatically accumulated into porous TiO_2 host films with a sufficiently large pore size. It has also been shown that this process was essentially irreversible and left the protein intact for electron transfer processes to occur.

Two distinct reduction processes were apparent and were associated with direct and reversible reduction of the protein in the vicinity of the ITO electrode surface and also indirect reduction was observed via conduction through the TiO_2 matrix.

However, although the voltammetric signals observed here are thought to be the Fe (III) to Fe (II) reduction of the haem unit in *P*450, it is important to keep in mind that overall, the mechanisms for the reduction of haem within *P*450 are complex and not well understood and more work would be required to resolve this.

6.7 References

1. Cooper J and Cass T **2004** *Biosensors*, Oxford University Press, Oxford UK

2. Wang C.H, Yang C, Song Y, Gao W, Xia X **2005** *Adv. Funct. Mater Adsorption and Direct electron transfer from haemoglobin into a three dimensionally ordered macrporous gold film.*15 pp1267-1275.

3. Roberts M, Bilewicz R, Stebe M, Hamidi A, Miclo A, Rogalska M. **2001** *Phys. Chem. Chem. Phys Fluorinated and hyrogenated cubic phases as matrices for immobilisation of cholesterol oxidase on electrodes.*3 pp240-245.

4. Fang A, Ng Y, Li S. **2003** *Biosens. & Bioelectron A high performance glucose biosensor based on momomlecular layer of glucose oxidase covalently immobilised on indium tin oxide surface.* 19 pp 43-49.

5. Shen L, Hu S, **2005** *Biomacromol. Electrostatic adsorption of haem proteins alternated with polyamidoamine dendrimers for layer by layer assembly of electroactive films.* 6 pp1475-1483.

6. Scheller F, Janchen M. Etzold G, Will H. **1974** *Bioelectrochem, Bioenerg Electrochemical reduction of bonded oxygen in oxyhemoglobin at gold electrodes modified by self-assembled cysteamine monolayers* 1 pp 478.

7. Rusling J F, **1998** *Acc.Chem.Res. Direct Electrochemistry and Electrocatalysis of Myoglobin Entrapped in Konjac Glucomannan Films* pp 31 363

8. Bartnicki L, Belser N, Castro C. **1978** *Biochemistry Epoxidation of styrene by hemoglobin and myoglobin. Transfer of oxidizing equivalents to the protein surface*17 pp 5582.

9. McKenzie K J , Marken F and Opallo M **2005** *Bioelectrochemistry, The effects of conductivity and electrochemical doping on the reduction of methemoglobin immobilized in nanoparticulate TiO2 films* . 66 (1-2) pp 41-47

10. N. F. González-Cadavid and P. N. Campbell. Biochem J. **1967** 105(2): 443–450.

11. J.F.Rusling. Biomolecular Films, Marcel Dekker, New York, **2003.**

12. C.G. Siontorou, D.P. Nikolelis, Cyanide ion mini sensor. Anal. Chim. Acta 355 **1997**, 227-234.

13. Y.Liu, H.Y. Liu, N.F. Hu, Core shell nanocluster of haemoglobin & clay. Direct electrochemistry & electroanalysis, Biophys. Chem. 117. **2005**. 27-37.

14. McKenzie K.J & Marken, F. Langmuir 19 (10) 4327 – 4331. May **2003,** 121.

15. McKenzie K.J, Marken F & Opallo M. Bioelectrochemistry, 66 (1-2) 41-47. **2005.**

16. Lewis, D.F.V. (2001). *Cytochromes P450. Structure and Function.* Taylor and Francis. London.

17. Ortiz de Montellano (1995). *Cytochrome P450. Structure, Mechanism and Biochemistry.* Kulwer Academic.

18. E.Topoglidis, A.E.G. Cass, J.R. Durrant. Anal. Chem. **1998**, 70. 5111.

19. Milsom, E. V.; Perrott, H. R.; Peter, L. M.;Marken, F. Langmuir; 2005; 21(21); 9482-9487.

20. Katy J. McKenzie, Frank Marken and Marcin Opallo. Bioelectrochemistry, Volume 66, Issues 1-2, April **2005**, Pages 41-47

21.Fabregat-Santiago, F.; Mora-Sero, I.; Garcia-Belmonte, G.; Bisquert, J. (J. Phys. Chem. B, 107 (3), 758 -768, 2003)

22. J. Phys. Chem. B, **107** (3), 758 -768, 2003 Electrochemistry Communications Vol 6, Issue 11 , Nov **2004,** 1153-1158.

23. Stoilov I, Jansson I, Sarfarazi M, Schenkman JB. Archives of Biochem & Biophys 385, 1, Jan **2001,** 78-87.

7 Conclusions and Outlook

7.1. Conclusions

7.2. Outlook

7.3. References

7.1 Conclusions

This project encompassed a number of key areas. Firstly, two functional Cytochrome *P*450 proteins were produced. Cyp101 from the bacteria Pseudomonas Putida by extraction and purification. Secondly, Cyp6g1 from the fruit fly Drosophila Melanogaster by an extraction method which yielded functional microsomal proteins. It was crucial to determine the purity of the extraction and purification processes at each step and most importantly, that both processes yielded functionally active proteins with structural integrity. The success of this protein production process allowed further experimental stages to go ahead.

The investigation of microsomal *P*450 proteins from the fruit fly *Drosophila Melanogaster* and their associated substrate biotransformation mechanisms were then shown in detail. This particular proteins' activity was probed using both electrochemical and fluorescent methods and focused on the *P*450 gene intrinsic in metabolic resistance in the fly.

Most importantly here, the work presented the first electrochemical study of the microsomal Cytochrome *P*450 protein Cyp6g1 from the fruit fly *Drosophila Melanogaster*. The extraction of microsomes containing this protein from two different fly strains was described. The electrochemical measurements of the biotransformation of substrate methoxy-resorufin ether allowed the effects of the over transcription of a single gene Cyp6g1 to be investigated. This proved to be an effective way of directly following substrate metabolism and compared well with what is already known about the genetic differences in the two strains of *Drosophila*.

The results reinforced the findings from the fluorescence study of the substrate metabolic product. Similar electrochemical approaches in tandem with fluorescent measurements will therefore be useful in further investigations of other xenobiotic metabolising *P*450s.

The next chapter investigates microsomal *P*450 proteins from the fruit fly on an electrode surface.

The project then went on to look at the reactivity of redox systems immobilised in TiO_2 films. This was shown to be strongly associated with and affected by the conductivity of the host matrix. Two distinct reduction processes were apparent and were associated with direct and reversible reduction of the protein in the vicinity of the ITO electrode surface and also indirect reduction was observed via conduction through the TiO_2

matrix. It was also shown that this process was essentially irreversible and left the protein intact for electron transfer processes to occur.

However, although the voltammetric signals observed here were considered to be the Fe (III) to Fe (II) reduction of the haem unit in *P*450, it is important to keep in mind that overall, the mechanisms for the reduction of haem within *P*450 are complex and not well understood and more work would be required to resolve this.

7.2 Outlook

Recent work has shown that both methaemoglobin and Cytochrome *P*450 proteins are likely to denature at an SnO_2 electrode surface and the observed electrochemical responses are likely to be the voltammetric response of Fe^{3+} released from the denatured protein. However, the mechanisms involved in this process are not clear and work continues in this area [1]. Similar work carried out by Brusova *et al* suggested that haem, which may be fully or partially removed from the protein entrapped in argarose hydrogel films, was likely to be responsible for observed electrochemical reactions [2, 3].

7.3 References

1. Milsom, E.V., Dash, H.A., Thetford, A., Bligh, N., Wojciech, N., Opallo, M & Marken F. Journal of Elecroanalytical Chemistry. April **2007**

2. Brusova, Z., Gorton, L. and Magner, E. Langmuir, 22 (26), 11453 -11455, **2006.**

3. E. V. Milsom , H. A. Dash , A. Thetford , N. Bligh , Wojciech Nogala , Marcin Opallo , F. Marken. Journal of Elecroanalytical Chemistry. July **2007**

8 Appendices

Appendix I - Methoxy Resorufin Ether as an electrochemically active biological probe for Cytochrome *P*450 *O* – demethylation

Appendix II - The effects of conductivity and electrochemical doping on the reduction of methemoglobin immobilised in nanoparticulate TiO_2 films